GEOMETRIC COMBINATORICS OF POLYNOMIALS II: POLYNOMIALS AND CELL STRUCTURES

MICHAEL DOUGHERTY AND JON MCCAMMOND

ABSTRACT. This article introduces a finite piecewise Euclidean cell complex homeomorphic to the space of monic centered complex polynomials of degree d whose critical values lie in a fixed closed rectangular region. We call this the *branched rectangle complex* since its points are indexed by marked d-sheeted planar branched covers of the fixed rectangle. The vertices of the cell structure are indexed by the combinatorial "basketballs" studied by Martin, Savitt and Singer. Structurally, the branched rectangle complex is a full subcomplex of a direct product of two copies of the order complex of the noncrossing partition lattice. Topologically, it is homeomorphic to the closed $2n$-dimensional ball where $n = d - 1$. Metrically, the simplices in each factor are orthoschemes. It can also be viewed as a compactification of the space of all monic centered complex polynomials of degree d.

We also introduce a finite piecewise Euclidean cell complex homeomorphic to the space of monic centered complex polynomials of degree d whose critical values lie in a fixed closed annular region. We call this the *branched annulus complex* since its points are indexed by marked d-sheeted planar branched covers of the fixed annulus. It can be constructed from the branched rectangle complex as a cellular quotient by isometric face identifications. And it can be viewed as a compactification of the space of all monic centered complex polynomials of degree d with distinct roots.

Finally, the branched annulus complex deformation retracts to the *branched circle complex*, which we identify with the dual braid complex. The space of polynomials with distinct roots is one of the earliest classifying spaces for the d-strand braid group, and the dual braid complex is a more recent classifying space derived from the braid group's dual Garside structure. Our explicit embedding of one classifying space as a spine of the other provides a direct proof that the two classifying spaces are homotopy equivalent.

INTRODUCTION

Let POLY_d^{mc} be the space of monic centered complex polynomials of degree d and let $\text{POLY}_d^{mc}(\mathbf{U})$ be the subspace of polynomials whose critical values lie in $\mathbf{U} \subset \mathbb{C}$. In this article we describe a finite piecewise Euclidean cell structure on $\text{POLY}_d^{mc}(\mathbf{U})$ in four cases: when $\mathbf{U}$ is a closed interval ⊶, a circle ○, a closed rectangle ▢, or a closed annulus ◉. Spaces homeomorphic to the first two have already appeared in the literature under different names. The last two are being introduced here.

The overall flavor of our results is best illustrated by a concrete example. Consider the case where $d = 3$ and $\mathbf{U} = $ ⊶ is the real interval $[-2, 2] \subset \mathbb{C}$. The space $\text{POLY}_3^{mc}(\text{⊶})$, of monic centered cubic polynomials with critical values in the interval $[-2, 2]$, includes the polynomial $p(z) = z^3 + b$ for any $b \in [-2, 2]$, since it has a double critical point at 0 and a double critical value at b, as well as the

$\mathrm{POLY}_3^{mc}(\rightarrowtail)$ 　　　　　　　　$\mathrm{MULT}_2(\rightarrowtail)$
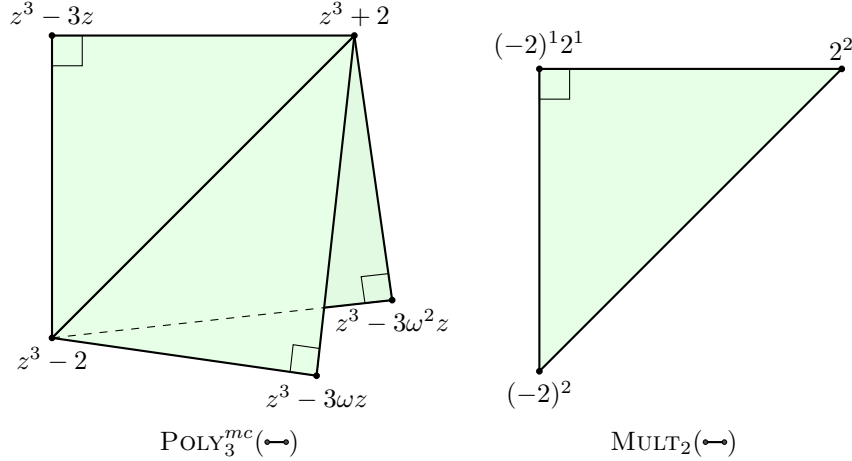
FIGURE 1. The right-angled triangle shown on the right is the space $\mathrm{MULT}_2(\rightarrowtail)$ of 2 unlabeled points in the closed interval $[-2, 2]$. The three right-angled triangles with a common hypotenuse shown on the left form the space $\mathrm{POLY}_3^{mc}(\rightarrowtail)$ of monic centered cubic polynomials with critical values in $[-2, 2]$. The extremal situations have been labeled in both cases.

(rescaled) Chebyshev polynomial $p(z) = z^3 - 3z$ with critical points ± 1 and critical values ± 2. More generally, it is straightforward to compute that the exact set of polynomials satisfying these conditions are those of the form $p(z) = z^3 - 3a^2\omega^k z + b$ with $a \in [0, 1]$, $b \in [2a^3 - 2, 2 - 2a^3]$, $k \in \{0, 1, 2\}$, and where $\omega = \frac{1+i\sqrt{3}}{2}$ is a cube root of unity. Note that when $a = 0$, the value of k is irrelevant. Topologically, the space is three triangles with a common hypotenuse, depicted in the left hand side of Figure 1. The metric is provided by the space of possible critical values. Two distinguishable critical values in $[-2, 2]$ are represented by a point in the square $[-2, 2]^2$, and removing our ability to distinguish them corresponds to folding the square along the diagonal line where they are equal to produce the space $\mathrm{MULT}_2(\rightarrowtail)$ of 2-element multisets in $[-2, 2]$. The right-angled triangle $\mathrm{MULT}_2(\rightarrowtail)$, shown on the right hand side of Figure 1, is also known as a 2-dimensional orthoscheme. The generically 3-to-1 map from $\mathrm{POLY}_3^{mc}(\rightarrowtail)$ on the left to $\mathrm{MULT}_2(\rightarrowtail)$ on the right is a restriction of the Lyashko–Looijenga map that sends a monic centered complex polynomial to (the monic polynomial determined by) its multiset of critical values.

More generally, $\mathrm{MULT}_d(\rightarrowtail)$ can be viewed as a metric simplex known as a standard d-dimensional orthoscheme, and we can pull back through the Lyashko–Looijenga map to obtain a simplicial structure for $\mathrm{POLY}_d^{mt}(\rightarrowtail)$, the space of monic degree-d polynomials up to precomposition with a translation[1] with critical values in $\rightarrowtail$. When the metric from the orthoscheme is pulled back through the Lyashko–Looijenga map, $\mathrm{POLY}_d^{mt}(\rightarrowtail)$ is assigned a *stratified Euclidean metric* (Definition 7.18) distinct from the usual Euclidean metric inherited from $\mathbb{C}^{d-1}$ when the coefficients of the monic centered polynomial are used as coordinates. For

---

[1]Considering polynomials up to precomposition with a translation is equivalent to centering the roots at the origin. The latter is preferable for concrete examples, but we will use the former for the statements of theorems. See Remark 7.6.

higher values of d, the combinatorial structure can be described using the lattice of noncrossing partitions NCPART_d and its order complex $|\mathrm{NCPART}_d|_\Delta$.

Theorem A (Intervals: Theorem 12.5). *The space* $\mathrm{POLY}_d^{mt}(\rightarrowtail)$ *of polynomials with critical values in a closed interval (with the stratified Euclidean metric) is isometric to the order complex* $|\mathrm{NCPART}_d|_\Delta$ *(with the orthoscheme metric).*

The noncrossing partition lattice NCPART_d, defined by Kreweras in 1972 [Kre72], has $C_d = \frac{1}{d+1}\binom{2d}{d}$ elements and d^{d-2} maximal chains, where the numbers C_d are the ubiquitous Catalan numbers [Sta15]. So by Theorem A, the simplicial complex $\mathrm{POLY}_d^{mt}(\rightarrowtail) \cong |\mathrm{NCPART}_d|_\Delta$ has C_d vertices and d^{d-2} top-dimensional simplices. Alternatively, every polynomial in $\mathrm{POLY}_d^{mt}(\rightarrowtail)$ can be uniquely labeled by a marked planar metric graph called a *banyan* or *branched line* (Example 3.19). The complex $\mathrm{BR}_d^m(\rightarrowtail)$ of all marked planar d-branched lines (Definition 12.6) is the same as the order complex $|\mathrm{NCPART}_d|_\Delta$, so one way to restate Theorem B is that $\mathrm{POLY}_d^{mt}(\rightarrowtail) \cong \mathrm{BR}_d^m(\rightarrowtail)$. See [BBG+19] and [McC06] for surveys of the various ways in which noncrossing partitions arise.

Noncrossing partitions started appearing in geometric group theory around the year 2000, starting with the work of Birman–Ko–Lee [BKL98] on a new "dual presentation" for the symmetric group SYM_d and the braid group BRAID_d. Tom Brady [Bra01] and David Bessis [Bes03] soon turned this presentation into a new classifying space for the braid group. More specifically, the dual presentation utilizes Biane's correspondence between NCPART_d and $[1, \delta]$, the set of permutations which appear in minimal length factorizations of the d-cycle $\delta = (1\ 2\ \cdots\ d)$ into transpositions [Bia97]. By an appropriate identification of cells in the order complex of NCPART_d, Brady defined a simplicial complex which is a classifying space for BRAID_d [Bra01], and this space was later endowed with the "orthoscheme metric" in work of Brady and the second author [BM10]. With the orthoscheme metric, this classifying space is called the *dual braid complex* K_d, and it is an example of an *interval complex* when the same construction is applied in more general settings. It was conjectured in [BM10] that the dual braid complex K_d is locally $\mathrm{CAT}(0)$, which would imply that BRAID_d is a $\mathrm{CAT}(0)$ group. This has been proven for $d \le 7$ [BM10, HKS16, Jeo23] but remains open in general. Our second main theorem provides a polynomial version of the dual braid complex K_d.

Theorem B (Circles: Theorem 13.3). *The space* $\mathrm{POLY}_d^{mt}(\bigcirc)$ *of polynomials with critical values in a circle is homeomorphic to a quotient of the complex* $\mathrm{POLY}_d^{mt}(\rightarrowtail)$ *by face identifications. As a metric Δ-complex,* $\mathrm{POLY}_d^{mt}(\bigcirc)$ *is the dual braid complex* K_d *with the orthoscheme metric.*

The quotient map transforming $\mathrm{POLY}_d^{mt}(\rightarrowtail)$ into $\mathrm{POLY}_d^{mt}(\bigcirc)$ identifies all of the vertices and many of the lower-dimensional faces. The cell structure on $\mathrm{POLY}_d^{mt}(\bigcirc)$ remains $(d-1)$-dimensional with d^{d-2} top-dimensional simplices, but now with only one vertex. Although it is no longer a simplicial complex, it is a Δ-complex in the sense of Hatcher [Hat02]. As in the interval case, there is an alternative way to label the points in $\mathrm{POLY}_d^{mt}(\bigcirc)$. Every polynomial in $\mathrm{POLY}_d^{mt}(\bigcirc)$ can be uniquely labeled by a marked planar metric graph called a *cactus* or *branched circle* (Example 3.20). The complex $\mathrm{BR}_d^m(\bigcirc)$ of all marked planar d-branched circles (Definition 13.4) is the same as the dual braid complex K_d, so one way to restate Theorem B is $\mathrm{POLY}_d^{mt}(\bigcirc) \cong \mathrm{BR}_d^m(\bigcirc)$.

Banyans and cacti were initially described in the first article of this series [DM22], although the approach we take here is both more general and more direct. Algebraically banyans and cacti can be viewed as encoding *linear* and *circular* factorizations of δ, respectively. This perspective is discussed in [DM24], where we introduce a continuous version of noncrossing partitions that is closely connected to the work of W. Thurston and his collaborators on the space of complex polynomials [TBY$^+$22].

The cell structure we put on the polynomial space $\mathrm{POLY}_d^{mt}(\square)$ is more complicated. A closed rectangle $\square \subset \mathbb{C}$ is a direct product $\rightarrowtail \times \rightarrowtail$ of two intervals and, somewhat surprisingly, we show that $\mathrm{POLY}_d^{mt}(\square)$ embeds as a subspace of the product $\mathrm{POLY}_d^{mt}(\rightarrowtail) \times \mathrm{POLY}_d^{mt}(\rightarrowtail)$. This is our third main theorem.

Theorem C (Rectangles: Theorem 14.4). *The space* $\mathrm{POLY}_d^{mt}(\square)$ *of polynomials with critical values in a closed rectangle (with the stratified Euclidean metric) is isometric to a subcomplex of* $|\mathrm{NCPERM}_d|_\Delta \times |\mathrm{NCPERM}_d|_\Delta$ *(with the orthoscheme metric).*

The cell structure on $\mathrm{POLY}_d^{mt}(\square)$ is *bisimplicial* in the sense that every cell is a product of two simplices. The vertices are enumerated by the Fuss–Catalan numbers $C_d^{(4)} = \frac{1}{3d+1}\binom{4d}{d}$ and labeled by the combinatorial "basketballs" (Definition 14.5) initially defined by Martin, Savitt and Singer in [MSS07]. There are $(d-1)!d^{d-2}$ top-dimensional cells. The compatibility condition between the noncrossing partitions in each factor arise from the fact that they need to be combinatorial aspects of a common marked planar d-branched cover of the rectangle $\square$. The complex $\mathrm{BR}_d^m(\square)$ is the same as $\mathrm{POLY}_d^{mt}(\square)$, but with points labeled by geometric and combinatorial information associated to marked planar d-branched rectangles (Definition 14.6) so one way to restate Theorem C is that $\mathrm{BR}_d^m(\square)$ embeds in $\mathrm{BR}_d^m(\rightarrowtail) \times \mathrm{BR}_d^m(\rightarrowtail)$. The compatibility condition on top-dimensional cells can be restated algebraically. The linear factorization of δ into transpositions coming from the first factor and the linear factorization of δ into transpositions coming from the second factor are related by the *Hurwitz action* of a simple braid. The d^{d-2} maximal factorizations and $(d-1)!$ simple braids parameterize the top-dimensional cells. This fact is related to the noncrossing hypertrees results in [McC].

Finally, the transition from $\square$ to $\circledcirc$ and its impact on $\mathrm{POLY}_d^{mt}(\square)$ is very similar to that from $\rightarrowtail$ to $\bigcirc$ and its impact on $\mathrm{POLY}_d^{mt}(\rightarrowtail)$. In particular, the side identification in $\mathbb{C}$ that turns the rectangle $\square$ into the annulus $\circledcirc$ induces a face identification on the corresponding polynomial cell complex.

Theorem D (Annuli: Theorem 15.1). *The space* $\mathrm{POLY}_d^{mt}(\circledcirc)$ *of polynomials with critical values in a closed annulus is homeomorphic to a quotient of the metric cell complex* $\mathrm{POLY}_d^{mt}(\square)$ *by face identifications.*

The vertices of the bisimplicial cell structure on $\mathrm{POLY}_d^{mt}(\circledcirc)$ are counted by the Catalan numbers C_d, and there are $(d-1)!d^{d-2}$ top-dimensional cells. The complex we call $\mathrm{BR}_d^m(\circledcirc)$ is the same as a the space $\mathrm{POLY}_d^{mt}(\circledcirc)$ but with points labeled by geometric and combinatorial information associated to marked planar d-branched annuli (Definition 15.4). A detailed exploration of the geometric combinatorics of the compact piecewise Euclidean cell complexes described by these first four theorems will appear later in this series.

The metric cell structures described in the preceding theorems are also connected to classical polynomial spaces via homeomorphisms, compactifications and deformation retractions. Our three final main theorems describe these connections.

Theorem E (Homeomorphisms: Theorem 10.7). *The complex plane $\mathbb{C}$, the punctured plane $\mathbb{C}_{\mathbf{0}}$ and the real line $\mathbb{R}$ are homeomorphic to the open rectangle $\blacksquare$, the open annulus $\odot$ and the open interval $\multimap$ respectively, and these induce homeomorphisms of polynomial spaces $\mathrm{POLY}_d^{mt}(\mathbb{C}) \cong \mathrm{POLY}_d^{mt}(\blacksquare)$, $\mathrm{POLY}_d^{mt}(\mathbb{C}_{\mathbf{0}}) \cong \mathrm{POLY}_d^{mt}(\odot)$ and $\mathrm{POLY}_d^{mt}(\mathbb{R}) \cong \mathrm{POLY}_d^{mt}(\multimap)$.*

Theorem F (Compactifications: Theorem 10.9). *The three spaces $\mathrm{POLY}_d^{mt}(\blacksquare)$, $\mathrm{POLY}_d^{mt}(\circledcirc)$ and $\mathrm{POLY}_d^{mt}(\bullet\!\!-\!\!\bullet)$ are compactifications of $\mathrm{POLY}_d^{mt}(\blacksquare)$, $\mathrm{POLY}_d^{mt}(\odot)$ and $\mathrm{POLY}_d^{mt}(\multimap)$.*

Combining Theorem E with Theorem F shows that $\mathrm{POLY}_d^{mt}(\blacksquare)$, $\mathrm{POLY}_d^{mt}(\circledcirc)$ and $\mathrm{POLY}_d^{mt}(\bullet\!\!-\!\!\bullet)$ can be viewed as compactifications of $\mathrm{POLY}_d^{mt}(\mathbb{C})$, $\mathrm{POLY}_d^{mt}(\mathbb{C}_{\mathbf{0}})$ and $\mathrm{POLY}_d^{mt}(\mathbb{R})$, respectively. In particular, the complex $\mathrm{POLY}_d^{mt}(\blacksquare)$ is a manifold, or more specifically a closed ball with corners. For comparison, the space $\mathrm{POLY}_d^{mt}(\bullet\!\!-\!\!\bullet)$ is not a manifold, and neither is the product of two copies of $\mathrm{POLY}_d^{mt}(\bullet\!\!-\!\!\bullet)$ which contains $\mathrm{POLY}_d^{mt}(\blacksquare)$ as a subcomplex (Theorem C).

Finally, some of these polynomial spaces are deformation retracts of others.

Theorem G (Deformation retractions: Theorem 10.15). *A deformation retraction of $\blacksquare$ onto any embedded arc $\bullet\!\!-\!\!\bullet \subset \blacksquare$ induces a deformation retraction from $\mathrm{POLY}_d^{mt}(\blacksquare)$ to $\mathrm{POLY}_d^{mt}(\bullet\!\!-\!\!\bullet)$. Similarly, a deformation retraction of $\circledcirc$ onto any core curve $\bigcirc \subset \circledcirc$ induces a deformation retraction from $\mathrm{POLY}_d^{mt}(\circledcirc)$ to $\mathrm{POLY}_d^{mt}(\bigcirc)$.*

This shows that the space of monic degree-d polynomials with distinct roots up to translation admits a compactification with a metric bisimplicial cell structure such that (1) there is a deformation retraction of this space to the subspace of polynomials with critical values on the unit circle, and (2) the induced cell structure on the resulting space is isometric to the dual braid complex K_d.

Connections to the literature. Many of the objects and ideas in our main theorems have appeared before in various forms, but we believe this is the first article to combine all of them. Any list of connections to the rich literature on these topics will be incomplete, but here are some of the previous appearances of the main characters: combinatorial data associated to polynomials, compactifications, cell structures, and the dual Garside structure for the braid group.

The preimages of lines and circles that arise in the combinatorial structures we derive from polynomials have appeared in many places over the years—we list a small fraction of them here. In this article, we label the points in $\mathrm{POLY}_d^{mt}(\bullet\!\!-\!\!\bullet)$ by preimages of line segments (*banyans* or *branched lines*). Similarly, Gauss's first proof of the Fundamental Theorem of Algebra [Gau99] utilizes the preimages of the real and imaginary axes under a complex polynomial. This idea was expanded upon by Martin, Savitt and Singer in [MSS07] and by Savitt in [Sav09] to introduce the notion of *basketballs*, which can be used to label the vertices of our cell structure on $\mathrm{POLY}_d^{mt}(\blacksquare)$. More recently, generalizations of these line preimages called *signatures* of polynomials have appeared in work of A'Campo [A'C20] and Combe [Com].

We use preimages of circles (*cacti* or *branched circles*) to label the points of $\text{POLY}_d^{mt}(\bigcirc)$. These graphs appeared previously (as quotients of an equivalence relation on a circle) in an unpublished manuscript of W. Thurston that was posthumously completed by his collaborators [TBY$^+$22]. See [DM24] for a more detailed account of the connections between Thurston's work and ours. Cacti have also appeared in fields such as complex geometry [CP91, CW91, EMHZZ96], complex dynamics [Nek14, Cal22], and algebraic topology [Sal22]. Special care must be taken when comparing results from different articles, as there are many variations (including markings and metrics) and definitions for cacti across subdisciplines.

Recent work by Wegert [Weg20], A'Campo [A'C22] and A'Campo–Papadopoulos [AP24] uses the pullbacks of both lines and circles to study polynomials in a manner which is similar to ours. In the latter two articles, the authors use this to introduce open cell structures for both the space $\text{POLY}_d^m(\mathbb{C})$ of monic degree-d polynomials with arbitrary roots and $\text{POLY}_d^m(\mathbb{C}_{\mathbf{0}})$, the subspace of polynomials with distinct roots. The numbers of top-dimensional cells in these complexes match the numbers of vertices in our cell structures on $\text{POLY}_d^{mt}(\square)$ and $\text{POLY}_d^{mt}(\circledcirc)$ respectively, so it seems likely that the two structures are dual to one another.

Several other recent articles in algebraic topology have featured ideas similar to ours. Following a presentation by the second author on the contents of this article at an Oberwolfach mini-workshop [McC24], Bianchi pointed out a connection with his recent work [Bia22, Bia23]. It appears that Bianchi defines an abstract cell structure for $\text{POLY}_d^m(\square)$ which matches ours, including an equivalent set of algebraic labels. His complex, however, does not include a metric. Other relevant work includes that of Salter [Sal23, Sal24] and Salvatore [Sal22]. Salter's articles provide an "equicritical" stratification on $\text{POLY}_d^m(\mathbb{C}_{\mathbf{0}})$ which is related to (but coarser than) the double stratification described in Section 7. The combinatorial tools used in Salter's work are similar to ours, but lead to distinct structures. Salvatore introduces a cell structure for $\text{POLY}_d^{mt}(\mathbb{C}_{\mathbf{0}})$ which uses similar objects (nested trees of cacti), but the resulting complex does not appear to be directly related to ours. We should also note that none of these authors connect their complexes to the dual structure on the braid group.

In this article, we compactify $\text{POLY}_d^{mt}(\mathbb{C})$ and $\text{POLY}_d^{mt}(\mathbb{C}_{\mathbf{0}})$ to obtain $\text{POLY}_d^{mt}(\square)$ and $\text{POLY}_d^{mt}(\circledcirc)$, respectively. The space $\text{POLY}_d^{mt}(\mathbb{C}_{\mathbf{0}})$ has several compactifications from algebraic geometry, and it would be interesting to know more about how our compactification relates to them. For example, our work is distinct from the well-known Fulton–MacPherson compactification of $\text{POLY}_d^{mt}(\mathbb{C}_{\mathbf{0}})$, in which collisions of distinct roots are recorded using their relative positions and velocities [FM94]. In contrast, each collision in our compactification is described using metric cacti which record the relative cyclic ordering of the colliding roots.

Another distinguishing feature of our work in comparison to the references mentioned above is the concrete connection with the dual presentation for the braid group. In particular, the identification of $\text{POLY}_d^{mt}(\rightarrowtail)$ with the order complex $|\text{NCPART}_d|_\Delta = \Delta([1, \delta])$ and of $\text{POLY}_d^{mt}(\bigcirc)$ with the interval complex $K_d = K([1, \delta])$ is new—although it was known to Bessis that $\text{POLY}_d^m(\mathbb{C}_{\mathbf{0}})$ deformation retracts onto a copy of $K_d = K([1, \delta])$ [Bes03, Proposition 10.6]. Similarly, W. Thurston et al. showed that $\text{POLY}_d^m(\mathbb{C}_{\mathbf{0}})$ deformation retracts onto $\text{POLY}_d^{mt}(\bigcirc)$ [TBY$^+$22], but without the cell structure, metric, or the connection with the dual presentation. Our explicit description of the cell structure for $\text{POLY}_d^{mt}(\circledcirc)$ and the

induced structure on $\text{POLY}_d^{mt}(\bigcirc)$ will hopefully provide a useful bridge between the geometric combinatorics of polynomials and the geometry of the braid group.

Generalizations and conjectures. The metric cell structures for the polynomial spaces $\text{POLY}_d^{mt}(\square)$ and $\text{POLY}_d^{mt}(\circledcirc)$ presented in this article prompt several immediate generalizations and conjectures. First, we believe that the stratified Euclidean metric is non-positively curved in the following sense.

Conjecture 1. *The stratified Euclidean metric on the space POLY_d^{mt} of all monic degree-d complex polynomials up to translation is* $\text{CAT}(0)$.

This conjecture about a natural piecewise Euclidean metric on the space of all polynomials has consequences for the study of braid groups. It is not too difficult to show that for any fixed d, the space $\text{POLY}_d^{mt} = \text{POLY}_d^{mt}(\mathbb{C})$ is $\text{CAT}(0)$ if and only if $\text{POLY}_d^{mt}(\square)$ is $\text{CAT}(0)$, which is true if and only if $\text{POLY}_d^{mt}(\circledcirc)$ is locally $\text{CAT}(0)$. In other words, these three spaces have closely related curvature properties. Similarly, $\text{POLY}_d^{mt}(\rightarrowtail)$ is $\text{CAT}(0)$ if and only if $\text{POLY}_d^{mt}(\bigcirc)$ is locally $\text{CAT}(0)$. Finally, when the first three are (locally) $\text{CAT}(0)$ the last two are (locally) $\text{CAT}(0)$. This means, in particular, that proving Conjecture 1 for a particular d would establish the main conjecture in [BM10] for this d, and show that the d-strand braid group BRAID_d is a $\text{CAT}(0)$ group. We conjecture that this implication is reversible.

Conjecture 2. *The stratified Euclidean metric on the space POLY_d^{mt} is $\text{CAT}(0)$ if and only if the orthoscheme metric on the dual braid complex K_d is locally $\text{CAT}(0)$.*

One natural extension of our results comes from generalizing the algebraic labels on our cell structures. For each Coxeter group W, there is a corresponding Artin group A_W which is the fundamental group of the *orbit configuration space* Y_W— the long-standing $K(\pi, 1)$ *conjecture* for Artin groups claims that Y_W is always a classifying space for A_W. See Paolini's survey [Pao21] for background and [CD95, DPS22, Hua24, PS21] for progress on this problem.

In this article, we are concerned with the case where W is the symmetric group SYM_d, A_W is the braid group BRAID_d, and Y_W is the complement of the complex braid arrangement in $\mathbb{C}_d$. Moreover, Y_W is homeomorphic to $\text{POLY}_d^{mc}(\mathbb{C}_\mathbf{0})$. The linear and rectangular factorizations of δ defined in this series of articles generalizes to an arbitrary Coxeter group W, with δ replaced by a *Coxeter element* of W. By mimicking our construction of the branched annulus complex with algebraic cell labels, we are able to define a metric bisimplicial structure on a manifold with corners $\text{BR}_{W,\delta}^m(\circledcirc)$. By Theorems D, E and F, the space $\text{BR}_d^m(\circledcirc)$ is a compactification of $\text{POLY}_d^{mt}(\mathbb{C}_\mathbf{0})$. We conjecture that this holds for at least some class of more general Coxeter groups.

Conjecture 3. *Let W be a Coxeter group and let $\delta \in W$ be a Coxeter element. Then the bisimplicial complex $\text{BR}_{W,\delta}^m(\circledcirc)$ is a compactification of the orbit configuration space Y_W.*

The fundamental group of $\text{BR}_{W,\delta}^m(\circledcirc)$ is the "dual Artin group" $A_{W,\delta}^*$, which has played an important role in several recent advances in the study of Artin groups [DPS22, MS17, PS21] and is conjectured to be isomorphic to the standard Artin group A_W in all cases. If Conjecture 3 can be proved with a similar compactification to that of Theorem F, this would imply the isomorphism $A_{W,\delta}^* \cong A_W$.

Structure of the article. The article is divided into three parts. Part 1 describes the geometric and combinatorial data that can be extracted from a single monic complex polynomial. Part 2 shifts attention to spaces of polynomials and proves Theorems E, F and G. And in Part 3 we combine the results from Parts 1 and 2 to establish Theorems A, B, C and D about specific cell complexes. Although some of the content included here already exists in the literature, it is almost always written to handle much more general situations. These discussions are intended to make our results accessible to a broader audience.

Finally, it is important to note that the geometric combinatorics described in Part 1 is similar to but distinct from those described in the first article in the series. In [DM22] the polynomial p had to have *distinct roots* and the constructions used the *polar* coordinates of its (necessarily nonzero) critical values. Here the polynomial p is *arbitrary* and the constructions use the *rectangular* coordinates of its (possibly zero) critical values. A connection between the two versions is discussed in Section 15.
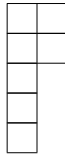
FIGURE 2. The Young diagram of the integer partition $\lambda = 2^2 1^3$.

Part 1. A Single Polynomial

The goal of Part 1 is to introduce 4 cell complexes constructed from a monic complex polynomial $p\colon \mathbb{C} \to \mathbb{C}$ with critical values in a fixed closed rectangle $\square$, and then to define a map based on the information they contain. The four complexes $\mathbf{P}_p$, $\mathbf{P}'_p$, $\mathbf{Q}_p$, and $\mathbf{Q}'_p$ focus on the regular points, critical points, regular values and critical values of p, respectively. The letter $\mathbf{P}$ stands for "polygon" and indicates a subdivided polygon in the domain. The letter $\mathbf{Q}$ stands for "quadrilateral" and indicates a subdivided rectangle in the range. The polynomial p sends the "point" complexes with a $\mathbf{P}$ to the "value" complexes with a $\mathbf{Q}$, and the "critical" complexes with primes are cellular duals of the "regular" complexes without primes. Since a cell complex and its dual contain essentially the same information, we are really just introducing two complexes in two different forms. In Part 3 we use the combinatorial structure of the regular point complex $\mathbf{P}_p$ and the metric structure of critical value complex $\mathbf{Q}'_p$ to construct compact piecewise Euclidean cell complexes.

Part 1 is structured as follows. Section 1 establishes conventions for combinatorial objects and maps. Section 2 does the same for polynomials and branched covers. Section 3 constructs the four complexes listed above. Section 4 reviews planar noncrossing combinatorics. And Section 5 defines a single map that collates the all of the geometric and combinatorial information extracted from monic polynomials.

1. Partitions and Multisets

This section records facts about basic combinatorial objects and the maps between them defined for any space $\mathbf{X}$. We begin with an example illustrating set partitions, multisets, and integer partitions, followed by the precise definitions.

Example 1.1 (Partitions and multisets). Let $\mathbf{X}$ be a space with five distinct points $a, b, c, d, e \in \mathbf{X}$ and consider the 7-tuple $\mathbf{x} = (a, b, a, c, d, c, e) \in \mathbf{X}^7$. The set partition recording which coordinates are equal is $[\lambda] = \{\{1, 3\}, \{2\}, \{4, 6\}, \{5\}, \{7\}\}$, or $13|2|46|5|7$. If we forget which entry came from which coordinate, the result is the 7-element multiset $M = \{a, a, b, c, c, d, e\} = \{a^2, b^1, c^2, d^1, e^1\}$, or $a^2 b^1 c^2 d^1 e^1$. The multiplicities of M, $\{2, 1, 2, 1, 1\}$, form a partition $\lambda = 2^2 1^3$ of the number 7, which can also be viewed as the sizes of the blocks of the set partition $[\lambda]$. See Figure 3. In symbols, $|M| = 7$ and $\lambda \vdash 7$. The Young diagram of λ is shown in Figure 2.

In this article, the structure of the space $\mathbf{X}$ is always extremely simple, and we indicate its shape using a visual shorthand.

Definition 1.2 (Visual shorthand). The symbol $\bigcirc$ is a visual shorthand for the closed unit disk $\mathbb{D}$ or, more generally, for any closed topological disk embedded as a subspace of $\mathbb{C}$, including $\square$, which is shorthand for a closed rectangle. Although

the intended meaning should be clear from context, it is also rarely necessary to sharply distinguish between the unit disk and a topological disk. See Corollary 10.3. Similarly, ◯ is the unit circle $\mathbb{T}$ (or any embedded circle), ⊷ is the closed unit interval $\mathbf{I} = [-1, 1]$ (or any embedded arc), and ◎ is the closed annulus formed by removing the open disk of radius $1/2$ from the closed unit disk $\mathbb{D}$ (or any embedded topological closed annulus). We write ▪, ◯, and ◉ for the points in the interior of ▢, ◯ and ◎ and ⊶ for the points in ⊷ other than its two endpoints. Finally, let ◯ denote the unit circle with the point -1 removed.

Remark 1.3 (Spaces)**.** The reader may assume that $\mathbf{X}$ is an elementary subset of $\mathbb{C}$, such as an interval ⊷, a rectangle ▢, a circle ◯, an annulus ◎, or $\mathbb{C}$ itself. In particular, $\mathbf{X}$ is a path-connected locally Euclidean Riemannian manifold of dimension $m > 0$, possibly with boundary and possibly with corners.

Definition 1.4 (Set partitions)**.** Let $[n] = \{1, 2, \ldots, n\}$. A *set partition of* $[n]$ is a partition of $[n]$ into pairwise disjoint nonempty subsets whose union is $[n]$. There is a standard shorthand notation for a set partition when n is small. Commas and brackets are removed, the elements in each block are listed in increasing order, and the blocks, separated by vertical bars, are listed in increasing order of their minimal elements. See Example 1.1. We write $\mathrm{SETPART}_n$ to denote the collection of all set partitions of $[n]$ partially ordered by refinement. The poset $\mathrm{SETPART}_n$ is also known as the (set) *partition lattice.* Its unique minimum element is the *discrete set partition* $1|2|\cdots|n$ with n blocks of size 1, and its unique maximum element is the *indiscrete set partition* $12\cdots n$ with 1 block of size n.

We often write $[\lambda] \vdash [n]$ as notation for a set partition to highlight the parallel with integer partitions, but it needs to be used with caution. See Remark 1.11.

Definition 1.5 (Multisets)**.** A (finite) *multiset* $M = (S, m)$ is a finite set S together with a *multiplicity function* $m \colon S \to \mathbb{N} = \{1, 2, \ldots\}$. The number $m(x)$ is the *multiplicity of* $x \in S$. A (finite) multiset can be concisely described using the notation $M = \{x_1^{m_1}, x_2^{m_2}, \ldots, x_k^{m_k}\}$ where the underlying set is $S = \{x_1, \ldots, x_k\}$, with $x_i = x_j$ if and only if $i = j$, and where the exponent $m_i = m(x_i)$ denotes the multiplicity of the element x_i. In the shorthand notation, the commas and braces are removed. All multisets in this article are finite and we drop the adjective. The *size* of a multiset is the sum of its multiplicities: $|M| = |M|_{\mathrm{MULT}} = n = \sum_i m_i$. This is the unmarked notion of size for multisets. The number of distinct elements in M is the *size of M as a set*: $|M|_{\mathrm{SET}} = |S| = k$ where $S = \mathrm{SET}(M)$. When $|M| = n$, M is an *n-element multiset*, and when its elements are in $\mathbf{X}$, it is a *multiset in* $\mathbf{X}$. The collection $\mathrm{MULT}_n(\mathbf{X})$ of all n-element multisets in $\mathbf{X}$ can also be viewed as $\mathrm{SYM}_n \backslash \mathbf{X}^n$, the orbits in $\mathbf{X}^n$ under the coordinate permuting symmetric group action, since being able to permute the coordinates makes their order irrelevant. Given our assumption on spaces (Remark 1.3) $\mathbf{X}^n$ a locally Euclidean manifold of dimension mn where $m = \dim(\mathbf{X})$, possibly with boundary and/or corners. The topology on $\mathrm{MULT}_n(\mathbf{X})$ comes from the quotient map $\mathbf{X}^n \to \mathrm{MULT}_n(\mathbf{X}) = \mathbf{X}^n / \mathrm{SYM}_n$. In this article, $\mathbf{X}$ is always a subset of $\mathbb{C}$, so all multisets have elements in $\mathbb{C}$, and MULT_n is used as shorthand for $\mathrm{MULT}_n(\mathbb{C})$. In general, we omit arguments in this manner only when the argument is all of $\mathbb{C}$.

Definition 1.6 (Integer partitions)**.** A *partition of a positive integer n* can be viewed as a multiset of positive integers whose sum is n, but care is required since

$$\mathbf{x} = (a, b, a, c, d, c, e) \longrightarrow [\lambda] = 13|2|46|5|7 \qquad\qquad \mathbf{X}^n \longrightarrow \text{SetPart}_n$$

$$\downarrow \qquad\qquad\qquad\qquad\qquad \downarrow \qquad\qquad\qquad\qquad \downarrow \qquad\qquad \downarrow$$

$$M = a^2 b^1 c^2 d^1 e^1 \longrightarrow \lambda = 2^2 1^3 \qquad\qquad \text{Mult}_n(\mathbf{X}) \longrightarrow \text{IntPart}_n$$

FIGURE 3. An n-tuple $\mathbf{x} \in \mathbf{X}^n$ determines a set partition $[\lambda] \vdash [n]$ in SetPart_n, an n-element multiset $M \in \text{Mult}_n(\mathbf{X})$, and an integer partition $\lambda \vdash n$ in IntPart_n. In the example $n = 7$.

partitions and multisets have distinct standard terminology. Let λ be a multiset of k positive integers whose sum is n. The elements of λ are its *parts*, the number k is its *length* and the number n is its *size*. We write $\text{len}(\lambda) = k$ and $\lambda \vdash n$. Note that the length of λ (as a partition) is its size as a multiset, and its size (as a partition) is its sum. The parts of a partition are typically listed in weakly decreasing order, summarized using exponents, and visualized using Young diagrams as in Example 1.1. Concretely, a typical partition is of the form $\lambda = \lambda_1^{a_1} \lambda_2^{a_2} \cdots \lambda_\ell^{a_\ell}$, where $\lambda_1 > \lambda_2 > \cdots > \lambda_\ell$ are its ℓ distinct parts, the number a_i indicates the number of times the part λ_i occurs, its length $k = a_1 + \cdots + a_\ell$ is the total number of parts, and its size $n = \sum_{i=1}^\ell a_i \cdot \lambda_i$ is the sum of its parts. We write IntPart_n to denote the collection of all integer partitions of n.

The maps in Figure 3 form a commuting square, and they are defined as follows.

Definition 1.7 (Maps). The map $\mathbf{X}^n \to \text{SetPart}_n$ sends each n-tuple $\mathbf{x}$ to the set partition $[\lambda]$ recording which of its coordinates are equal. The map $\mathbf{X}^n \to \text{Mult}_n(\mathbf{X})$ sends each n-tuple $\mathbf{x}$ to its multiset M of coordinates. The map $\text{Mult}_n(\mathbf{X}) \to \text{IntPart}_n$ sends a multiset M to its multiset of multiplicities. And the map $\text{SetPart}_n \to \text{IntPart}_n$ sends the set partition $[\lambda]$ to the multiset of its blocks sizes. The vertical maps are always onto and the horizontal maps are onto since $\mathbf{X}$ has infinitely many elements (Remark 1.3). For the top and left maps, we name the maps by their output, writing $M = \text{Mult}(\mathbf{x})$ and $[\lambda] = \text{SetPart}(\mathbf{x})$. For the three maps (horizontal, vertical and implicit diagonal) that end at IntPart_n, we describe λ as the *shape of M*, the *shape of $[\lambda]$* and the *shape of $\mathbf{x}$*. and write $\lambda = \text{Shape}(M) = \text{Shape}([\lambda]) = \text{Shape}(\mathbf{x})$. The common name for these maps is unambiguous in practice since the object being evaluated determines the domain.

Remark 1.8 (Functions). The elements of the four spaces in Figure 3 can also be interpreted as functions. A point $\mathbf{x} \in \mathbf{X}^n$ corresponds to a function $f \colon [n] \to \mathbf{X}$, and note that both the domain and range have distinguishable elements. If we make the elements of the domain / the range / both the domain and the range indistinguishable, then f carries less information, and the remaining information is captured by the multiset M / the set partition $[\lambda]$ / the shape λ.

The integer partitions of n can be viewed as a poset or as an acyclic category.

Remark 1.9 (Acyclic categories). An *acyclic category* is a category where (1) the only arrows starting and ending at the same object are the identity arrows, and (2) if there is a nonidentity arrow f from a to b, there is no arrow from b to a. Acyclic categories are to posets as Hatcher's Δ-complexes are to simplicial complexes. Every poset can be viewed as an acyclic category by using the elements as objects and drawing a single arrow $p \to q$ if and only if $p \leq q$. In the other
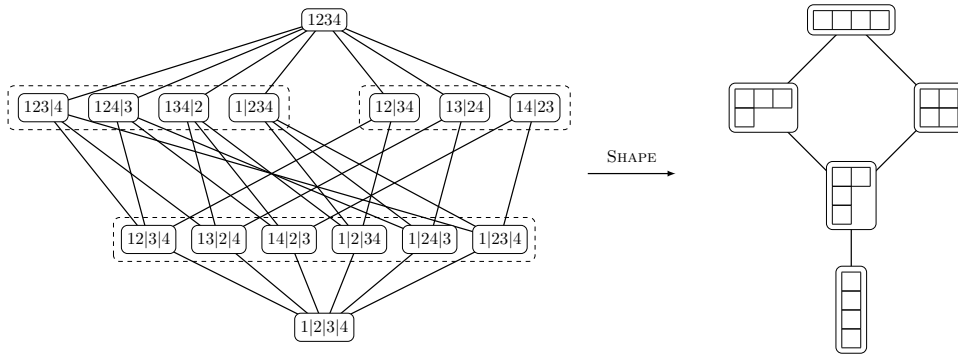
FIGURE 4. The poset homomorphism SHAPE from the 15 element poset SETPART$_4$ to the 5 element poset INTPART$_4$. The dashed lines enclose set partitions sent to the same integer partition.

direction, every acyclic category has an underlying poset structure by defining $p \leq q$ if there exists an arrow $p \to q$. Note that sequentially applying both constructions to a poset reproduces the origin poset, but applying both constructions to an acyclic category produces a quotient category where all arrows with the same endpoints have been identified. Acyclic categories were introduced by Andre Haefliger under the name "small categories without loops" to study complexes of groups [Hae91]. See also [BH99]. The "acyclic category" terminology is from [Koz08].

Definition 1.10 (Ordering integer partitions). If λ is an integer partition and π is a partition of the parts of λ then there is a new partition μ whose parts are the sums of the numbers in the blocks of π. We write $\lambda \xrightarrow{\pi} \mu$, or simply $\lambda \to \mu$ when the partition π is implicitly understood. If $\lambda = 3^1 2^1 1^2 \vdash 7$ and $\pi = \{\{3, 2\}, \{1, 1\}\}$, for example, then $\mu = 5^1 2^1$. Note that multiple arrows can exist with the same endpoints. In our example, $\pi' = \{\{3, 1, 1\}, \{2\}\}$ is a distinct partition that also turns λ into μ. The collection of all arrows of this form turn the set INTPART$_n$ into an acyclic category. And it can be simplified to its underlying poset structure by defining $\lambda \leq \mu$ if there exists a partition π with $\lambda \xrightarrow{\pi} \mu$. With this partial order INTPART$_n$ becomes a bounded graded poset. It is bounded below by the *discrete partition* $\lambda = 1^n$, bounded above by the *indiscrete partition* $\lambda = n^1$ and the grading is determined by the number of parts. The map SHAPE from SETPART$_n$ to INTPART$_n$ can be viewed as a functor between acyclic categories, which simplifies to an order-preserving rank-preserving poset homomorphism if the acyclic category structure on INTPART$_n$ is replaced with its underlying poset structure. See Figure 4.

The acyclic category of integer partitions is used to index stratifications of polynomial spaces. See Section 7.

Remark 1.11 (Set partition notation). Although we write $[\lambda] \vdash [n]$ to denote a set partition of shape $\lambda \vdash n$, the reader should note that this notation is ambiguous. In Figure 4, for example, there are 4 distinct set partitions of shape $3^1 1^1$, and $[3^1 1^1]$ could refer to any one of them. There is no such ambiguity at either extreme since the discrete set partition $1|2|\cdots|n$, with n blocks of size 1, is the unique set partition of shape 1^n and the indiscrete set partition $12 \cdots n$, with 1 block of size n, is the unique set partition of shape n^1.

2. Polynomials and Branched Covers

This section records basic facts about polynomials (2.1), branched covers between surfaces (2.2), and planar branched covers between disks (2.3).

2.1. **Polynomials.** For any $U \subset \mathbb{C}$, let $\mathbb{C}_U$ be the complement $\mathbb{C} \setminus U$, so that $\mathbb{C}_{\mathbf{0}}$ is $\mathbb{C}^*$ with $\mathbf{0} = \{0\}$. Let $\mathbb{D}$ be the closed unit disk with unit circle boundary $\mathbb{T} = \partial\mathbb{D}$.

Definition 2.1 (Polynomials). For each $d \in \mathbb{N}$, let $\mathrm{POLY}_d \subset \mathbb{C}[z]$ be the collection of *complex polynomials of degree d*. Concretely, for $p \in \mathrm{POLY}_d$, we write $p(z) = c_0 z^d + c_1 z^{d-1} + \cdots + c_{d-1} z + c_d$ with $c_0 \in \mathbb{C}_{\mathbf{0}}$ and $c_i \in \mathbb{C}$ for $i \in [d]$. The polynomial p is *monic* if $c_0 = 1$ and *centered* if $c_1 = 0$. Let POLY_d^m be the subspace of monic polynomials and let POLY_d^{mc} be the subspace of monic, centered polynomials. Using *coefficient coordinates*, there are natural homeomorphisms $\mathrm{POLY}_d^m \cong \mathbb{C}^d$ and $\mathrm{POLY}_d^{mc} \cong \mathbb{C}^n$ where $n = d - 1$.

Definition 2.2 (Points and values). Let $p \colon \mathbb{C} \to \mathbb{C}$ be a degree-d polynomial. The roots of the derivative p' form an n-element multiset (where $n = d - 1$) called the *critical points* of p. In symbols, if $p'(z) = d \cdot c_0 \cdot (z - z_1)^{n_1} \cdots (z - z_k)^{n_k}$, then $\mathbf{cpt} = \mathbf{cpt}(p) = \{z_1^{n_1}, \ldots, z_k^{n_k}\}$. The z_i are the k critical points, the $n_i = n_{z_i}$ are their multiplicities, and we typically order the z_i so that the n_i are weakly decreasing. Note that $n = n_1 + \cdots + n_k = d - 1$ is the size of $\mathbf{cpt}$. The *critical values* of p are the images of the critical points, and the n-element multiset $\mathbf{cvl} = \mathbf{cvl}(p)$ is $p(\mathbf{cpt})$. The points in the domain and the values in the range that are not critical are *regular points* and *regular values*. A subset is *regular* if every element is regular. Finally, denote the full preimage of $\mathbf{cvl}$ by $\mathbf{cpt}^+ = \{z_1, \ldots, z_m\} = p^{-1}(\mathbf{cvl})$, where $m \geq k$. If $m > k$, the regular points in $\mathbf{cpt}^+$ are listed at the end. We still have $n_1 + \cdots + n_m = n$ since $n_i = 0$ for regular points.

The following polynomial is going to be our running example throughout Part 1.

Example 2.3. Let p be the complex polynomial

$$z^5 + \left(\frac{-17 + 6i}{4}\right) z^4 + \left(\frac{73 - 63i}{15}\right) z^3 + \left(\frac{34 - 12i}{25}\right) z^2 + \left(\frac{-308 + 252i}{125}\right) z.$$

Its critical points are $\mathbf{cpt}(p) = \{-\frac{2}{5}, \frac{2}{5}, \frac{7-7i}{5}, \frac{10+i}{5}\}$, all with multiplicity 1, and its (rounded) critical values are $\mathbf{cvl}(p) \approx \{.8 - .6i, -.6 + .5i, -8.5 - 4.3i, 3.6 - 6.9i\}$, again all with multiplicity 1. The critical values are listed in the same order as the critical points: for example, $p(\frac{2}{5}) \approx -.6 + .5i$. Figure 7 on page 20 shows the range of p with its 4 critical values marked as yellow dots. Figure 10 on page 25 shows the domain of p with its 4 critical points marked as yellow dots.

Polynomials are examples of planar branched covers, and general branched covers are locally modeled on degenerate polynomials.

Definition 2.4 (Degenerate polynomials). The polynomial $p(z) = a \cdot (z - b)^d + c$ of degree $d > 1$ is *degenerate* in the sense that both its critical point multiset $\mathbf{cpt}(p) = \{b^n\}$ and its critical value multiset $\mathbf{cvl}(p) = \{c^n\}$ are indiscrete, and as far from generic as possible. Regular values have d point preimages under p, but the critical value c has only one, so c has $n = d - 1$ missing preimages. The *power polynomial* $p \colon \mathbb{C} \to \mathbb{C}$ with $p(z) = z^d$ is the identity when $d = 1$ and degenerate for $d > 1$.

$$
\begin{array}{ccc}
X \xrightarrow{\ p\ } Y & \qquad & Z \xrightarrow{\ p\ } W \\
\uparrow{\scriptstyle f} \quad \downarrow{\scriptstyle g} & \qquad & \uparrow{\scriptstyle h} \quad \| \\
Z \xrightarrow{\ q\ } W & \qquad & Z \xrightarrow{\ q\ } W
\end{array}
$$

FIGURE 5. The maps p and q on the left look alike. The maps p and q on the right are topologically equivalent. The three labeled vertical maps are homeomorphisms, and both squares commute.

Definition 2.5 (Branched even coverings). Let $\mathbf{d} = (d_1, \ldots, d_m) \in \mathbb{N}$ be an m-tuple of natural numbers with sum $d = d_1 + \cdots + d_m$. Let $\mathbf{p_d} \colon \mathbf{Z} \to \mathbf{W}$ be the map where $\mathbf{W} = \mathbb{D}$, $\mathbf{Z} = \bigsqcup_{i \in [m]} \mathbb{D}$ is a disjoint union of m copies of the closed unit disk $\mathbb{D}$, and the ith component map $\mathbf{p}_i \colon \mathbb{D} \to \mathbb{D}$ is the power map $\mathbf{p}_i(z) = z^{d_i}$. And let $p_{\mathbf{d}} \colon Z \to W$ be the map from the interior of the domain to the interior of the range. When $\mathbf{d} = \mathbf{1} = (1, 1, \ldots, 1)$, each p_i is a homeomorphism and $p_{\mathbf{d}}$ is the prototypical *even covering* used to define a (finite sheeted) covering map. For general $\mathbf{d}$ we say that $p_{\mathbf{d}}$ is a *branched even covering*. When a degenerate component map exists, $0 \in W$ is a (unique) critical value and its multiplicity is $d - m$. The critical points are at the origin in components where the component map is degenerate.

2.2. **Branched covers.** Branched covers are surface maps that locally look like branched even covers. Here is what we mean by "surface" and "looks like".

Definition 2.6 (Surfaces). Unless otherwise stated, all surfaces in this article are either closed compact oriented 2-dimensional manifolds, possibly with boundary, or open surfaces homeomorphic to the interior of one of our closed surfaces. We use boldface letters for closed surfaces, non-bold letters for open surfaces, and the same letter for a closed surface and its open interior, i.e. a closed surface $\mathbf{Z}$ has interior Z. For a connected closed surface $\mathbf{Z}$, let $\widehat{\mathbf{Z}}$ be the closed surface without boundary obtained by attaching a disk to each circle of $\partial \mathbf{Z}$. If $\widehat{\mathbf{Z}}$ has genus g, then we say $\mathbf{Z}$ has genus g. The *Euler characteristics* are $\chi(\widehat{\mathbf{Z}}) = 2 - 2g$ and $\chi(\mathbf{Z}) = \chi(Z) = 2 - 2g - b$ where b is the number of components of $\partial \mathbf{Z}$. In particular, for connected closed surfaces, $\chi(\mathbf{Z}) = 1$ if and only if $\mathbf{Z}$ is a closed disk with $g = 0$, $b = 1$.

Definition 2.7 (Maps). For maps between surfaces we make a standing assumption that the range is always connected, but the domain is allowed to be disconnected. Note, however, that the number of connected components for any surface considered here is finite. Let $\mathbf{q} \colon \mathbf{Z} \to \mathbf{W}$ be a map between surfaces. A *component map of* $\mathbf{q}$ is a restriction of $\mathbf{q}$ to a component of its domain. If these have been indexed, $\mathbf{q}_i$ is the restriction of $\mathbf{q}$ to the ith component $\mathbf{Z}_i$.

Definition 2.8 (Equivalent maps). We say that a map $q \colon Z \to W$ *looks like* a map $p \colon X \to Y$ if there are homeomorphisms $f \colon Z \to X$ and $g \colon Y \to W$ such that $q = g \circ p \circ f$. There is also a more restricted notion when $X = Z$ and $Y = W$ and the homeomorphism of the range must be the identity map. We say that q is *topologically equivalent* to p if there is a self-homeomorphism $h \colon Z \to Z$ of the domain so that $q = p \circ h$. In the language of [LZ04], the first version is a *flexible* notion of equivalence, and the second is a *rigid* one. See Figure 5.

Definition 2.9 (Branched covers). Let $q \colon Z \to W$ be a map between open surfaces (Definition 2.6). Let $D \subset W$ be an open disk and let $C = q^{-1}(D)$ be its preimage.

We say that D is *branched evenly covered* if the restricted map $q\colon C \to D$ looks like (Definition 2.8) a branched even covering map $p_{\mathbf{d}}$ for some tuple $\mathbf{d}$ (Definition 2.5). The map q is an *(open) branched covering map* if every point $w \in W$ has a neighborhood D which is branched evenly covered. For maps $\mathbf{q}\colon \mathbf{Z} \to \mathbf{W}$ between closed surfaces (Definition 2.6), we say that $\mathbf{q}$ is a *(closed) branched covering map* if it restricts to an open branched cover $q\colon Z \to W$ on the interiors and an ordinary covering map $\partial\mathbf{q}\colon \partial\mathbf{Z} \to \partial\mathbf{W}$ on the boundaries. Not only do closed branched covers restrict to open branched covers, but every open branched cover (of the open surfaces being considered) extends to a closed branched cover.

Branched covering maps retain many properties of ordinary covering maps.

Lemma 2.10 (Surjective maps). *If $\mathbf{q}\colon \mathbf{Z} \to \mathbf{W}$ is a branched cover, then $\mathbf{q}$ is surjective. In particular, for any $w \in \mathbf{W}$, the natural map that sends a preimage of w to the (index of the) component containing it is onto.*

Proof. Let $\mathbf{Z}_1$ be a component of $\mathbf{Z}$ with $z_1 \in \mathbf{Z}_1$ and $w_1 = \mathbf{q}(z_1)$. Since $\mathbf{W}$ is connected (Definition 2.7), for any $w_2 \in \mathbf{W}$ there is a regular path β from a value near w_1 to a value near w_2, where "near" means in a branched evenly covered neighborhood D_i of w_i. Once β is lifted to start in the component of $\mathbf{q}^{-1}(D_1)$ containing z_1, it ends in a component of $\mathbf{q}^{-1}(D_2)$ containing a lift of w_2. $\qquad\square$

Definition 2.11 (Branch points). Let $q\colon Z \to W$ be an open branched cover. By definition, every $z \in Z$ has an open disk neighborhood sent to an open disk neighborhood containing $w = q(z)$ that looks like a power map $p(z) = z^d$ for some unique $d = d_z$. The positive integer d_z is the *degree of z* and the nonnegative integer $n_z = d_z - 1$ is the *multiplicity of z*. When $d_z = 1$ and $n_z = 0$, $p(z) = z$ is the identity map and q is a local homeomorphism near z. When $d_z > 1$ and $n_z > 0$, the point z is a *branch point of multiplicity n_z*. Branch points are also called *critical points* or *ramification points*. The critical values, regular values, regular points, and the preimage set $\mathbf{cpt}^+$ of q are defined exactly as in Definition 2.2. For closed branched covers $\mathbf{q}\colon \mathbf{Z} \to \mathbf{W}$, the points $z \in \partial\mathbf{Z}$, being regular, have degree $d_z = 1$ and multiplicity $n_z = 0$.

A polynomial is a branched cover, its critical points are its branch points, and the two notions of multiplicity agree, so the rest of the terminology is also consistent. Globally, a branched cover is a covering map away from finitely many points.

Definition 2.12 (Degree and metric). Let $\mathbf{q}\colon \mathbf{Z} \to \mathbf{W}$ be a closed branched cover. If $V = \textsc{Set}(\mathbf{cvl}) \subset W$ is the set of critical values and $U = \mathbf{q}^{-1}(V) = \mathbf{cpt}^+ \subset Z$ is the full set of preimages, then the restricted map $\mathbf{q}\colon (\mathbf{Z}\setminus U) \to (\mathbf{W}\setminus V)$ is a covering map. Moreover, since $\mathbf{W}$ is connected (Definition 2.7), $\mathbf{W} \setminus V$ is connected, and $\mathbf{q}$ has a constant *global degree d*, making $\mathbf{q}$ a *d-branched cover*. Branched covers are also called *ramified covers*. And note that if $\mathbf{W}$ has a metric, there is a unique *induced metric* on $\mathbf{Z}$ so that $\mathbf{q}$ is a local isometry except at $\mathbf{cpt}$.

Remark 2.13 (Riemann–Hurwitz formula). Let $\mathbf{q}\colon \mathbf{Z} \to \mathbf{W}$ be a d-branched cover. If $m = |\mathbf{cpt}^+|$ and $\ell = |\mathbf{cvl}|_{\textsc{Set}}$, then $\mathbf{q}$ satisfies the *Riemann–Hurwitz formula*: $(\chi(\mathbf{Z}) - m) = d \cdot (\chi(\mathbf{W}) - \ell)$, because Euler characteristic is multiplicative for covering maps.

Lemma 2.14 (Disk preimages). *If $\mathbf{q}\colon \mathbf{Z} \to \mathbf{W}$ is a closed branched cover where $\mathbf{Z}$ is connected and $\mathbf{W}$ is a closed disk with one critical value, then $\mathbf{Z}$ is a closed disk*

with one critical point. Similarly, if $q \colon Z \to W$ is an open branched cover where Z is connected and W is an open disk with one critical value, then Z is an open disk with one critical point.

Proof. Open branched covers extend to closed branched covers in our setting, so we only need to prove the closed version. Let g be the genus of $\mathbf{Z}$, let b be the number of components of $\partial\mathbf{Z}$ and let $m = |\mathbf{cpt}^+|$. Since $\chi(\mathbf{W}) = 1$ and $|\mathbf{cvl}|_{\mathrm{SET}} = 1$, we have $\chi(\mathbf{Z}) = |\mathbf{cpt}^+|$ by Remark 2.13, so $2-2g-b = m$ and therefore $2 = 2g+b+m$. We know that $g \geq 0$ by definition, $b > 0$ because $\partial\mathbf{Z} = \mathbf{q}^{-1}(\partial\mathbf{W})$ is nonempty, and $m > 0$ because $\mathbf{q}$ has at least one critical point, so the only solution is $g = 0$ and $b = m = 1$, making $\mathbf{Z}$ a closed disk. $\square$

Lemma 2.15 (Degree and preimages)**.** *Let $\mathbf{q} \colon \mathbf{Z} \to \mathbf{W}$ be a d-branched cover. For any $w \in \mathbf{W}$, the sum of the degrees of its preimages is d.*

Proof. Let $\mathbf{q}^{-1}(w) = \{z_1, \ldots, z_m\}$ and let d_i be the degree of z_i. Let D be a branched evenly covered neighborhood of w with preimage $C = \mathbf{q}^{-1}(D)$. The $\sum d_i$ must be equal to d since any regular point in D has d_i preimages in the component of C containing z_i, and d preimages total. $\square$

Lemma 2.16 (Degree and multiplicity)**.** *If $\mathbf{q} \colon \mathbf{Z} \to \mathbf{W}$ is a d-branched cover and n is the common size of the multisets $\mathbf{cpt}$ and $\mathbf{cvl}$, then $n + \chi(\mathbf{Z}) = d \cdot \chi(\mathbf{W})$. In particular, when $\mathbf{W}$ is a disk and $\mathbf{Z}$ is a disjoint union of b disks, $n + b = d$.*

Proof. Suppose $U = \mathbf{cpt}^+ = \{z_1, \ldots, z_m\}$ and $V = \mathrm{SET}(\mathbf{cvl}) = \{w_1, \ldots, w_\ell\}$. The sum of the degrees of the z_i is $\sum_i d_i = \sum_i (n_i + 1) = n + m$. By Lemma 2.15, the sum of degrees of $q^{-1}(w_j) = d$ for each $j \in [\ell]$, so the sum of the degrees of the z_i is $d \cdot \ell$. Thus $n + m = d \cdot \ell$. By Remark 2.13, $(\chi(\mathbf{Z}) - m) = d \cdot (\chi(\mathbf{W}) - \ell)$. Adding these two equations completes the proof. $\square$

These results hold, of course, for our running example.

Example 2.17. The polynomial p of Example 2.3 has degree $d = 5$ and multiplicity $n = 4$ (Lemma 2.16). It has 4 critical values, so $|V| = |\mathbf{cvl}|_{\mathrm{SET}} = 4$. Each critical value has 4 preimages, one critical point of degree 2 and three regular points of degree 1, so the sum of the degrees of every value is 5 (Lemma 2.15) and $|U| = |\mathbf{cpt}^+| = 16$. Finally, the domain and range are $\mathbb{C}$ with $\chi(\mathbb{C}) = 1$, so the Riemann–Hurwitz formula (Remark 2.13) is satisfied since $(1 - 16) = 5 \cdot (1 - 4)$.

2.3. **Planar branched covers.** We now restrict attention to branched covers between subsurfaces of spheres.

Definition 2.18 (Surfaces in spheres)**.** For any closed surface $\mathbf{W} \subset \mathbb{C} \subset \widehat{\mathbb{C}} = \mathbb{C}P^1$ with interior W, let $\beta = \partial\mathbf{W}$ be the union of its simple closed boundary curves, let W^c be the complement of $\mathbf{W}$ in $\widehat{\mathbb{C}}$ and let $\mathbf{W}^c = W^c \sqcup \beta$ be the closed surface which is the complement of W in $\widehat{\mathbb{C}}$. We call $\mathbf{W}^c$ the *closed complement of* $\mathbf{W}$. Note that $\widehat{\mathbb{C}} = W \sqcup \beta \sqcup W^c = \mathbf{W} \cup \mathbf{W}^c$, and $\mathbf{W}$ is a closed disk if and only if β is a Jordan curve if and only if $\mathbf{W}^c$ is a closed disk. More generally, $\mathbf{W}$ is a disjoint union of closed disks if and only if its closed complement $\mathbf{W}^c$ is connected.

Definition 2.19 (Planar branched covers)**.** A *(closed) planar branched cover* is a branched cover $\mathbf{q} \colon \mathbf{Z} \to \mathbf{W}$ where $\mathbf{Z}$ and $\mathbf{W}$ are closed disks, and an *(open) planar branched cover* is a branched cover $q \colon Z \to W$ where Z and W are open disks.

Closed planar branched covers restrict to open planar branched covers and every open planar branched cover extends to a closed planar branched cover. Also, open planar branched covers look like branched covers $p\colon \mathbb{C} \to \mathbb{C}$, hence the name. Closed planar branched covers look like branched covers $\mathbf{p}\colon \mathbb{D} \to \mathbb{D}$. A planar branched cover with only one critical point is *degenerate*.

Example 2.20 (Degenerate branched covers). The map $p\colon \mathbb{C} \to \mathbb{C}$ defined by $p(z) = z^d$ extends to a map $\widehat{p}\colon \widehat{\mathbb{C}} \to \widehat{\mathbb{C}}$, where $\widehat{\mathbb{C}} = \mathbb{C}P^1$. The map $\widehat{p}$ preserves the decomposition $\widehat{\mathbb{C}} = \mathbb{D} \cup \mathbb{D}^c$, so it splits into two degenerate planar d-branched covers $\mathbf{p}\colon \mathbb{D} \to \mathbb{D}$ and $\mathbf{p}^c\colon \mathbb{D}^c \to \mathbb{D}^c$ with critical points 0 and ∞, respectively, that overlap on the d-fold cover $\partial\mathbf{p}\colon \mathbb{T} \to \mathbb{T}$.

Complex polynomials form the most natural examples of open planar branched covers, and in the sense described below, the two notions actually coincide.

Remark 2.21 (Polynomials and Branched Covers). Let $[p]_{\text{top}}$ denote the topological equivalence class of a planar branched cover $p\colon \mathbb{C} \to \mathbb{C}$ presented in Definition 2.8. When $p, q\colon \mathbb{C} \to \mathbb{C}$ are complex polynomials, we say that p and q are *linearly equivalent* if there is a linear function $h(z) = az + b$ so that $p = q \circ h$, i.e. $p(z) = q(az + b)$. Let $[p]_{\text{lin}}$ denote the linear equivalence class of a complex polynomial p. Since polynomials are planar branched covers and linear maps are homeomorphisms, there is a well defined function $[p]_{\text{lin}} \mapsto [p]_{\text{top}}$ from polynomials up to linear equivalence to planar branched covers up to topological equivalence. In fact, this function is a bijection: every planar branched cover $p\colon \mathbb{C} \to \mathbb{C}$ is topologically equivalent to a polynomial (surjectivity), and two polynomials that are topologically equivalent are linearly equivalent (injectivity). See [LZ04, Chapter 1].

Definition 2.22 (Spherical branched covers). A *spherical branched cover* is a branched cover $\widehat{\mathbf{q}}\colon \widehat{\mathbf{Z}} \to \widehat{\mathbf{W}}$ where $\widehat{\mathbf{Z}}$ and $\widehat{\mathbf{W}}$ are 2-spheres. Every planar d-branched cover $\mathbf{q}\colon \mathbf{Z} \to \mathbf{W}$ extends to a spherical d-branched cover $\widehat{q}\colon \widehat{\mathbf{Z}} \to \widehat{\mathbf{W}}$ by attaching the degenerate planar d-branched cover $\mathbf{p}^c\colon \mathbb{D}^c \to \mathbb{D}^c$ (Example 2.20) to the boundaries. This completes $\mathbf{Z}$ to $\widehat{\mathbf{Z}}$ and $\mathbf{W}$ to $\widehat{\mathbf{W}}$, and $\mathbf{p}^c$ agrees with $\mathbf{q}$ on the boundary map $\partial\mathbf{q}\colon \partial\mathbf{Z} \to \partial\mathbf{W}$. In the other direction, if $\widehat{\mathbf{q}}\colon \widehat{\mathbf{Z}} \to \widehat{\mathbf{W}}$ is a spherical branched cover and there is a point $w^c \in \widehat{\mathbf{W}}$ with only one preimage $z^c \in \widehat{\mathbf{Z}}$, then removing a branched evenly covered neighborhood W^c of w^c and its preimage Z^c containing z^c leaves a planar d-branched cover.

Example 2.23 (Non-disk preimages). Let $\mathbf{W}$ be a closed disk in $\widehat{\mathbb{C}}$ that does not contain 0 or ∞, and let $\mathbf{W}^c$ be its closed disk complement. Under $\widehat{p}$, the spherical d-branched cover of Example 2.20, the preimage $\mathbf{Z}$ of $\mathbf{W}$ is d disjoint topological disks since $\mathbf{W}$ is regular and the preimage $\mathbf{Z}^c$ of $\mathbf{W}^c$ is a connected surface with d boundary components. In particular, $\mathbf{Z}^c$ is not a disk, even though $\mathbf{W}^c$ is a disk.

The preimage of a disk under a spherical branched cover need not be a disk, but the preimage under a planar branched cover is a union of disks.

Proposition 2.24 (Disks and preimages). *Let $\mathbf{p}\colon \mathbb{D} \to \mathbb{D}$ be a closed planar branched cover and let $\mathbf{W}$ be a closed disk in the range. If $\partial\mathbf{W}$ is regular, then $\mathbf{Z} = \mathbf{p}^{-1}(\mathbf{W})$ is a disjoint union of b closed disks $\mathbf{Z}_i$, its closed complement $\mathbf{Z}^c$ is connected, and its boundary $\partial\mathbf{Z}$ is a set of disjoint nonnested simple closed curves. Moreover, the component maps $\mathbf{p}_i\colon \mathbf{Z}_i \to \mathbf{W}$ are closed planar branched covers, and*

the number of components b is equal to $d - n_w$, where n_w is the total multiplicity of the critical values in $\mathbf{W}$.

Proof. Since $\partial \mathbf{W}$ is regular, its preimage $\partial \mathbf{Z}$ is a collection of simple closed curves, and $\mathbf{Z}^c = \widehat{\mathbf{p}}^{-1}(\mathbf{W}^c)$ is a closed submanifold in $\widehat{\mathbb{C}}$ with $\infty \in \mathbf{Z}^c$. Since ∞ is the only preimage of ∞ (Definition 2.22), $\mathbf{Z}^c$ is connected (Lemma 2.10), so $\mathbf{Z} = \mathbf{Z}_1 \sqcup \cdots \sqcup \mathbf{Z}_k$ is disjoint union of disks (Definition 2.18). The restricted maps $\mathbf{p}_i \colon \mathbf{Z}_i \to \mathbf{W}$ between spaces homeomorphic to $\mathbb{D}$ is itself a branched cover since it still satisfies the required conditions: local conditions are local, a connected component of a cover is a cover, and the boundary map is a covering. And $b = d - n_w$ by Lemma 2.16. $\square$

3. Cell Complexes and Cellular Maps

Given a branched cover $p \colon \mathbb{C} \to \mathbb{C}$ and a rectangle $\square$ in the range, we use the critical values $\mathbf{cvl}(p)$ to define 4 complexes: two coordinate complexes $\mathbf{Q}_p$ and $\mathbf{Q}'_p$ in the range and two branched coordinate complexes $\mathbf{P}_p$ and $\mathbf{P}'_p$ in the domain. The focus here is on rectangular coordinates, but similar constructions using polar coordinates were given in the first paper in this series [DM22]. After defining the coordinate complexes $\mathbf{Q}_p$ and $\mathbf{Q}'_p$ in the range (3.1), we record the properties of branched cellular maps (3.2) that make it possible to define the branched coordinate complexes $\mathbf{P}_p$ and $\mathbf{P}'_p$ in the domain (3.3).

3.1. **Complexes in the range.** The constructions in the range are very straight-forward since we are simply subdividing a rectangle $\square$ vertically and horizontally through the critical values of p in the case of $\mathbf{Q}'_p$ and at representative regular values in the case of $\mathbf{Q}_p$. The two constructions are not quite "dual" to each other, since taking cellular duals is not an involution on planar cell complexes with boundary. We begin with an example of two cell complexes in $\mathbb{R}$, followed by the definitions to make it precise.

Example 3.1 ($\mathbf{I}_p$ and $\mathbf{I}'_p$). The real critical value interval $\mathbf{I}'_p$ for the polynomial of Example 2.3 is the interval $[-10, 5]$ subdivided at $C' = \{x'_1, x'_2, x'_3, x'_4\}$, the real parts of $\mathbf{cvl}(p)$. The real regular value interval $\mathbf{I}_p$ is an interval that has $\mathbf{I}'_p$ as its cellular dual. Figure 6 shows $\mathbf{I}_p$ on the top and $\mathbf{I}'_p$ on the bottom. In the "critical" interval $\mathbf{I}'_p$ the x'_i label vertices and in the "regular" interval $\mathbf{I}_p$ they label edges.

Definition 3.2 (Intervals). Let $[x_l, x_r] \subset \mathbb{R}$ be a compact interval and let $\mathbf{I}$ be $[x_l, x_r]$ with the structure of a cell complex. The *basepoint of* $\mathbf{I}$ is x_ℓ. The *combinatorial cell structure* of $\mathbf{I}$ is completely determined by the number k of vertices in its interior. The cell structure of the original interval has 1 edge and 2 vertices and we say it has been 0-subdivided. More generally we say that $\mathbf{I}$ has been k-*subdivided* when it has $k + 2$ vertices $x_\ell = v_0 < v_1 < \cdots < v_k < v_{k+1} = x_r$ indexed in the order they occur in $\mathbb{R}$, and $k + 1$ open edges e_i with endpoints v_{i-1} and v_i, $i \in [k + 1]$. A *metric cell structure* on $\mathbf{I}$ corresponds to a *metric k-subdivision*. It has an *absolute* description that records the locations $x_i \in (x_l, x_r) = I = \mathrm{int}(\mathbf{I})$ of the vertices v_i, $i \in [k]$. This is a k-element set $C = \{x_1, \ldots, x_k\} \in \mathrm{SET}_k(I)$, and we write $\mathbf{I}_C$ for $\mathbf{I}$ with this metric cell structure. Alternatively, it is sufficient to give a *relative* description, by listing the relative widths of the $k + 1$ subintervals. The *weight* or *relative width* $\mathbf{wt}_i$ of the ith subinterval (x_{i-1}, x_i) is the positive real $\mathbf{wt}_i = \frac{|x_i - x_{i-1}|}{|x_r - x_\ell|}$. Note that $\mathbf{wt}_1 + \cdots + \mathbf{wt}_{k+1} = 1$. The metric cell structures
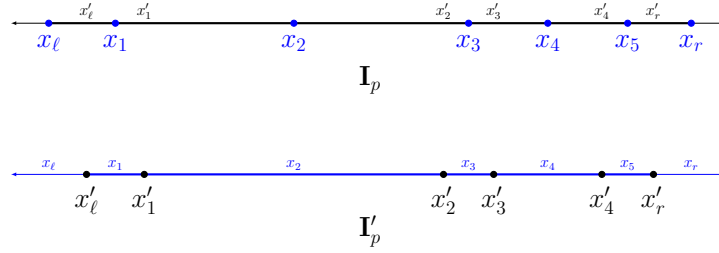
FIGURE 6. The real critical value interval $\mathbf{I}'_p$, shown on the bottom, is the interval $[-10, 5]$ subdivided at $C' = \{x'_1, x'_2, x'_3, x'_4\}$, the real parts of the critical values of our running example. The real regular value interval $\mathbf{I}_p$, shown on the top, is an undual of $\mathbf{I}'_p$. It is a subdivision of $[-11, 6]$, subdivided at the midpoints of the midpoints of the edges of $\mathbf{I}'_p$. In the "critical" interval $\mathbf{I}'_p$ the points in C' label vertices and in the "regular" interval $\mathbf{I}_p$ they label edges.

on an interval $\mathbf{I}_C$ that has been k-subdivided are in bijection with $(k + 1)$-tuples $\mathrm{BARY}(\mathbf{I}_C) = (\mathbf{wt}_1, \ldots, \mathbf{wt}_{k+1})$ of positive reals with sum 1. In Definition 5.12, the $\mathbf{wt}_i$ are used as the barycentric coordinates of a point in an open k-simplex, hence the name.

Definition 3.3 (Dual intervals). Let $\mathbf{I}, \mathbf{I}' \subset \mathbb{R}$ be subdivided intervals $\mathbf{I} = \mathbf{I}_k$ and $\mathbf{I}' = \mathbf{I}'_{k'}$. We say that $\mathbf{I}' = (\mathbf{I})'$ is a *dual* of $\mathbf{I}$ and $\mathbf{I} = \int(\mathbf{I}')$ is an *undual* of $\mathbf{I}'$ if the $k' + 2$ vertices of $\mathbf{I}'$ are in bijection with the $k + 1$ edges of $\mathbf{I}$ and each vertex of $\mathbf{I}'$ is contained in the corresponding edge of $\mathbf{I}$. Concretely, $k' = k - 1$ and the vertices V of $\mathbf{I}$ and the vertices V' of $\mathbf{I}'$ strictly alternative in $\mathbb{R}$, with $x_i < x'_i < x_{i+1}$ for $i = 0, \ldots, k' + 2$. Given $\mathbf{I}$, creating a dual $\mathbf{I}' = (\mathbf{I})'$ involves choosing a point from each bounded component of $\mathbb{R} \setminus V$. Given $\mathbf{I}'$, creating an undual $\mathbf{I} = \int(\mathbf{I}')$ involves choosing a point from each component of $\mathbb{R} \setminus V'$.

The derivative and integral metaphor of Definition 3.3 is inspired by Rolle's Theorem. If the vertices x_i of $\mathbf{I}$ are the distinct simple roots of real polynomial p, then the roots of its derivative p' are one choice for the vertices x'_i of its dual $\mathbf{I}'$.

Example 3.4 (Critical value complex $\mathbf{Q}'_p$). Let p be the polynomial of Example 2.3 and let $\square = [-10, 5] \times [-9, 2] \subset \mathbb{R}^2 = \mathbb{C}$ be a rectangle in its range, chosen to contain $\mathbf{cvl}(p)$. The *critical value complex* $\mathbf{Q}'_p$ *of p with rectangle* $\square$ is the rectangle $\square$ after it has been subdivided vertically and horizontally through the critical values of p. Figure 7 shows the range of p with its 4 critical values marked as yellow dots. The metric cell complex $\mathbf{Q}'_p$ is the product of factor metric cell complexes $\mathbf{I}'_p$ and $\mathbf{J}'_p$ which subdivide the factors of $\square$ at the real and imaginary parts of $\mathbf{cvl}(p)$. The real parts of $\mathbf{cvl}(p)$, listed in increasing order, are $C' = \{x'_1, x'_2, x'_3, x'_4\} \approx \{-8.5, -.6, .8, 3.6\}$, and the imaginary parts in increasing order, are $D' = \{y'_1, y'_2, y'_3, y'_4\} \approx \{-6.9, -4.3, -.6, .5\}$. The metric on $\mathbf{Q}'_p$ can be recorded by listing the relative widths of the open subintervals of $\mathbf{I}'_p$ and $\mathbf{J}'_p$. In this case, $\mathrm{BARY}(\mathbf{I}'_p) \approx (.102, .528, .089, .191, .091)$ and $\mathrm{BARY}(\mathbf{J}'_p) \approx (.190, .241, .334, .098, .136)$. Since we are recording relative widths, the sum of each list is 1. They are used as barycentric coordinates in Definition 5.12.
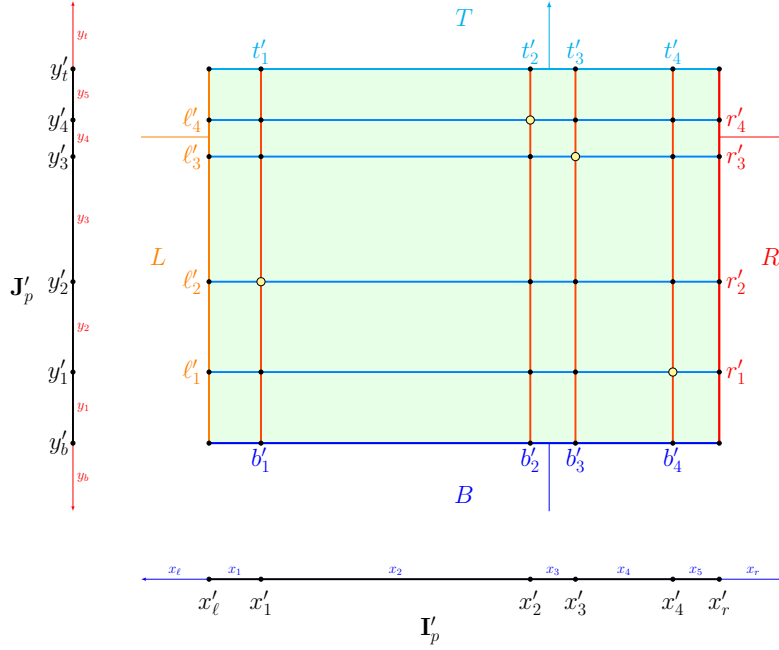
FIGURE 7. The range of the polynomial p of Example 2.3 with its 4 critical values marked as yellow dots. They are shown inside a rectangle $[-10, 5] \times [-9, 2] \subset \mathbb{R}^2 = \mathbb{C}$ that has been subdivided into the critical value complex $\mathbf{Q}'_p$.

Example 3.5 (Regular value complex $\mathbf{Q}_p$)**.** The regular value complex $\mathbf{Q}_p$ for the polynomial p of Example 2.3 with rectangle $\square$ is constructed from the critical value complex $\mathbf{Q}'_p$ and its factor complexes $\mathbf{I}'_p$ and $\mathbf{J}'_p$. Specially, if $\mathbf{I}_p$ is any interval complex whose dual is $\mathbf{I}'_p$ and $\mathbf{J}_p$ is any interval complex whose dual is $\mathbf{J}'_p$, then the complex $\mathbf{Q}_p = \mathbf{I}_p \times \mathbf{J}_p$ whose dual is $\mathbf{Q}'_p$ is the *regular value complex for p with rectangle $\square$*. The choices made when constructing $\mathbf{Q}_p$ from $\mathbf{Q}'_p$ impact the metric on $\mathbf{Q}_p$, but its combinatorial cell structure is well-defined. Let $\mathbf{I}$ and $\mathbf{J}$ be the intervals that are subdivided to form $\mathbf{I}_p$ and $\mathbf{J}_p$, and let $\mathbf{Q}$ be the rectangle that is subdivided to form $\mathbf{Q}_p$. Figure 7 shows one choice for $\mathbf{Q} = \mathbf{I} \times \mathbf{J}$. The enlarged rectangle is $[-11, 6] \times [-10, 3]$, and points $C = \{x_1, \ldots, x_5\}$ and $D = \{y_1, \ldots, y_5\}$ are chosen to be the midpoints of the corresponding intervals in $\mathbf{I}'_p$ and $\mathbf{J}'_p$, respectively. The vertex $z = (x_\ell, y_b)$ is its *basepoint* and the opposite vertex $w = (x_r, y_t)$ is its *breakpoint*.

Definition 3.6 (Coordinate rectangles)**.** Let $\mathfrak{R} \colon \mathbb{C} \to \mathbb{R}$ and $\mathfrak{I} \colon \mathbb{C} \to \mathbb{R}$ be maps so that for any $z = x + yi \in \mathbb{C}$, $\mathfrak{R}(z) = x$ is its *real part*, and $\mathfrak{I}(z) = y$ is its *imaginary part*. Let $I = (x_\ell, x_r)$ and $J = (y_b, y_t)$ be two non-empty open intervals in $\mathbb{R}$. Their closures $\mathbf{I} = [x_\ell, x_r]$ and $\mathbf{J} = [y_b, y_t]$ have a natural cell structure with open edges I and J, vertices x_ℓ, x_r, y_b and y_t, and *basepoints* x_ℓ and y_b. They determine a *coordinate rectangle* $\mathbf{Q} = \mathbf{I} + \mathbf{J}i = \{z \mid \mathfrak{R}(z) \in \mathbf{I}, \mathfrak{I}(z) \in \mathbf{J}\}$. Equivalently, $\mathbf{Q} = \mathbf{I} \times \mathbf{J}$ under the natural identification of $\mathbb{C}$ with $\mathbb{R}^2$.
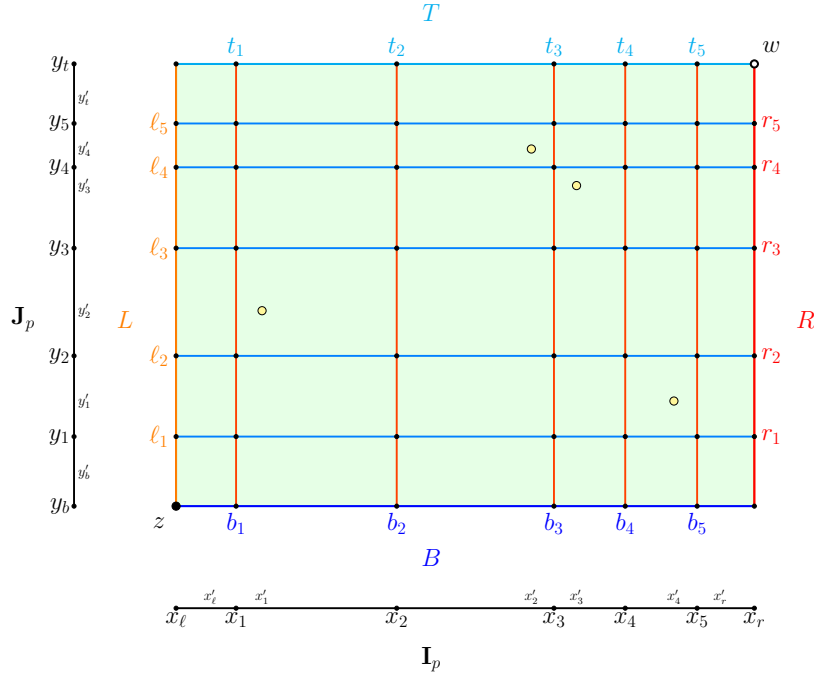
FIGURE 8. The range of the polynomial of Example 2.3 with its 4 critical values marked as yellow dots. They are shown inside a rectangle $[-11, 6] \times [-10, 3] \subset \mathbb{R}^2 = \mathbb{C}$ that has been subdivided into the regular value complex $\mathbf{Q}_p$. The basepoint z and breakpoint w are also marked.
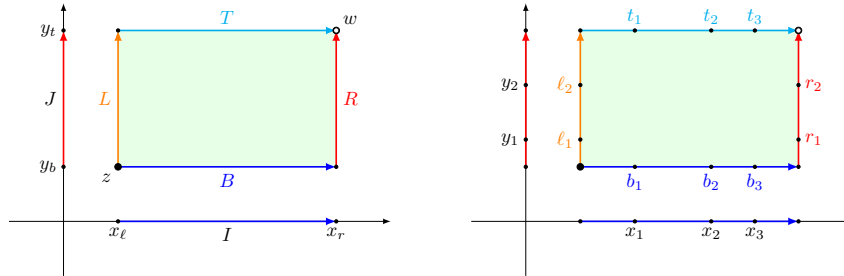
FIGURE 9. The vertices and sides of $\mathbf{Q} = \mathbf{I} + \mathbf{J}i$ are shown on the left, including its basepoint z and its breakpoint w. The 10 points of a $(3, 2)$-configuration induced by $C = \{x_1, x_2, x_3\} \subset I$ and $D = \{y_1, y_2\} \subset J$ are shown on the right.

Definition 3.7 (Sides and cells). The rectangle $\mathbf{Q}$ has a natural cell structure. The *sides* of $\mathbf{Q}$ are the open edges of the *top side* $\mathbf{T} = \mathbf{I} \times \{y_t\}$, *bottom side* $\mathbf{B} = \mathbf{I} \times \{y_b\}$, *left side* $\mathbf{L} = \{x_\ell\} \times \mathbf{J}$, and *right side* $\mathbf{R} = \{x_r\} \times \mathbf{J}$. The vertex $z = (x_\ell, y_b)$ is its *basepoint* and the opposite vertex $w = (x_r, y_t)$ is its *breakpoint*. The isometric *side identifications* $f_{\mathbf{B}} \colon \mathbf{B} \to \mathbf{I}$, $g_{\mathbf{R}} \colon \mathbf{R} \to \mathbf{J}$, $f_{\mathbf{T}} \colon \mathbf{T} \to \mathbf{I}$, and $g_{\mathbf{L}} \colon \mathbf{L} \to \mathbf{J}$, drop the fixed coordinate. The intervals $\mathbf{I}$ and $\mathbf{J}$ are oriented left-to-right as subsets of $\mathbb{R}$

and the sides of $\mathbf{Q}$ are oriented via their side identifications: $\mathbf{B}$ and $\mathbf{T}$ are oriented left-to-right; $\mathbf{L}$ and $\mathbf{R}$ are oriented bottom-to-top. In the boundary $\partial\mathbf{Q}$, $\mathbf{L}$ and $\mathbf{T}$ are oriented clockwise while $\mathbf{B}$ and $\mathbf{R}$ are oriented counterclockwise.

Cell structures on $\mathbf{I}$ and $\mathbf{J}$ produce a product cell structure on $\mathbf{Q} = \mathbf{I} \times \mathbf{J}$.

Definition 3.8 (Rectangles and subdivisions). Let $\mathbf{Q} = \mathbf{I} \times \mathbf{J}$ be a coordinate rectangle (Definition 3.6). When $\mathbf{I}$ is k-subdivided and $\mathbf{J}$ is l-subdivided, we say $\mathbf{Q}$ has been (k,l)-*subdivided* and has a (k,l)-*structure*. It has $(k+1)(l+1)$ 2-cells, $(k+1)(l+2)$ horizontal edges, $(k+2)(l+1)$ vertical edges, and $(k+2)(l+2)$ vertices $v_{i,j} = (x_i, y_j)$. The $k \cdot l$ new vertices in the interior are those with $i \in [k]$ and $j \in [l]$. When $\mathbf{I}$ and $\mathbf{J}$ have been given metric cell structures $\mathbf{I}_C$ and $\mathbf{J}_D$, the rectangle $\mathbf{Q}$ has a metric cell structure $\mathbf{Q}_{C,D}$. Using the side identifications, the sides of $\mathbf{Q}_{C,D}$ have metric cell structures $\mathbf{T}_C$, $\mathbf{B}_C$, $\mathbf{L}_D$, and $\mathbf{R}_D$. When $C = \{x_1, x_2, \ldots, x_k\}$ and $D = \{y_1, y_2, \ldots, y_l\}$, we write $C_T = \{t_1, \ldots, t_k\}$, $C_B = \{b_1, \ldots, b_k\}$, $D_L = \{\ell_1, \ldots, \ell_l\}$, and $D_R = \{r_1, \ldots, r_l\}$, for the interior vertices of $\mathbf{T}_C$, $\mathbf{B}_C$, $\mathbf{L}_D$, and $\mathbf{R}_D$, respectively. The $2(k+l)$ new vertices in $\partial\mathbf{Q}_{C,D}$ are a metric (C,D)-*configuration* and a combinatorial (k,l)-*configuration*. The right hand side of Figure 9 shows the 10 points of a $(3,2)$-configuration.

Definition 3.9 (Critical value complex $\mathbf{Q}'_p$). Let $p \colon \mathbb{C} \to \mathbb{C}$ be a planar branched cover, and let $\square = [x'_\ell, x'_r] \times [y'_b, y'_t]$ be a coordinate rectangle in the range with $\mathbf{cvl}(p) \subset \square$. Define $E' = \mathrm{Set}(\mathbf{cvl}(p))$ and let $C' = \Re(E') \cap I'$ and $D' = \Im(E') \cap J'$, the real and imaginary parts of E' in the open intervals I' and J', respectively. Let $\mathbf{I}'_p = \mathbf{I}'_{C'}$, $\mathbf{J}'_p = \mathbf{J}'_{D'}$ and $\mathbf{Q}'_p = \mathbf{Q}'_{C',D'}$ (Definitions 3.2 and 3.8). This is the unique minimal horizontal and vertical subdivision of $\square$ so that $\mathbf{cvl}(p)$ is in the 0-skeleton. We call $\mathbf{Q}'_p$ the *critical value complex* on $\square$, whose factors are the *real critical value complex* $\mathbf{I}'_p$ and the *imaginary critical value complex* $\mathbf{J}'_p$ of p on $\square$.

Remark 3.10 (Cells and sides). The cell structure $\mathbf{Q}'_p$ is almost entirely independent of the choice of $\square$, but changes occur depending on whether or not the sides of $\square$ are regular. For example, if a rectangle $\square \supset \mathbf{cvl}(p)$ contains a critical value in its right side and we slightly extend I' to the right so that this doesn't happen, then the new extended $\mathbf{I}'_p$ has one more subdivision than the old $\mathbf{I}'_p$ and the new extended version of $\mathbf{Q}'_p$ has an extra row of 2-cells on the right compared to the previous $\mathbf{Q}'_p$. Similar comments apply to the other sides. Given a branched cover p, one could simply choose a rectangle $\square$ large enough so that its sides are regular, eliminating this dependency, but we need to allow critical values in the boundary of $\square$ in order to create compact spaces of polynomials. See Lemma 10.5 in Part 2.

Definition 3.11 (Regular value complex $\mathbf{Q}_p$). Let $\mathbf{I}_p$ be a subdivision of an interval $\mathbf{I} = [x_\ell, x_r]$ and let $\mathbf{J}_p$ be a subdivision of an interval $\mathbf{J} = [y_b, y_t]$ so that $\mathbf{I}'_p = (\mathbf{I}_p)'$ and $\mathbf{J}'_p = (\mathbf{J}_p)'$ as cellular duals. In other words $\mathbf{I}_p = \int(\mathbf{I}'_p)$ is an undual of $\mathbf{I}'_p$ and $\mathbf{J}_p = \int(\mathbf{J}'_p)$ is an undual of $\mathbf{J}'_p$. The product of the *real regular value complex* $\mathbf{I}_p$ and the *imaginary regular value complex* $\mathbf{J}_p$ is the *regular value complex* $\mathbf{Q}_p = \mathbf{I}_p \times \mathbf{J}_p$ for p based on $\square$. It is based on $\square$ in the sense of Remark 3.10, but it is drawn on the larger rectangle $\mathbf{Q}$ with $\square = \mathbf{Q}' \subset \mathrm{int}(\mathbf{Q})$ by construction. Extending the notation of Definition 3.3, we write $\mathbf{Q}_p = \int(\mathbf{Q}'_p)$ since $\mathbf{Q}_p$ is an undual of $\mathbf{Q}'_p$. Note that if $\mathbf{Q}'_p$ is (k',l')-subdivided, then $\mathbf{Q}_p$ is (k,l)-subdivided with $k = k' + 1$ and $l = l' + 1$. The basepoint $z = (x_\ell, y_b)$ and breakpoint $w = (x_r, y_t)$ are marked because they are needed. The basepoint is used when computing

fundamental groups (Definition 11.1), and the breakpoint is used when indexing the sides of a branched rectangle (Definition 5.2). Note that we mark a basepoint and a breakpoint only on the regular value complex $\mathbf{Q}_p$ where both are regular, and not on the critical value complex $\mathbf{Q}'_p$ where they may not be regular.

3.2. **Branched cellular maps.** A cell complex in the range of a planar branched cover with regular edges induces a cell structure on its preimage and there is a branched cellular map between them. A cellular map between cell complexes is one that maps each cell in the domain homeomorphically to a cell of the same dimension in the range. A branched cellular map allows branching in 2-cells.

Definition 3.12 (Branched cellular maps)**.** Let $\mathbf{p}\colon \mathbf{Z} \to \mathbf{W}$ be a branched covering map between surfaces that restricts to a map $\mathbf{p}\colon \mathbf{X} \to \mathbf{Y}$ from a cell complex $\mathbf{X} \subset \mathbf{Z}$ to a cell complex $\mathbf{Y} \subset \mathbf{W}$. We say that the restricted map $\mathbf{p}$ is a *branched cellular map* when (1) for each open i-cell in $\mathbf{X}$ there is an open i-cell in $\mathbf{Y}$ that contains its image under $\mathbf{p}$, (2) the maps between 1-cells are homeomorphisms and (3) the maps between open 2-cells are open planar branched covers (Definition 2.19). In particular, every branched cellular map looks like a cellular map between cell complexes if you only look near the 1-skeleton.

Lemma 3.13 (Disk preimages)**.** *Let* $\mathbf{p}\colon \mathbf{Z} \to \mathbf{W}$ *be a planar branched cover and let* $\mathbf{Y} \subset \mathbf{W}$ *be a cell complex. For every open* 2-*cell* F *in* $\mathbf{Y}$*, the preimage* $\mathbf{p}^{-1}(F)$ *is a disjoint union of open* 2-*cells and the component maps are planar branched covers.*

Proof. Let $\mathbf{W}_F \subset F$ be a closed disk such that all of the critical values of p in F are in the interior of $\mathbf{W}_F$. By Proposition 2.24, its preimage $\mathbf{Z}_F = \mathbf{p}^{-1}(\mathbf{W}_F)$ is a union of disks, and the preimage of the open annulus region $F \setminus \mathbf{W}_F$, being regular, is a union of open annuli which provide an annular padding around the components of $\mathbf{Z}_F$, showing that the components of $\mathbf{p}^{-1}(F)$ are open disks. $\square$

Let $\mathbf{Y} \subset \mathbf{W}$ be a cell complex in the range of a branched cover. We say that $\mathbf{Y}$ is 1-*regular* if the open 1-cells of $\mathbf{Y}$ are regular. Note that the regular value complex $\mathbf{Q}_p$ and the critical value complex $\mathbf{Q}'_p$ are both 1-regular by construction: in the regular case because the critical values lie in 2-cells and in the critical case because the critical values are 0-cells. For 1-regular cell complexes in the range of a branched cover, the preimage has a cell structure.

Definition 3.14 (Induced cell structures)**.** Let $\mathbf{p}\colon \mathbf{Z} \to \mathbf{W}$ be a planar branched cover. If $\mathbf{Y} \subset \mathbf{W}$ is a 1-regular cell complex, then its preimage $\mathbf{X} = \mathbf{q}^{-1}(\mathbf{Y})$ has an *induced cell structure from* $\mathbf{Y}$ *via* $\mathbf{q}$ and the restricted map $\mathbf{p}\colon \mathbf{X} \to \mathbf{Y}$ is a branched cellular map. The *i-regions* of $\mathbf{X}$ are the connected components of the preimages of the open i-cells of $\mathbf{Y}$ with the obvious attaching maps. The 1-regions in $\mathbf{X}$ are open 1-cells (since the open 1-cells are evenly covered), and the 2-regions are open 2-cells by Lemma 3.13. The assumption that $\mathbf{p}$ is a *planar* branched cover is crucial here, since Example 2.23 gives an example where a preimage of a closed disk is a closed surface with multiple boundary cycles. Finally, if $\mathbf{Y}$ has a metric and $\mathbf{X}$ has the induced metric, then $\mathbf{p}$ is a local isometry away from the critical points in $\mathbf{X}$.

For our purposes, the most important cell complexes are disk diagrams.

Definition 3.15 (Disk diagrams)**.** A *disk diagram* $\mathbf{Y}$ is a compact contractible cell complex embedded in a surface $\mathbf{W}$. If $\mathbf{Y}$ is homeomorphic to a closed disk, it is *nonsingular*, otherwise it is *singular*. For disk diagrams, being singular is equivalent

to having a cut point, or even a local cut point, whose removal (locally) disconnects $\mathbf{Y}$. Disk diagrams can also be characterized as cell complexes embedded in a surface where there are arbitrarily small neighborhoods that are topological disks. When the surface $\mathbf{W}$ containing the (singular or nonsingular) disk diagram $\mathbf{Y}$ is itself a disk, $\mathbf{W}$ deformation retracts to $\mathbf{Y}$.

Remark 3.16 (Components and critical complexes). Let $\mathbf{p} \colon \mathbf{Z} \to \mathbf{W}$ be a planar branched cover, let $\mathbf{Y} \subset \mathbf{W}$ be a disk diagram and let $\mathbf{W}^{\mathbf{Y}}$ be a small closed disk neighborhood of $\mathbf{Y}$ so that any critical values of $\mathbf{p}$ in $\mathbf{W}^{\mathbf{Y}}$ are in $\mathbf{Y}$. By Proposition 2.24, the preimage $\mathbf{Z}^{\mathbf{Y}} = \mathbf{p}^{-1}(\mathbf{W}^{\mathbf{Y}})$ is a union of disks and the component maps $\mathbf{p}_i^{\mathbf{Y}} \colon \mathbf{Z}_i^{\mathbf{Y}} \to \mathbf{W}^{\mathbf{Y}}$ are planar branched covers. In particular, working component-by-component, restricting $\mathbf{Z}$ to $\mathbf{Z}_i^{\mathbf{Y}}$, $\mathbf{W}$ to $\mathbf{W}^{\mathbf{Y}}$, and $\mathbf{p}$ to $\mathbf{p}_i^{\mathbf{Y}}$, reduces the general case to a set of special cases in with $\mathbf{cvl}(\mathbf{q}_i^{\mathbf{Y}}) \subset \mathbf{Y}$.

Corollary 3.17 (Disk diagrams). *If $\mathbf{p} \colon \mathbf{Z} \to \mathbf{W}$ is a planar branched cover and $\mathbf{Y} \subset \mathbf{W}$ is a 1-regular disk diagram, then $\mathbf{X} = \mathbf{p}^{-1}(\mathbf{Y})$ is a disjoint union of disk diagrams. In particular, if $\mathbf{cvl}(\mathbf{p}) \subset \mathbf{Y}$, then $\mathbf{X}$ itself is a disk diagram.*

Proof. By Remark 3.16 it is sufficient to prove this when $\mathbf{cvl}(\mathbf{p}) \subset \mathbf{Y}$ and $\mathbf{Z}$ is a disk. In this case, $\mathbf{X}$ is a cell complex and the map $p \colon \mathbf{X} \to \mathbf{Y}$ is a branched cellular map (Definition 3.12). Moreover, the deformation retraction from $\mathbf{W}$ to $\mathbf{Y}$ (Definition 3.15) lifts to a deformation retraction from $\mathbf{Z}$ to $\mathbf{X}$ (since the complement of $\mathbf{Y}$ is covered by the complement of $\mathbf{X}$). Since $\mathbf{X}$ and $\mathbf{Z}$ are homotopy equivalent, $\mathbf{X}$ is contractible. $\square$

It is easy to determine whether or not the preimage disk diagram is singular.

Corollary 3.18 (Singular diagrams). *Let $\mathbf{p} \colon \mathbf{Z} \to \mathbf{W}$ be a planar branched cover that restricts to a map $\mathbf{X} \to \mathbf{Y}$ between disk diagrams. When $\mathbf{Y}$ is singular, $\mathbf{X}$ is singular. And when $\mathbf{Y}$ is nonsingular, $\mathbf{X}$ is singular if and only if $\partial \mathbf{X}$ contains a critical point of p.*

Proof. Suppose $\mathbf{Y}$ is singular and let v be a local cut vertex in $\partial \mathbf{Y}$ (Definition 3.15). Any u in $\partial \mathbf{X}$ sent to v is also a local cut vertex, regardless of whether the local model is branched, so $\mathbf{X}$ is also singular. Next, suppose $\mathbf{Y}$ is nonsingular and there are no critical points in the boundary of $\mathbf{X}$. Then the local models are homeomorphisms, there are no local cut points in the boundary of $\mathbf{X}$, so $\mathbf{X}$ is also nonsingular. Finally, suppose $\mathbf{Y}$ is nonsingular and there is a critical point u in the boundary of $\mathbf{X}$. Its image v is a critical value in the boundary of $\mathbf{Y}$, the branched local model near u shows that u is a local cut vertex, and $\mathbf{X}$ is singular. $\square$

Example 3.19 (Branched lines and banyans). Let $\mathbf{q} \colon \mathbf{Z} \to \mathbf{W}$ be a planar branched cover, and let $\mathbf{Y} \subset \mathbf{W}$ be a closed interval. If $\mathbf{Y}$ is subdivided so that any critical values in $\mathbf{Y}$ are vertices, then its preimage $\mathbf{X} = \mathbf{q}^{-1}(\mathbf{Y})$ is a 1-complex (Definition 3.14) with components $\mathbf{X} = \mathbf{X}_1 \sqcup \cdots \sqcup \mathbf{X}_k$. The 1-complexes $\mathbf{X}_i$ are trees because they are contractible (Corollary 3.17). We call them *branched lines* or *banyan trees*, a type of tree with multiple branches and multiple roots. The cell complex $\mathbf{X}$ is a *banyan grove*, a type of forest.

Example 3.20 (Branched disks and cacti). Let $\mathbf{q} \colon \mathbf{Z} \to \mathbf{W}$ be a planar branched cover, and let $\mathbf{Y} \subset \mathbf{W}$ be a closed disk. If $\mathbf{Y}$ is given the cell structure of a nonsingular 2-complex with only one 2-cell and a subdivided boundary $\partial \mathbf{Y}$ with regular edges, then its preimage $\mathbf{X} = \mathbf{q}^{-1}(\mathbf{Y})$ is a 2-complex (Definition 3.14)
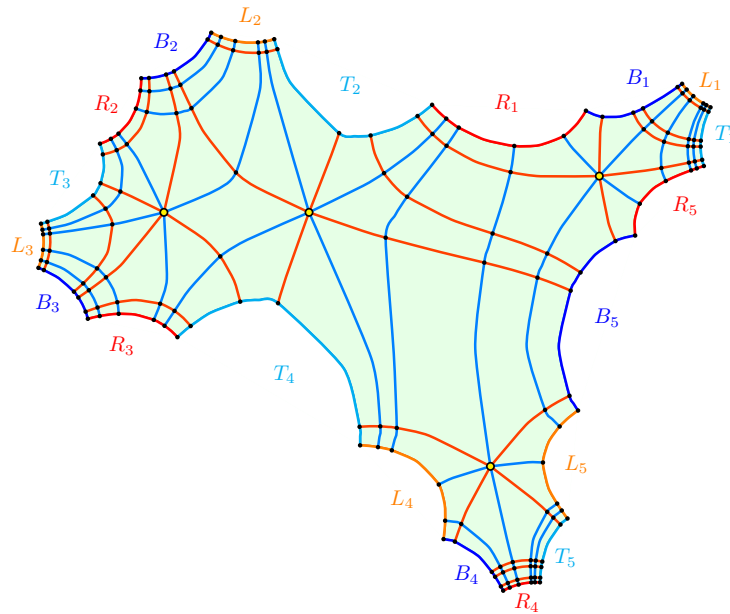
FIGURE 10. The domain of the polynomial p of Example 2.3 with its 4 critical points marked as yellow dots. They are shown inside the critical point complex $\mathbf{P}'_p$, which is the preimage of the critical value complex $\mathbf{Q}'_p$ shown in Figure 7.

with components $\mathbf{X} = \mathbf{X}_1 \sqcup \cdots \sqcup \mathbf{X}_k$. The 2-dimensional cell complexes $\mathbf{X}_i$ are disk diagrams (Corollary 3.17) called *branched disks* or *cactus diagrams*, since they resemble prickly pear cacti. The cell complex $\mathbf{X}$ is a *garden of cactus diagrams*. The components $\partial \mathbf{X}_i$ of $\partial \mathbf{X}$ are the boundaries of the components $\mathbf{X}_i$ of $\mathbf{X}$. The component $\partial \mathbf{X}_i$ is a *branched circle* or *cactus graph*, and the full 1-skeleton $\partial \mathbf{X}$ is a *garden of cactus graphs*.

Metric banyans and metric cacti appeared in the first paper in this series [DM22], but the definitions given here are more concise.

3.3. **Complexes in the domain.** We now define the regular point complex $\mathbf{P}_p$ and the critical point complex $\mathbf{P}'_p$ using Definition 3.14.

Example 3.21 (Point complexes $\mathbf{P}'_p$ and $\mathbf{P}_p$). Let p be the polynomial of Example 2.3, let $\mathbf{Q}'_p$ be the critical value complex in the range of p shown in Figure 7, and let $\mathbf{Q}_p$ be the regular value complex in the range of p shown in Figure 8. The *critical point complex* $\mathbf{P}'_p$ in the domain of p is shown in Figure 10. The pullback metric on $\mathbf{P}'_p$ makes each of the 125 topological 2-cells into a Euclidean rectangle with a metric determined by its image in $\mathbf{Q}'_p$. The disk diagram $\mathbf{P}'_p$ is nonsingular, in this case, because $\partial \mathbf{Q}'_p$ is regular (Corollary 3.18). The *regular point complex* $\mathbf{P}_p$ in the domain of p is shown in Figure 11. Since the branching occurs in the interior of 2-cells, the 1-skeleton of $\mathbf{P}_p$ is a 5-sheeted cover of the 1-skeleton of $\mathbf{Q}_p$, and it has a 5-branched $(5,5)^5$-structure. The side labels are explained in Section 5.
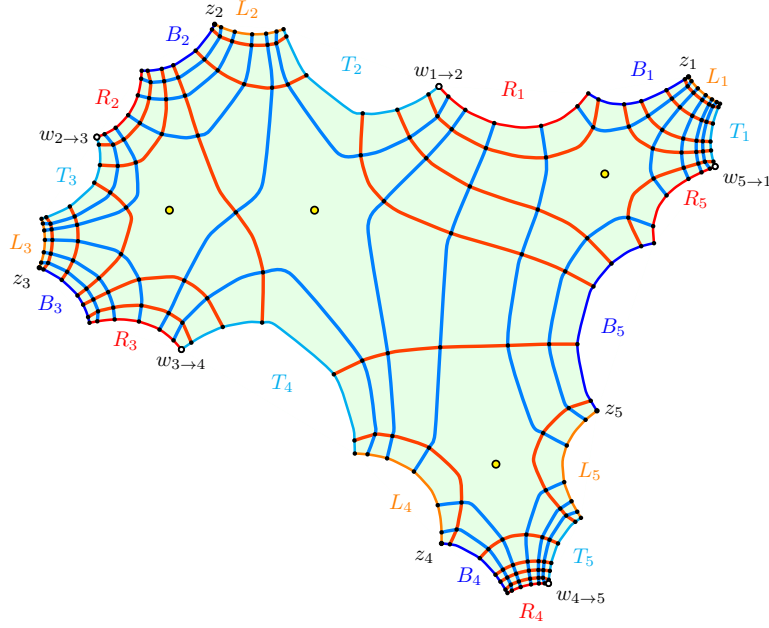
FIGURE 11. The domain of the polynomial p of Example 2.3 with its 4 critical points marked as yellow dots. They are shown inside the regular point complex $\mathbf{P}_p$, which is the preimage of the regular value complex $\mathbf{Q}_p$ shown in Figure 7. The breakpoint preimages $w_{m \to m+1}$ and basepoint preimages z_i are also marked.

Definition 3.22 (Point complexes $\mathbf{P}_p$ and $\mathbf{P}'_p$). Let $p \colon \mathbb{C} \to \mathbb{C}$ be a planar branched cover, and let $\square = [x'_\ell, x'_r] \times [y'_b, y'_t]$ be a coordinate rectangle in the range with $\mathbf{cvl}(p) \subset \square$. The coordinate complexes $\mathbf{Q}_p$ and $\mathbf{Q}'_p$ in the range are both 1-regular, and by Definition 3.14 their preimages under p have induced cell structures. We call these cell complexes in the domain the *regular point complex* $\mathbf{P}_p$ and the *critical point complex* $\mathbf{P}'_p$. The map p restricts to the *regular complex map* $\mathbf{P}_p \to \mathbf{Q}_p$ and the *critical complex map* $\mathbf{P}'_p \to \mathbf{Q}'_p$. Note that the cell structure on $\mathbf{Q}'_p$ and the critical complex map $\mathbf{P}'_p \to \mathbf{Q}'_p$ can be reconstructed simply from the cell structure of $\mathbf{P}'_p$. The regular complex map is a branched cellular map, and the the critical complex map is a cellular map since the rectangular 2-cells of the critical value complex $\mathbf{Q}_p$ are regular by construction. The regular complex map is a d-sheeted covering map between their 1-skeletons because the 1-skeleton of $\mathbf{Q}_p$ is regular. If $\mathbf{Q}_p$ has a (k,l)-structure (Definition 3.8), then we say that $\mathbf{P}_p$ has a d-branched $(k,l)^d$-*structure*.

Remark 3.23 (Unique geodesics). The critical map from $\mathbf{P}'_p$ to $\mathbf{Q}'_p$ is a cellular map between piecewise Euclidean complexes built out of Euclidean rectangles. The complex $\mathbf{Q}'_p$, as a subdivided rectangle, is obviously a CAT(0) metric space, and so is $\mathbf{P}'_p$ since every interior vertex has an integer multiple of 2π in angle. In particular, both spaces have unique geodesics [BH99].

Remark 3.24 (Combinatorial invariance). Technically speaking, the construction of the regular point complex $\mathbf{P}_p$ depends on the regular value complex $\mathbf{Q}_p$ which

in turn depends on a choice of subdivided intervals $\mathbf{I}_p$ and $\mathbf{J}_p$ that have $\mathbf{I}'_p$ and $\mathbf{J}'_p$ as cellular duals, but the combinatorial structures of $\mathbf{I}_p$, $\mathbf{J}_p$, $\mathbf{Q}_p$ and $\mathbf{P}_p$ are independent of these choices. In particular, continously varying the choice of vertices of $\mathbf{I}_p$ and $\mathbf{J}_p$, continuously varies the 1-skeleton of $\mathbf{Q}_p$ and continuously varies the 1-skeleton of $\mathbf{P}_p$ (since this is taking place in the regular portion of the range) without changing any of their cell structures. It does, of course, still depend on the choice of rectangle $\square$ since this changes the cell structure of the critical value complex $\mathbf{Q}'_p$ (Remark 3.10).

4. Noncrossing Combinatorics

The combinatorial structure of the regular point complex $\mathbf{P}_p$ can be described using planar noncrossing combinatorics. This section establishes conventions for noncrossing partitions (4.1), drawn on planar branched rectangles (4.2), and it connects them to noncrossing matchings (4.3) and noncrossing permutations (4.4). Since these structures are associated to planar d-branched covers and degree-d polynomials, we use $[d]$ as our indexing set.

4.1. **Noncrossing partitions.** Noncrossing partitions can be defined combinatorially, metrically, and topologically. The combinatorial version is the simplest, the metric version explains the name, and the topological version, introduced here, is the most convenient to use in our context. We begin with some basic notation for points and subsets of the complex plane.

Definition 4.1 (Points and subsets). Recall that $\mathbb{D}$ is the closed unit disk and $\mathbb{T} = \partial\mathbb{D}$ is its unit circle boundary. Let $e \colon \mathbb{C} \to \mathbb{C_0}$ be the function $e(z) = \exp(2\pi i z)$ that sends $\mathbb{R}$ to $\mathbb{T}$ with kernel $\mathbb{Z}$. The dth roots of unity $\sqrt[d]{1} = \{e(j/d) \mid j \in [d]\}$ are indexed by $j \in [d]$, viewed as residue classes of the integers mod d. More generally, every d-element subset of $\mathbb{T}$ can be identified with the integers mod d by sending 1 to the element with smallest positive argument, and proceeding in a counterclockwise fashion around the circle.

Definition 4.2 (Combinatorial noncrossing partitions). A set partition $[\lambda] \vdash [d]$ is a (combinatorial) *noncrossing partition* if whenever there is a 4-element subset $i < j < k < \ell$ in $[d]$ with i and k in the same block, and j and ℓ in the same block, then all four are in the same block. The collection NCPART_d of all noncrossing partitions of $[d]$, ordered by refinement, is an induced subposet of $\mathrm{SETPART}_d$.

Definition 4.3 (Metric noncrossing partitions). Let $\sqrt[d]{1} \subset \mathbb{C}$ be the dth roots of unity with $j \in [d]$ labeling $e(j/d)$ (Definition 4.1). A set partition $[\lambda] \vdash [d]$ is a (metric) *noncrossing partition*, if the convex hulls of the dth roots labeled by the numbers in each block of $[\lambda]$ form pairwise disjoint subspaces of $\mathbb{C}$.

Definition 4.4 (Topological noncrossing partitions). Let $\mathbf{X}$ be a closed disk in the complex plane, let $S \subset \partial\mathbf{X}$ be a subset of its boundary with d path components and fix a bijective labeling of the components of S by the numbers in $[d]$ in the counterclockwise order they occur in the boundary of $\mathbf{X}$. For every subspace $\mathbf{U}$ (typically a closed subsurface) with $S \subset \mathbf{U} \subset \mathbf{X}$ we define a set partition $\mathrm{NCPART}(\mathbf{U})$ where i and j are in the same block of $\mathrm{NCPART}(\mathbf{U})$ if and only if the path components of S labeled i and j are in the same path component of $\mathbf{U}$. A set partition $[\lambda] \vdash [d]$ is a (topological) *noncrossing partition* if there exists a subspace

$\mathbf{U}$ with $S \subset \mathbf{U} \subset \mathbf{X}$ such that $\mathrm{NCPART}(\mathbf{U}) = [\lambda]$. Note that if we view the subspaces of $\mathbf{X}$ containing S as a poset under inclusion, then the map to NCPART_d is weakly order-preserving. In other words, if $S \subset \mathbf{U}_1 \subset \mathbf{U}_2 \subset \mathbf{X}$ as subspaces, then $\mathrm{NCPART}(\mathbf{U}_1) \leq \mathrm{NCPART}(\mathbf{U}_2)$ as set partitions.

The three definitions are, of course, equivalent.

Proposition 4.5 (Noncrossing partitions). *The combinatorial, metric and topological definitions of noncrossing partitions define the same collection of set partitions.*

Proof. (C $\Leftrightarrow$ M) The equivalence of the combinatorial and metric definitions is classical [Kre72]. (M $\Rightarrow$ T) Given $\mathbf{X}$ and S as in Definition 4.4, fix an identification of $\mathbf{X}$ with closed unit disk $\mathbb{D}$ so that the path component of S labeled j contains $e(j/d) \in \sqrt[d]{1}$. For each metric noncrossing partition $[\lambda]$, the union of its convex hulls (union S), viewed as a subspace $\mathbf{U} \subset \mathbf{X} = \mathbb{D}$, shows that $[\lambda]$ is a topological noncrossing partition. If we need $\mathbf{U}$ to be a subsurface, simply replace the subspace with a small closed neighborhood in $\mathbb{D}$. (T $\Rightarrow$ C) Let $[\lambda]$ be a topological noncrossing partition in a disk $\mathbf{X}$, let $\mathbf{U}$ be a subspace with $\mathrm{NCPART}(\mathbf{U}) = [\lambda]$ and let $i < j < k < \ell$ be numbers in $[n]$ with i and k in the same block and j and ℓ in the same block. If $\alpha \colon \mathbf{I} \to \mathbf{U}$ is a path in $\mathbf{U}$ from the ith component of S to the kth component of S, and $\beta \colon \mathbf{I} \to \mathbf{U}$ is a path in $\mathbf{U}$ from the jth component of S to the ℓth component of S, then α and β intersect.[2] Thus all four points are in the same path component of $\mathbf{U}$, the numbers are in the same block of $\mathrm{NCPART}(\mathbf{U}) = [\lambda]$, and $[\lambda]$ is a combinatorial noncrossing partition. $\square$

4.2. **Branched rectangles.** The topological noncrossing partitions of interest here are induced by subspaces of planar branched covers of rectangles. This subsection establishes our conventions for such spaces. We first specify a standard rectangle.

Definition 4.6 (Standard rectangle). The *standard rectangle* is $\mathbf{Q} = \mathbf{I} + \mathbf{J}i \subset \mathbb{C}$ where both $\mathbf{I}$ and $\mathbf{J}$ are the *standard interval* $[-1, 1]$. The sides of $\mathbf{Q}$ touch the unit circle at their midpoints $\sqrt[4]{1}$ with $i \in T$, $-1 \in L$, $-i \in B$ and $1 \in R$, and these are their *representatives*. The vertices of $\mathbf{Q}$ are $\{\pm(1 \pm i)\} = \sqrt[4]{-4}$. The breakpoint is $w = 1 + i$ and the basepoint is $z = -(1 + i)$.

Similar conventions apply to the power map preimages of the standard rectangle.

Definition 4.7 (Standard branched rectangles). Let $p(z) = z^d$ be the power map (Definition 2.4) and let $\mathbf{Q}$ is the standard rectangle (Definition 4.6). The *standard d-branched rectangle* is $\mathbf{P} = p^{-1}(\mathbf{Q})$. The d-fold covering map $\partial\mathbf{p} \colon \partial\mathbf{P} \to \partial\mathbf{Q}$ between their boundaries is used to partition the $4d$ open edges, or *sides*, S, into d *top sides* S_T, d *left sides* S_L, d *bottom sides* S_B, and d *right sides* S_R. For example $S_T = p^{-1}(T)$. The midpoints of the sides of $\mathbf{P}$ touch the unit circle at the $4d$ points $\sqrt[4d]{1}$, and these are their *standard representatives*. More precisely, the top sides are represented by the points $\sqrt[d]{i}$, the left sides by the points $\sqrt[d]{-1}$, the bottom sides by the points $\sqrt[d]{-i}$ and right sides are by the points $\sqrt[d]{1}$. Sides are indexed by the indexing of their representatives (Definition 4.1). For example, T_m contains $e(\frac{4m-3}{4d})$, the mth element of $\sqrt[d]{i} = \{e(\frac{4m-3}{4d}) \mid m \in [d]\}$. The *basepoint preimage*

---

[2]If not, then $(s, t) \mapsto (\beta(t) - \alpha(s))$ is a contractible map $\mathbf{I}^2 \to \mathbb{C}^*$ whose boundary cycle is sent to a loop of winding number 1, contradiction. The winding number can be computed by assuming $\mathbf{X}$ is a rectangle and α and β connect opposite corners. The map in this case sends the vertices of $\mathbf{I}^2$ to the coordinate axes and its sides to paths in specific quadrants.
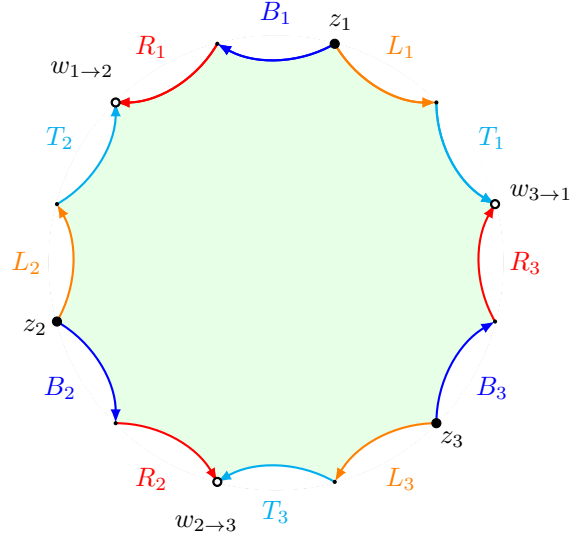
FIGURE 12. A standard 3-branched rectangle with labeled cells. The 3 large white dots are the indexed breakpoints $w_{m \to m+1}$ and the 3 large black dots are the indexed basepoints z_i.

between sides L_m and B_m is z_m, and the *breakpoint preimage* between sides R_m and T_{m+1} is $w_{m \to m+1}$. See Figure 12.

The standard $4d$-gon **P** roughly looks like a regular hyperbolic polygon, but more precisely, the sides are portions of the curves $r^d \cos(d\theta) = \pm 1$ (for the preimages of the right and left sides) and $r^d \sin(d\theta) = \pm 1$ (for the preimages of the top and bottom sides). Nevertheless, we often treat **P** as though it was in the Poincaré disk model with a hyperbolic metric. Arcs and convex hulls are drawn with this hyperbolic approximation in mind. See Figure 12 for an example when $d = 3$.

The standard branched rectangle has side-based noncrossing partitions.

Definition 4.8 (Noncrossing partitions of sides)**.** Let NCPart_d^T be the (topological) noncrossing partitions of the top sides S_T in **P**, with NCPart_d^L, NCPart_d^B, and NCPart_d^R defined similarly. There are canonical isomorphisms $\mathrm{NCPart}_d \cong \mathrm{NCPart}_d^T \cong \mathrm{NCPart}_d^L \cong \mathrm{NCPart}_d^B \cong \mathrm{NCPart}_d^R$ based on the indexing of the sides, and we write $[\lambda]^T$, $[\lambda]^L$, $[\lambda]^B$, $[\lambda]^R$, for the image of a noncrossing partition $[\lambda] \in \mathrm{NCPart}_d$ in these other copies.

Since the identifications in Definition 4.8 are based on subscripting conventions, they necessarily break certain symmetries.

Remark 4.9 (Broken symmetries)**.** Iteratively rotating **P** through a counterclockwise angle of $2\pi/4d$ sends a subsurface defining $[\lambda]^T$ to a subsurface defining $[\lambda]^L$, then to a subsurface defining $[\lambda]^B$, then to a subsurface defining $[\lambda]^R$, then to a subsurface defining $[\lambda^+]^T$. The plus indicates that the (combinatorial) noncrossing partition $[\lambda] \vdash [d]$ stays the same until the last step, when $[\lambda^+]$ is $[\lambda]$ with every number increased by one (mod d). In Figure 12, for example, a component of a subsurface containing T_2 is sent to one containing L_2, then B_2, then R_2, then T_3.

The map $p(z) = z^d$ lifts subsets of the sides of $\mathbf{Q}$ to subsets of the sides of $\mathbf{P}$.

Definition 4.10 (Points in branched sides)**.** Given subsets $C \subset I$ and $D \subset J$, we define corresponding subsets of the sides of $\mathbf{P}$ using the map $p(z) = z^d$. For example, $S_{T,C} = p^{-1}(C_T) = \bigcup_{m \in [d]} C_{T_m}$ where $C_{T_m} = p^{-1}(C_T) \cap T_m$ and C_T is given as in Definition 3.8. When C and D are finite, we index the points in the sides of $\mathbf{P}$ by indicating the side in the first subscript and the point in the second subscript. For example, we write $t_{m,i}$ for the point in C_{T_m} with $p(t_{m,i}) = t_i \in C_T$, where $f_T(t_i) = x_i \in C$. If $|C| = k$ and $|D| = l$, then there are $2d(k+l)$ lifted points in the sides S, with $|S_{T,C}| = |S_{B,C}| = dk$ and $|S_{L,D}| = |S_{R,D}| = dl$. We call this a $(k,l)^d$-*configuration of points* in the boundary of the d-branched rectangle $\mathbf{P}$.

If we select a point in I and a point in J, these lift to a point in each side of $\mathbf{P}$.

Definition 4.11 (Representative points)**.** A point $x \in I$ with $C = \{x\}$ determines a $(1,0)^d$-configuration of $2d$ points, one in each of the d top sides and d bottom sides. In particular, there is $t_{m,x} \in T_m$ and $b_{m,x} \in B_m$. Similarly, a point $y \in J$ with $D = \{y\}$ determines a $(0,1)^d$-configuration of $2d$ points, one in each of the d left sides and d right sides. In particular, there is $\ell_{m,y} \in L_m$ and $r_{m,y} \in R_m$. The combination of these two is a $(1,1)^d$-configuration with $4d$ points, one in each side. In all three cases, we say these points *represent* the corresponding side.

4.3. **Noncrossing matchings.** A noncrossing matching is both a special type of noncrossing partition on $[2d]$ points and an encoding of a noncrossing partition on $[d]$ points. Both viewpoints can be illustrated on d-branched rectangles.

Definition 4.12 (Noncrossing matchings)**.** A (combinatorial) *noncrossing matching* $[\mu]$ is a noncrossing partition of the set $[2d]$, necessarily of even size, where every block has size 2. In other words, $\textsc{Shape}([\mu]) = 2^d$. Note that the numbers in a block are forced to have opposite parity since they are separated by an even number of ends of noncrossing arcs. In particular, a (metric) noncrossing matching can be viewed as a noncrossing bijection between the d points in $\sqrt[d]{1}$ with even labels and the d points in $\sqrt[d]{-1}$ with odd labels. A bijection between two sets is sometimes called a *matching*, hence the name. Let NCMat_{2d} denote the set of all noncrossing matchings of $[2d]$.

There is also a topological definition.

Definition 4.13 (Side matchings)**.** The d-branched rectangle $\mathbf{P}$ contains $2d$ top and bottom sides, $T_1, B_1, T_2, B_2, \ldots, T_d, B_d$ in counterclockwise order, starting at the first breakpoint $w_{d \to 1}$, containing the $2d$ points $\sqrt[2d]{1}$ as their midpoints. A (topological noncrossing) *top-bottom matching* is a topological noncrossing partition of $S_T \cup S_B$ where every block contains exactly 2 sides. Let NCMat_{2d}^{TB} denote the collection of all such top-bottom matchings. The bijection $S_T \cup S_B \to [2d]$ sending T_m to $2m - 1$ and B_m to $2m$ extends to a bijection $\text{NCMat}_{2d}^{TB} \to \text{NCMat}_{2d}$. Alternatively, a top-bottom matching can be viewed as a noncrossing matching of the $2d$ points in a $(1,0)^d$-configuration (Definition 4.11). Similarly, $\mathbf{P}$ contains $2d$ left and right sides, $L_1, R_1, L_2, R_2, \ldots, L_d, R_d$ in counterclockwise order, starting at the first breakpoint $w_{d \to 1}$. A (topological noncrossing) *left-right matching* is a topological noncrossing partition of $S_L \cup S_R$ where every block contains exactly 2 sides. Let NCMat_{2d}^{LR} denote the collection of all such left-right matchings. The bijection $S_L \cup S_R \to [2d]$ sending L_m to $2m-1$ and R_m to $2m$ extends to a bijection
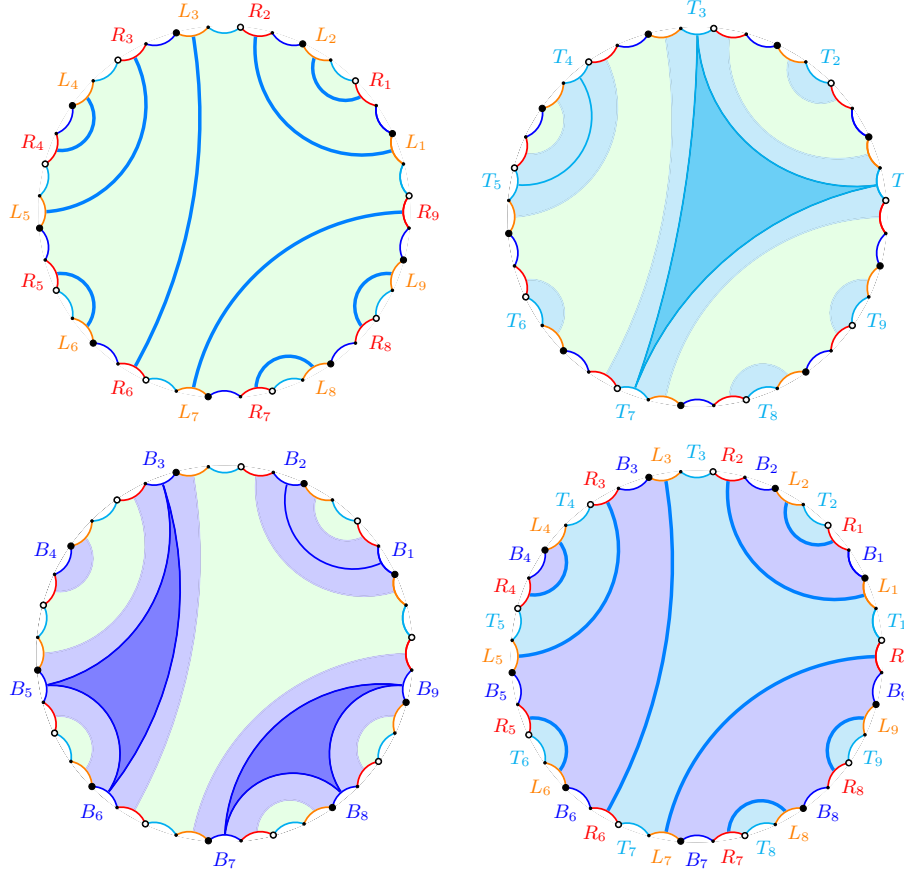
FIGURE 13. The noncrossing left-right matching $[\mu]^{LR}$ (upper left), the noncrossing top partition $[\lambda]^T = 137|2|45|6|8|9$ (upper right), the noncrossing bottom partition $[\lambda]^B = 12|356|4|789$ (lower left), and the 2-coloring (lower right), all contain the same combinatorial information. The partition figures include the convex hulls of representative points to make them easier to see.

$\mathrm{NCMAT}_{2d}^{LR} \to \mathrm{NCMAT}_{2d}$. Alternatively, a left-right matching can be viewed as a noncrossing matching of the $2d$ points in a $(0,1)^d$-configuration (Definition 4.11). We write $[\mu]^{LR}$ and $[\mu]^{TB}$ for the left-right and top-bottom matchings that correspond to $[\mu] \in \mathrm{NCMAT}_{2d}$.

There are bijections between NCMAT_{2d}^{LR}, NCPART_d^T and NCPART_d^B, and between NCMAT_{2d}^{TB}, NCPART_d^L and NCPART_d^R. We begin with an example.

Example 4.14. Let **P** be a standard 9-branched rectangle and let $[\mu]^{LR}$ be a left-right matching in NCMAT_{18}^{LR} with blocks $\{L_1, R_2\}$, $\{L_2, R_1\}$, $\{L_3, R_6\}$, $\{L_4, R_4\}$, $\{L_5, R_3\}$, $\{L_6, R_5\}$, $\{L_7, R_9\}$, $\{L_8, R_7\}$, and $\{L_9, R_8\}$. The upper left corner of Figure 13 shows the multiarc whose arcs are convex hulls of the representative points in a $(0,1)^9$-configuration (e.g. the "hyperbolic" arc from $\ell_{1,y}$ to $r_{2,y}$). The

$$\text{NCPART}_d^T$$

$$\text{NCPART}_d \qquad \qquad \uparrow \text{KREW}^{BT}$$

$$\text{NCPART}_d^B$$

FIGURE 14. Three bijections that do not form a commutative diagram, since the composition of all three starting at NCPART_d is the Kreweras complement map KREW, a non-trivial order-reversing automorphism.

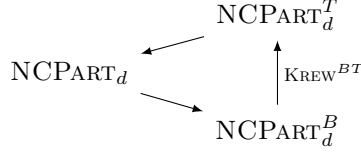complementary regions of $\mathbf{P}$ with these arcs removed can be 2-colored: a lighter sky blue if it contains a top side and a darker sea blue if it contains a bottom side (lower right). The sky blue subsurface $\mathbf{U}_T$ contains S_T and the corresponding (topological) noncrossing partition of top sides is $[\lambda]^T = 137|2|45|6|8|9 \in \text{NCPART}_9^T$ (upper right). The sea blue subsurface $\mathbf{U}_B$ contains S_B and the corresponding (topological) noncrossing partition of bottom sides is $[\lambda]^B = 12|356|4|789 \in \text{NCPART}_9^B$ (lower left). The convex hulls of representative points in each block (e.g. the "hyperbolic" triangle connecting $b_{3,x}$, $b_{5,x}$, and $b_{6,x}$), are also included. This process is also reversible in the sense that the original left-right matching can be recovered from either the top or the bottom noncrossing partition. Given $[\lambda]^T$, for example, we can define $\mathbf{U}_T$ to be an ϵ-neighborhood of convex hulls of the representative points in each block union the sides S_T. The 9 arcs of $\partial \mathbf{U}_T$ in the interior of $\mathbf{P}$ are a multiarc that defines the left-right matching $[\mu]^{LR}$.

Arguing as in Example 4.14 establishes the following result.

Proposition 4.15 (Matchings and partitions). *There are bijections*

$$\text{NCPART}_d^T \leftrightarrow \text{NCMAT}_{2d}^{LR} \leftrightarrow \text{NCPART}_d^B$$

and

$$\text{NCPART}_d^L \leftrightarrow \text{NCMAT}_{2d}^{TB} \leftrightarrow \text{NCPART}_d^R.$$

The bijections between different types of noncrossing partitions are related to the Kreweras complement map.

Definition 4.16 (Kreweras complement maps). A *topological Kreweras complement* is a bijection $\text{KREW}^{XY} \colon \text{NCPART}_d^X \to \text{NCPART}_d^Y$ from Proposition 4.15, where X is T, L, B or R and $Y = X^{\text{op}}$ is the *opposite side* B, R, T or L, respectively. Combining a topological Kreweras complement map with the bijections of Definition 4.8 produces the classical order-reversing *Kreweras complement map* (see [Kre72]) $\text{KREW} \colon \text{NCPART}_d \to \text{NCPART}_d$, or its inverse. The bottom-to-top and right-to-left maps produce the Kreweras complement, and the top-to-bottom and left-to-right maps produce its inverse. Figure 14 illustrates the process.

4.4. **Noncrossing permutations.** When noncrossing partitions are converted to noncrossing permutations, the Kreweras map has an algebraic description.

Definition 4.17 (Noncrossing permutations). A set partition $[\lambda] \vdash [d]$ can be converted into a permutation $\pi \in \text{SYM}_d$ by turning each block of $[\lambda]$ of size k into a k-cycle in which the elements of the block are listed in increasing order. For

example, if $[\lambda] = 137|2|45|6|8|9$, then $\pi = \text{PERM}([\lambda]) = (1\ 3\ 7)(4\ 5)$ in SYM_9. This defines a map $\text{PERM}\colon \text{SETPART}_d \hookrightarrow \text{SYM}_d$ which is injective because the set partition can be reconstructed from its permutation image. When $[\lambda]$ is a noncrossing partition, we call $\pi = \text{PERM}([\lambda])$ a *noncrossing permutation*. Let NCPERM_d denote the collection of noncrossing permutations in SYM_d. The restriction $\text{PERM}\colon \text{NCPART}_d \to \text{NCPERM}_d$ is a bijection as shown by Biane in [Bia97]. In the metric version of noncrossing partitions, the disjoint cycles of $\text{PERM}([\lambda])$ record the order in which vertices occur in the counterclockwise boundary cycle of the convex hull of each block of $[\lambda]$.

The bijection from NCPART_d to NCPERM_d makes the latter into a partially ordered set, and this has a useful interpretation which is purely algebraic.

Definition 4.18 (Absolute order). Let T be the set of all transpositions in the symmetric group SYM_d and, for each $\sigma \in \text{SYM}_d$, define the *absolute reflection length* $\ell(\sigma)$ to be the length of a minimal factorization of σ into elements of T. Declaring $\sigma \le \tau$ if $\ell(\sigma) + \ell(\sigma^{-1}\tau) = \ell(\tau)$ makes SYM_d into a partially ordered set which happens to be a lattice. If we define δ to be the d-cycle $(1\ 2\ \cdots\ d)$, then the interval $[1, \delta]$ in SYM_d is the set NCPERM_d, so the set of noncrossing permutations is partially ordered with the *absolute order*. One should think of the interval $[1, \delta]$ as a union of geodesics from the identity to δ in the Cayley graph of SYM_d with respect to the generating set T. Moreover, the map $\text{PERM}\colon \text{NCPART}_d \to \text{NCPERM}_d$ is a poset isomorphism.

Definition 4.19 (Noncrossing permutations of sides). Composing the identifications in Definition 4.8 with the function in Definition 4.17 produces new functions $\text{PERM}\colon \text{NCPART}_d^X \to \text{NCPERM}_d$ where X is T, L, B, or R. We write π^X when $\pi^X = \text{PERM}([\lambda]^X)$ for some $[\lambda]^X \in \text{NCPART}_d^X$. Alternatively, let $\mathbf{U}$ be a closed, possibly disconnected, subsurface of $\mathbf{P}$ with contractible components and $\text{NCPART}(\mathbf{U}) = [\lambda]$. The sides S_X occur in the boundary $\mathbf{U}$ and the disjoint cycles of π^X record the counterclockwise ordering of the sides in the boundaries of each component.

Definition 4.20 (Permutations and matchings). Let $[\mu] \vdash [2d]$ be a noncrossing matching. By Proposition 4.15, the left-right matching $[\mu]^{LR}$ determines noncrossing partitions $[\lambda]^T$ and $[\lambda]^B$. The corresponding noncrossing permutations, π^T and π^B, are the *top and bottom permutations* associated with $[\mu]^{LR}$. Similarly, the top-bottom matching $[\mu]^{TB}$ determines noncrossing partitions $[\lambda]^L$ and $[\lambda]^R$, and the corresponding noncrossing permutations, π^L and π^R, are the *left and right permutations* associated with $[\mu]^{TB}$.

There is a close algebraic connection between the two noncrossing permutations associated with a noncrossing side-to-side matching.

Example 4.21. The noncrossing matching $[\mu]^{LR}$ in Example 4.14 determines the noncrossing partitions $[\lambda]^T = 137|2|45|6|8|9$ and $[\lambda]^B = 12|356|4|789$, which become the noncrossing permutations $\pi^T = (1\ 3\ 7)(4\ 5)$ and $\pi^B = (1\ 2)(3\ 5\ 6)(7\ 8\ 9)$ in SYM_9. Note that the composition $\pi^T \cdot \pi^B = (1\ 2\ \cdots\ 9)$. This can be understood geometrically. The permutation π^B is applied first. It identifies 6 with the side B_6 which is connected to B_3 in the counterclockwise order in the boundary of the block $\{3, 5, 6\}$ and this side is identified with the number 3. The permutation π^T identifies 3 with the side T_3 which is connected to T_7 in the counterclockwise order

in the boundary of the block $\{1, 3, 7\}$ and this is identified with the number 7. This can be visualized as a path from B_6 to B_3 to T_3 (passing through L_3) to T_7. This is nearly a full circuit around the arc from R_6 to L_3, from the bottom side B_6 adjacent to R_6 to the top side T_7, also adjacent to R_6. Between the start and end sides there is exactly one vertex where the indexing changes (Remark 4.9), so 6 goes to 7 in the composition. Similarly, i goes to $i + 1 \bmod 9$ for every $i \in [9]$.

Arguing as in Example 4.21 establishes the following.

Proposition 4.22 (Factors). *Let $[\mu] \vdash [2d]$ be a noncrossing matching and let δ be the d-cycle $(1\ 2\ \cdots\ d)$. The top and bottom permutations associated to the left-right matching $[\mu]^{LR}$ satisfy the equation $\pi^T \cdot \pi^B = \delta$, and the left and right permutations associated to the top-bottom matching $[\mu]^{TB}$ satisfy the equation $\pi^L \cdot \pi^R = \delta$.*

Proposition 4.22 gives an algebraic description of the Kreweras complement map.

Remark 4.23 (Kreweras complements). Proposition 4.22 shows, for example, that the permutation version of KREW^{BT} sends π^B to $\pi^T = \delta \cdot (\pi^B)^{-1}$, its *left complement* with respect to $\delta = (1\ 2\ \cdots\ d)$. Similarly, the permutation version of KREW^{TB} sends π^T to $\pi^B = (\pi^T)^{-1} \cdot \delta$, its *right complement* with respect to δ.

5. Geometric Combinatorics

As we transition from looking at a single polynomial (Part 1) to looking at spaces of polynomials (Part 2), we introduce a way of sending each monic polynomial to a point in a product of order complexes. After turning the combinatorics of the regular complex $\mathbf{P}_p$ into two chains in noncrossing partition lattices (5.1), we combine this with the metric of the critical value complex $\mathbf{Q}'_p$ to create the GeoCom map from a polynomial space to a product of two simplicial complexes (5.2).

5.1. **Chains of side partitions.** The combinatorial structure of the regular point complex $\mathbf{P}_p$ encodes two chains of noncrossing partitions. We begin by listing our standing assumptions.

Remark 5.1 (Standing assumptions). In this section $p \colon \mathbb{C} \to \mathbb{C}$ is a monic complex polynomial of degree d with fixed coordinate rectangle $\square \supset \mathbf{cvl}(p)$. The critical value complex $\mathbf{Q}'_p$, regular value complex $\mathbf{Q}_p$ and regular point complex $\mathbf{P}_p$ are as defined in Section 3. We assume that $\mathbf{Q}'_p$ is (k', l')-subdivided and $\mathbf{Q}_p$ is (k, l)-subdivided, with $k = k' + 1$ and $l = l' + 1$. All illustrations in this section use the degree 5 polynomial p of Example 2.3.

Since we are only interested in its combinatorial structure, we redraw the regular point complex $\mathbf{P}_p$ as a cell structure on a standard branched rectangle. We do this using a standard labeling that comes from the fact that p is monic.

Definition 5.2 (Labeling $\mathbf{P}_p$). Recall that cell structure of $\mathbf{Q}'_p$ depends on the choice of rectangle $\square$ (Remark 3.10), but once that choice has been made, the cell structure of $\mathbf{Q}_p$ (and $\mathbf{P}_p$) is unaffected by the size of the larger rectangle on which $\mathbf{Q}$ is built (Remark 3.24). Thus we are free to assume that interval $\mathbf{J}$ includes 0. Let γ be the portion of the x-axis that starts in the right side $\mathbf{R}$ of $\mathbf{Q}_p$ and extends to the right. Because p is monic, the preimage of this regular ray lifts to d topological rays that start in the right sides of $\mathbf{P}_p$ and end up asymptotic to the rays in the dth root of unity directions. The side $\mathbf{R}_d = \mathbf{R}_0$ in $\mathbf{P}_p$ is the one whose
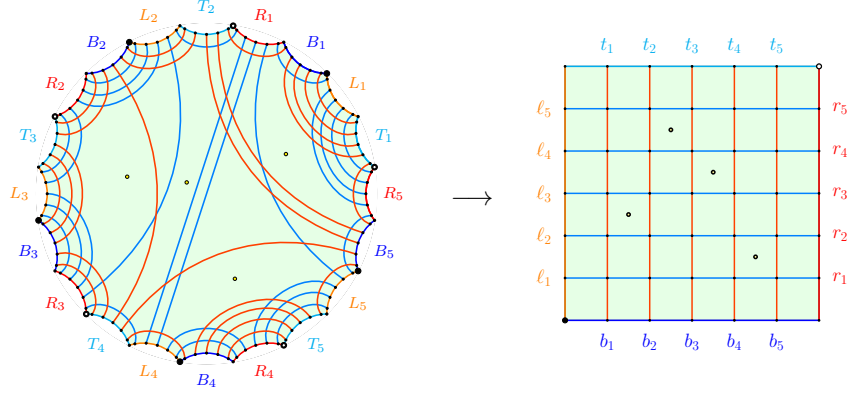
FIGURE 15. The "regular" map $\mathbf{p}\colon \mathbf{P}_p \to \mathbf{Q}_p$ for the polynomial p of Example 2.3 is shown in standardized form. The regular value complex $\mathbf{Q}_p$ of Figure 8 is shown here as a standard rectangle with an equally spaced $(5,5)$-subdivision. Similarly, the regular point complex $\mathbf{P}_p$ of Figure 11 is shown here in a 20-sided standard 5-branched rectangle.

ray ends up asymptotic to the positive x-axis, and the remaining sides and vertices are indexed so that its boundary labels look like a standard d-branched rectangle (Definition 4.7). See Figure 11.

Definition 5.3 (Standard representations)**.** A *standard representation of $\mathbf{Q}_p$* is one where the small rectangles in its (k, l)-subdivision are the same size, and a *standard representation of $\mathbf{P}_p$* is one where its cell structure is drawn on the $4d$-gon that is the standard d-branched rectangle (Definition 4.7), according to the monic polynomial labels (Definition 5.2).

Figure 15 shows standard representations for our running example. The representations of Definition 5.3 are possible because the regular point complex $\mathbf{P}_p$ is always a nonsingular disk diagram. This would not always be possible for the critical point complex $\mathbf{P}'_p$ since it is singular when the critical value complex $\mathbf{Q}'_p$ has critical values in its boundary (Corollary 3.18). The subdivision of $\mathbf{Q}_p$ can be viewed as a horizontal subdivision and a vertical subdivision that have been superimposed.

Definition 5.4 (Arcs)**.** The regular value complex $\mathbf{Q}_p = \mathbf{I}_p \times \mathbf{J}_p$ is a cell structure on the rectangle $\mathbf{Q} = \mathbf{I} \times \mathbf{J}$. As intermediate steps we have $\mathbf{Q}_{\Re(p)} = \mathbf{I}_p \times \mathbf{J}$ and let $\mathbf{Q}_{\Im(p)} = \mathbf{I} \times \mathbf{J}_p$, which have a $(k, 0)$-subdivision and a $(0, l)$-subdivision. Let α_i be the edge in $\mathbf{Q}_{\Re(p)}$ from b_i in the bottom side to t_i in the top side, with $i \in [k]$. Let β_j be the edge in $\mathbf{Q}_{\Im(p)}$ from ℓ_j in the left side to r_j in the right side, with $j \in [l]$. These persist as subdivided arcs in the (k, l)-subdivided $\mathbf{Q}_p$ and we call them the *vertical arcs α_i* and the *horizontal arcs β_j*.

For our standard example, Figure 16 shows the structures associated with a single vertical arc. Here are the definitions to make this precise.

Definition 5.5 (Subsurfaces of $\mathbf{P}_p$ and $\mathbf{Q}_p$)**.** The closed complementary regions (as in Definition 2.18) of the vertical arc α_i from b_i to t_i are the *left subsurface $\mathbf{V}_i^L$*
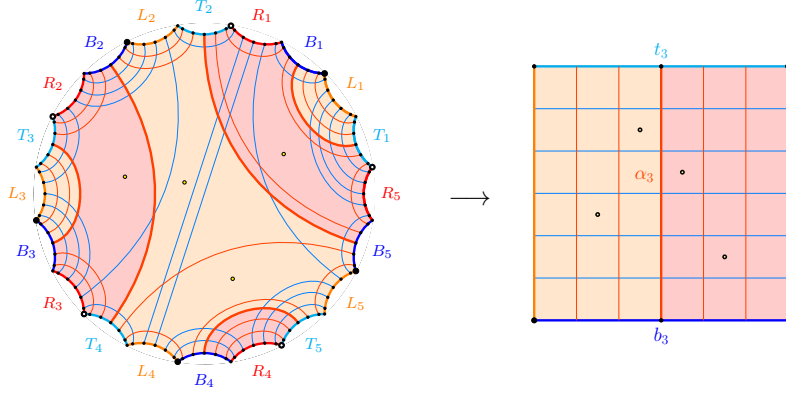
FIGURE 16. The vertical arc α_3 from b_3 to t_3 in the range divides the regular value complex $\mathbf{Q}_p$ into an orange left subsurface $\mathbf{V}_3^L$ and a red right subsurface $\mathbf{V}_3^R$. Their preimages divide the regular point complex $\mathbf{P}_p$ into an orange "left" subsurface $\mathbf{U}_3^L = p^{-1}(\mathbf{V}_3^L)$ and a red "right" subsurface $\mathbf{U}_3^R = p^{-1}(\mathbf{V}_3^R)$ separated by the multiarc $\widetilde{\alpha}_3 = p^{-1}(\alpha_3)$. The corresponding topological noncrossing partitions are $\mathrm{NCPART}^L(\mathbf{U}_3^L) = 1|245|3$ of the 5 left sides of $\mathbf{P}_p$, and $\mathrm{NCPART}^R(\mathbf{U}_3^R) = 15|23|4$ of the 5 right sides of $\mathbf{P}_p$.

and the *right subsurface* $\mathbf{V}_i^R$. The complementary regions of a horizontal regular arc β_j from ℓ_j to r_j are the *top subsurface* $\mathbf{V}_j^T$ and the *bottom subsurface* $\mathbf{V}_j^B$. Collectively these the $2(k+l)$ *side subsurfaces of* $\mathbf{Q}_p$. Their preimages are the *left subsurface* $\mathbf{U}_i^L = p^{-1}(\mathbf{V}_i^L)$, the *right subsurface* $\mathbf{U}_i^R = p^{-1}(\mathbf{V}_i^R)$, the *top subsurface* $\mathbf{U}_j^T = p^{-1}(\mathbf{V}_j^T)$, and the *bottom subsurface* $\mathbf{U}_j^B = p^{-1}(\mathbf{V}_j^B)$. These are the $2(k+l)$ *side subsurfaces of* $\mathbf{P}_p$. See Table 1.

As in Example 4.14, these subsurfaces produce noncrossing partitions.

Definition 5.6 (Side partitions and side matchings)**.** For each vertical arc α_i from b_i to t_i, we have $L \subset \mathbf{V}_i^L \subset \mathbf{Q}_p$, so $S_L \subset \mathbf{U}_i^L \subset \mathbf{P}_p$. The ith *left partition* $[\lambda_i]^L = \mathrm{NCPART}^L(\mathbf{U}_i^L)$ (Definition 4.8) is the corresponding noncrossing partition of the left sides of $\mathbf{P}_p$. The preimage $\widetilde{\alpha}_i = p^{-1}(\alpha_i)$ of α_i is a multiarc, a collection of d noncrossing arcs that connect the d top sides and the d bottom sides. The mulitarc $\widetilde{\alpha}_i$ defines a *top-bottom matching* $[\mu_i]^{TB}$ and forms the common boundary between the two subsurfaces $\mathbf{U}_i^L$ and $\mathbf{U}_i^R$. Similarly, the ith *right partition* is $[\lambda_i]^R = \mathrm{NCPART}^R(\mathbf{U}_i^R)$. And for any horizontal arc β_j, the jth *top partition* is $[\lambda_j]^T = \mathrm{NCPART}^T(\mathbf{U}_j^T)$ and the jth *bottom partition* is $[\lambda_j]^B = \mathrm{NCPART}^B(\mathbf{U}_j^B)$. The preimage $\widetilde{\beta}_j = p^{-1}(\beta_j)$ of β_j is a multiarc, a collection of d noncrossing arcs that connect the d left sides and the d right sides. The multiarc $\widetilde{\beta}_j$ defines a *left-right matching* $[\mu_j]^{LR}$ and form the common boundary between the two subsurfaces $\mathbf{U}_j^T$ and $\mathbf{U}_j^B$. These are the *side partitions* and *side matchings* of $\mathbf{P}_p$.

Nested subsurfaces in $\mathbf{Q}_p$ lift to nested subsurfaces in $\mathbf{P}_p$ and comparable noncrossing partitions. For our standard example Figure 17 shows the structures associated with the vertical subdivisions of $\mathbf{Q}_p$, and Figure 18 shows the structures

name	partition	permutation	in $\mathbf{P}_p$	in $\mathbf{Q}_p$
TB matching	$[\mu_i]^{TB} \in \mathrm{NCMat}_{2d}^{TB}$	—	$\widetilde{\alpha}_i$	α_i
LR matching	$[\mu_j]^{LR} \in \mathrm{NCMat}_{2d}^{LR}$	—	$\widetilde{\beta}_j$	β_j
top partition	$[\lambda_j]^T \in \mathrm{NCPart}_d^T$	π_j^T	$\mathbf{U}_j^T$	$\mathbf{V}_j^T$
left partition	$[\lambda_i]^L \in \mathrm{NCPart}_d^L$	π_i^L	$\mathbf{U}_i^L$	$\mathbf{V}_i^L$
bottom partition	$[\lambda_j]^B \in \mathrm{NCPart}_d^B$	π_j^B	$\mathbf{U}_j^B$	$\mathbf{V}_j^B$
right partition	$[\lambda_i]^R \in \mathrm{NCPart}_d^R$	π_i^R	$\mathbf{U}_i^R$	$\mathbf{V}_i^R$

TABLE 1. Notations for the side matchings and side partitions of the regular point complex $\mathbf{P}_p$ (Definition 5.6).
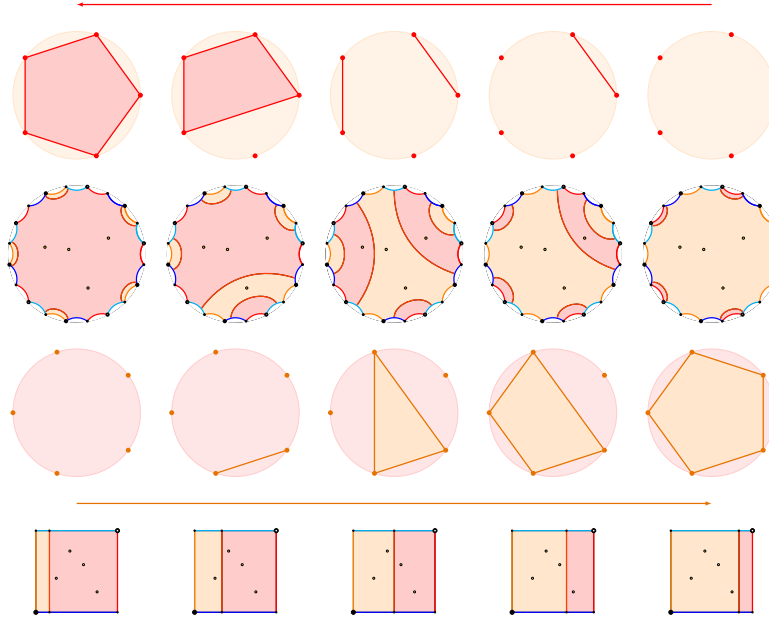
FIGURE 17. The bottom row shows the left and right subsurfaces $\mathbf{V}_i^L, \mathbf{V}_i^R \subset \mathbf{Q}_p$ separated by the vertical arcs α_i. The second row shows the corresponding left and right subsurfaces $\mathbf{U}_i^L, \mathbf{U}_i^R \subset \mathbf{P}_p$ separated by the 5 arcs of the multi arc $\widetilde{\alpha}_i$ which defines the top-bottom matching $[\mu_i]^{TB}$. The third row shows the chain $1|2|3|4|5 < 1|2|3|45 < 1|245|3 < 1|2345 < 12345$ of left noncrossing partitions $[\lambda_i]^L \in \mathrm{NCPart}_5^L$. And the top row shows the chain $12345 > 1235|4 > 15|23|4 > 15|2|3|4 > 1|2|3|4|5$ of right noncrossing partitions $[\lambda_i]^R \in \mathrm{NCPart}_5^R$.

associated with the horizontal subdivisions of $\mathbf{Q}_p$. The side chains are strictly monotonic because of the way in which the cell complexes for p are defined.

Lemma 5.7 (Distinct). *Nested side surfaces of $\mathbf{P}_p$ have distinct partitions.*

Proof. We prove this for nested left subsurfaces. For any $i_1, i_2 \in [k]$ with $i_1 < i_2$, we have $\mathbf{U}_{i_1}^L \subset \mathbf{U}_{i_2}^L$ and $[\lambda_{i_1}]^L \leq [\lambda_{i_2}]^L$ (Definition 4.4). We know that there is at least one critical value of p in $\mathbf{V}_{i_2}^L \setminus \mathbf{V}_{i_1}^L$ by construction. As a consequence the subsurface $\mathbf{U}_{i_1}^L$ has more connected components than $\mathbf{U}_{i_2}^L$ (Proposition 2.24) and the noncrossing permutation $\text{PERM}([\lambda_{i_1}]^L)$ has more disjoint cycles than $\text{PERM}([\lambda_{i_2}]^L)$ (Definition 4.12), so the inequality is strict. $\qquad\square$

Definition 5.8 (Side chains of $\mathbf{P}_p$). The k vertical arcs α_i from b_i to t_i define nested left subsurfaces $L \subset \mathbf{V}_1^L \subset \mathbf{V}_2^L \subset \cdots \subset \mathbf{V}_k^L \subset \mathbf{Q}_p$ which lift to $S_L \subset \mathbf{U}_1^L \subset \mathbf{U}_2^L \subset \cdots \subset \mathbf{U}_k^L \subset \mathbf{P}_p$ which in turn define an increasing chain $[\lambda_1]^L < [\lambda_2]^L < \cdots < [\lambda_k]^L$ of left noncrossing partitions in NCPART_d^L (Definition 4.4 and Lemma 5.7). In the other direction, the nested right subsurfaces $\mathbf{Q}_p \supset \mathbf{V}_1^R \supset \mathbf{V}_2^R \supset \cdots \supset \mathbf{V}_k^R \supset R$ lift to $\mathbf{P}_p \supset \mathbf{U}_1^R \supset \mathbf{U}_2^R \supset \cdots \supset \mathbf{U}_k^R \supset S_R$ which define a decreasing chain $[\lambda_1]^R > [\lambda_2]^R > \cdots > [\lambda_k]^R$ of right noncrossing partitions in NCPART_d^R. Similarly, the l horizontal arcs β_j from ℓ_j to r_j define an increasing chain $[\lambda_1]^B < [\lambda_2]^B < \cdots < [\lambda_l]^B$ of bottom noncrossing partitions in NCPART_d^B, and a decreasing chain $[\lambda_1]^T > [\lambda_2]^T > \cdots > [\lambda_j]^T$ of top noncrossing partitions in NCPART_d^T. These are the 4 *side chains of $\mathbf{P}_p$*. Since the right and left chains are related by the topological Kreweras complement map (Definition 4.16), they contain the same information, and the same is true for the top and bottom chains. We focus on the increasing left and bottom chains.

In our example, the side chains start at the discrete partition and end at the indiscrete partition because $\partial \mathbf{Q}_p'$ is regular.

Lemma 5.9 (Discrete and indiscrete). *The side chains of $\mathbf{P}_p$ start at the discrete partition if and only if the corresponding start side of $\mathbf{Q}_p'$ is regular, and they end at the indiscrete partition if and only if the corresponding end side of $\mathbf{Q}_p'$ is regular.*

Proof. It is sufficient to prove this for the start of the left chain. By the same reasoning as in the proof of Lemma 5.7, the first partition $[\lambda_1]^L$ is discrete if and only if the first column of $\mathbf{Q}_p$ is regular, which is true if and only if the left side of $\mathbf{Q}_p' = \square$ has no critical values. $\qquad\square$

Remark 5.10 (Real and imaginary Morse functions). The left chain of $\mathbf{P}_p$ essentially encodes the changes in the topology of the preimages of lower intervals for the *real Morse function* $\Re \circ p \colon \mathbb{C} \to \mathbb{R}$, but with slight modifications because of the rectangle $\square = [x_\ell', x_r'] \times [y_b', y_t']$ surrounding the critical values. The critical values of this Morse function are the points $C' = \{x_1', \dots, x_k'\}$ with the possible addition of x_ℓ' and x_r', if there is a critical value in the left and/or right side of $\square$. The values x_i used to define $\mathbf{I}_p$ are representatives of the equivalence classes of regular levels of this Morse function, with possible duplication at the extremes if there are no critical values in the left and/or right side of $\square$. To see the connection with Morse level sets, note that the regular point x_i used to define the vertical arc α_i and the left subsurface $\mathbf{V}_i^L$, also defines the left half-space $\mathbf{H}_i^L$ with the vertical line $\{x_i\} \times \mathbb{R}$ as its boundary. And since each $\mathbf{H}_i^L \setminus \mathbf{V}_i^L$ is regular, the preimages
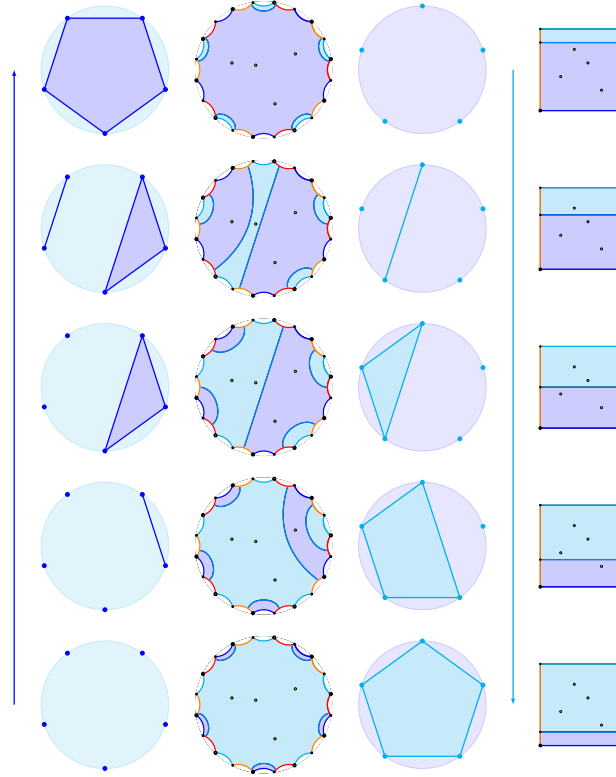
FIGURE 18. The last column shows the top and bottom subsurfaces $\mathbf{V}_j^T, \mathbf{V}_j^B \subset \mathbf{Q}_p$ separated by the horizontal arcs β_j. The second column shows the corresponding top and bottom subsurfaces $\mathbf{U}_j^T, \mathbf{U}_j^B \subset \mathbf{P}_p$ separated by the 5 arcs of the multiarc $\widetilde{\beta}_j$ which defines the left-right matching $[\mu_j]^{LR}$. The first column shows the chain $1|2|3|4|515|2|3|4 < 145|2|3 < 145|23 < 12345$ of bottom noncrossing partitions $[\lambda_j]^B \in \mathrm{NCPART}_5^B$. And the third column shows the chain $1|2|3|4|5 < 1|24|3|5 < 1|234|5 < 1|2345 < 12345$ of top noncrossing partitions $[\lambda_j]^T \in \mathrm{NCPART}_5^T$.

under p have the same homotopy type. In particular, the portion of the domain shown in the diagrams in the second row of Figure 17 contains all of the interesting information. Similar comments hold for the bottom chain of $\mathbf{P}_p$ and the *imaginary Morse function* $\Im \circ p \colon \mathbb{C} \to \mathbb{R}$.

5.2. **The geometric combinatorics map.** We now assemble all of the geometric combinatorial information about monic polynomials with critical values in a fixed closed rectangle $\square$ into a single continuous map from a polynomial space to a bisimplicial cell complex. The range is built out of order complexes.

Definition 5.11 (Order complex). Let $|\mathrm{NCPART}_d|_\Delta$ be the ordered simplicial complex that is the *order complex* of NCPART_d. Its vertices are labeled by the elements of NCPART_d and it has an ordered k-simplex on vertices $[\lambda_1], [\lambda_2], \ldots, [\lambda_k]$ for every chain $[\lambda_1] < [\lambda_2] < \cdots < [\lambda_k]$ in NCPART_d. A point in $|\mathrm{NCPART}_d|_\Delta$ is a

formal sum $\sum_{i\in[k]} \mathbf{wt}_i \cdot [\lambda_i]$, where the $[\lambda_i]$ label the vertices of an ordered simplex in $|\mathrm{NCPART}_d|_\Delta$ and the real numbers $\mathbf{wt}_i \in (0,1)$ with $\sum_{i\in[k]} \mathbf{wt}_i = 1$ are the barycentric coordinates of a point in the interior of that simplex.

Definition 5.12 (Geometric combinatorics map)**.** Let $\mathrm{POLY}_d^{mc}(\blacksquare)$ be the set of monic centered complex polynomials of degree d with $\mathbf{cvl}(p)$ in a fixed coordinate rectangle $\blacksquare$. There is a well-defined *geometric combinatorics map*

$$\mathrm{GEOCOM}\colon \mathrm{POLY}_d^{mc}(\blacksquare) \to |\mathrm{NCPART}_d^L|_\Delta \times |\mathrm{NCPART}_d^B|_\Delta$$

defined by sending a polynomial p to

$$\mathrm{GEOCOM}(p) = \left(\sum_{i\in[k]} \mathbf{wt}_i^I \cdot [\lambda_i]^L, \sum_{j\in[l]} \mathbf{wt}_j^J \cdot [\lambda_j]^B \right).$$

The left side partitions $[\lambda_i]^L$ of Definition 5.8 label the vertices of a simplex in the order complex $|\mathrm{NCPART}_d^L|_\Delta$, and the numbers $(\mathbf{wt}_1^I, \ldots, \mathbf{wt}_k^I) = \mathrm{BARY}(\mathbf{I}_p')$ of Definition 3.2 are the barycentric coordinates of a point in the interior of that simplex (Definition 5.11). Similarly, the bottom side partitions $[\lambda_i]^B$ label the vertices of a simplex in the order complex $|\mathrm{NCPART}_d^B|_\Delta$ and the relative widths $(\mathbf{wt}_1^J, \ldots, \mathbf{wt}_l^J) = \mathrm{BARY}(\mathbf{J}_p')$ are the barycentric coordinates of a point in in the interior of that simplex. The map $\mathrm{PERM}\colon \mathrm{NCPART}_d \to \mathrm{NCPERM}_d$ (Definition 4.17) sends side partitions such as $[\lambda_i]^L$ to *side permutations* $\pi_i^L = \mathrm{PERM}([\lambda_i]^L)$. See Table 1 on page 37. This means that $|\mathrm{NCPART}_d|_\Delta = |\mathrm{NCPERM}_d|_\Delta$ with relabeled vertices. There is an alternative version of the geometric combinatorics map

$$\mathrm{GEOCOM}\colon \mathrm{POLY}_d^{mc}(\blacksquare) \to |\mathrm{NCPERM}_d^L|_\Delta \times |\mathrm{NCPERM}_d^B|_\Delta$$

using noncrossing permutations, and defined by the formula

$$\mathrm{GEOCOM}(p) = \left(\sum_{i\in[k]} \mathbf{wt}_i^I \cdot (\pi_i^L), \sum_{j\in[l]} \mathbf{wt}_j^J \cdot (\pi_j^B) \right).$$

In both formulations, the simplices are determined by the combinatorial structure of the regular point complex $\mathbf{P}_p$, and the points in these simplices are selected using the metric structure of the critical value complex $\mathbf{Q}_p'$.
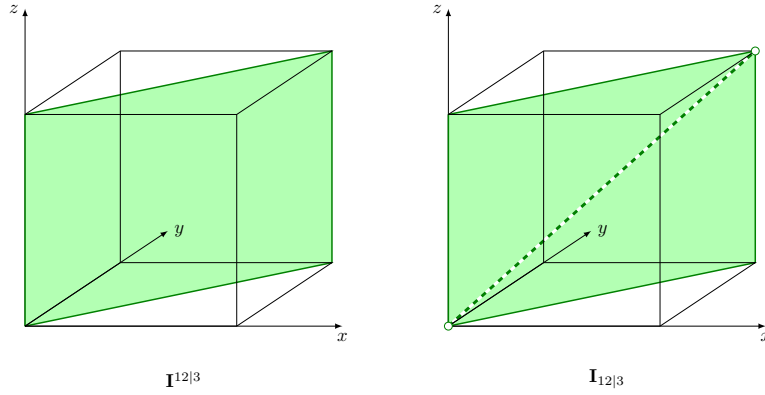
FIGURE 19. On the left, the subspace $\mathbf{I}^{12|3}$ forms a rectangular subspace with side lengths of $\sqrt{2}$ and 1 inside the 3-cube $\mathbf{I}^3$. On the right, the stratum $\mathbf{I}_{12|3}$ is the same rectangle, but with the long diagonal $\mathbf{I}^{123} = \mathbf{I}_{123}$ removed.

Part 2. Spaces of Polynomials

In this part the focus shifts from a single polynomial to spaces of polynomials. The Lyashko–Looijenga map, or LL map, is a stratified covering map from a polynomial space to a multiset space. Its structure makes it possible to lift certain types of multiset paths (a continuously varying families of multisets) to a polynomial path (a continuously varying family of polynomials). And lifted polynomial paths lead to polynomial homotopies that continuously modify spaces of polynomials. The goal of Part 2 is to prove Theorems E, F and G using these polynomial homotopies.

Part 2 is structured as follows. Section 6 discusses the MULT map as a stratified covering MULT: $\mathbf{X}^n \to \text{MULT}_n(\mathbf{X})$. Section 7 discusses the Lyashko–Looijenga map, or LL map, as a stratified covering LL: $\text{POLY}_d^{mt}(\mathbf{X}) \to \text{MULT}_n(\mathbf{X})$. Section 8 shows that paths in $\text{MULT}_n(\mathbf{X})$ with weakly increasing shapes can be uniquely lifted to $\text{POLY}_d^{mt}(\mathbf{X})$ through the LL map, using path lifting to $\mathbf{X}^n$ through the MULT map as a model. Section 9 turns these unique polynomial lifts into polynomial homotopies, and Section 10 uses these to establish relationships between spaces of polynomials, including homeomorphisms, compactifications, deformations and quotients.

6. PRODUCTS AND MULTISETS

This section describes stratifications of the product space $\mathbf{X}^n$ and the multiset space $\text{MULT}_n(\mathbf{X})$ that turn the MULT map into a stratified covering. After discussing product strata (6.1) we discuss multiset strata (6.2).

6.1. **Product strata.** The horizontal map SETPART: $\mathbf{X}^n \to \text{SETPART}_{[n]}$ in Figure 3 on page 11 subdivides $\mathbf{X}^n$ into strata we call $\mathbf{X}_{[\lambda]}$ and into subspaces we call $\mathbf{X}^{[\lambda]}$. We begin with an example and then define the notation.

Example 6.1 (Cubes). Let $\mathbf{I} = [0,1]$, or more generally let $\mathbf{I} = [x_\ell, x_r]$ be an interval of length s. The subspace $\mathbf{I}^{12|3}$ inside the 3-cube $\mathbf{I}^3$ is an $(\sqrt{2})s \times s$ rectangle containing the long diagonal subspace $\mathbf{I}^{123}$. The stratum $\mathbf{I}_{12|3}$ is the same rectangle

with this long diagonal removed. Note that the closure of the stratum $\mathbf{I}_{12|3}$ is the subspace $\mathbf{I}^{12|3}$. The stratum $\mathbf{I}_{12|3}$ is homeomorphic but not isometric to $\mathrm{CONF}_2(\mathbf{I})$, the space of two distinct unlabeled points in $\mathbf{I}$. See Figure 19. More generally, $\mathbf{I}^n$ is an n-dimensional cube of side length s. For each set partition $[\lambda] \vdash [n]$ with k blocks of size $a_1, \ldots, a_k$, the subspace $\mathbf{I}^{[\lambda]}$ is a product of k line segments with lengths $(\sqrt{a_1})s, \ldots, (\sqrt{a_k})s$. There is a unique minimal simplicial cell structure on $\mathbf{I}^n$ that contains all of these subspaces $\mathbf{I}^{[\lambda]}$ as subcomplexes.

Definition 6.2 (Product strata)**.** Let $\mathbf{X}_{[\lambda]} = \{\mathbf{x} \in \mathbf{X}^n \mid \mathrm{SETPART}(\mathbf{x}) = [\lambda]\}$ for each $[\lambda] \in \mathrm{SETPART}_n$. These are the *strata of* $\mathbf{X}^n$, and $\mathbf{X}^n$ is a disjoint union of these nonempty subspaces (Definition 1.7). The indiscrete stratum $\mathbf{X}_{[n^1]}$, where all coordinates are equal, is the *long thin diagonal* of $\mathbf{X}^n$. It is a topological diagonal copy of $\mathbf{X}$ with its metric dilated by a factor of $\sqrt{n}$. The discrete stratum $\mathbf{X}_{[1^n]}$ is $\mathrm{CONF}_n(\mathbf{X})$, the *configuration space* of all collections of n distinct labeled points.

In addition to the strata $\mathbf{X}_{[\lambda]}$, we also define a different, overlapping collection of subspaces $\mathbf{X}^{[\lambda]}$, also indexed by set partitions, whose structure is easier to describe.

Definition 6.3 (Product subspaces)**.** For a set partition $[\lambda] \vdash [n]$ let $\mathbf{X}^{[\lambda]}$ be the collection of points $\mathbf{x}$ where coordinates belonging to the same block of $[\lambda]$ are required to be equal. Unlike the definition of $\mathbf{X}_{[\lambda]}$, we do *not* require that distinct blocks have distinct coordinate values. For example, $\mathbf{X}^{13|2|4} = \{(a, b, a, c) \in X^4\}$ while $\mathbf{X}_{13|2|4} = \{(a, b, a, c) \in X^4 \mid a, b, c \text{ distinct}\}$. Since an n-tuple $\mathbf{x}$ is in $\mathbf{X}^{[\lambda]}$ if and only if $\mathrm{SHAPE}(\mathbf{x}) \geq [\lambda]$, $\mathbf{X}^{[\lambda]}$ is a disjoint union of strata:

$$\mathbf{X}^{[\lambda]} = \bigsqcup_{[\mu] \geq [\lambda]} \mathbf{X}_{[\mu]}.$$

The rectangular boxes in the n-cube (Example 6.1) illustrate the general properties of product subspaces and their strata. Let $[\lambda] \vdash [n]$ be a set partition with k blocks. We show that the subspace $\mathbf{X}^{[\lambda]}$ is a rescaled version of $\mathbf{X}^k$ (Proposition 6.6), the stratum $\mathbf{X}_{[\lambda]}$ is a rescaled version of $\mathrm{CONF}_k(\mathbf{X})$ (Proposition 6.7), and the topological closure of $\mathbf{X}_{[\lambda]}$ is $\mathbf{X}^{[\lambda]}$ (Proposition 6.8). The proofs use natural maps between set partitions and indexing sets.

Definition 6.4 (Set partition maps)**.** Let $[\lambda] \vdash [n]$ be a set partition with k blocks and let $\lambda = \lambda_1^{a_1} \cdots \lambda_\ell^{a_\ell}$ be its shape. There are canonical maps $[n] \to [\lambda] \to [\ell]$. The first sends $i \in [n]$ to the block containing i in $[\lambda]$, The second sends a block of $[\lambda]$ of size λ_j to $j \in [\ell]$. If we pick a bijection $[\lambda] \to [k]$ fixing an ordering of the blocks, we get maps $[n] \to [k] \to [\ell]$ between standard sets of integers. Note that functions to and from $[\lambda]$ are technically functions to and from the set of blocks of $[\lambda]$.

Remark 6.5 (Points as functions)**.** In the language of Remark 1.8, the points in $X^{[\lambda]}$ bijectively correspond to functions $[\lambda] \to \mathbf{X}$, whereas the points in $\mathbf{X}_{[\lambda]}$ correspond to the injective functions $[\lambda] \hookrightarrow \mathbf{X}$. A "point" $[n] \to \mathbf{X}$ in $\mathbf{X}^{[\lambda]}$ factors through the set partition map $[n] \to [\lambda]$ (Definition 6.4) to yield a "point" $[\lambda] \to \mathbf{X}$, and composition with this set partition map reverses the process. If $[\lambda]$ has k blocks and we fix a bijection $[k] \to [\lambda]$ ordering the blocks of $[\lambda]$, then composition establishes an additional bijection, in fact a homeomorphism, between "points" in $\mathbf{X}^{[\lambda]}$ and "points" in $\mathbf{X}^k$.
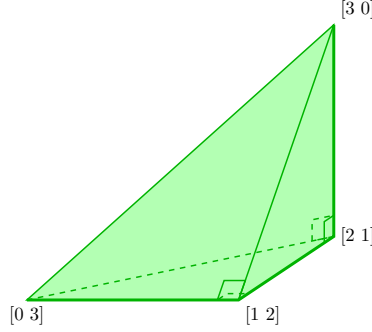
FIGURE 20. A standard 3-orthoscheme $\mathrm{MULT}_3(\mathbf{I})$. The vertices are multisets of the form $x_\ell^{a_\ell} x_r^{a_r}$ with $a_\ell + a_r = 3$, so we label them using the shorthand $[a_\ell\ a_r]$. The spine of the orthoscheme is indicated by the thick path from [0 3] to [1 2] to [2 1] to [3 0].

Proposition 6.6 (Subspace metrics). *Let $[\lambda] \vdash [n]$ be a set partition with k blocks. Ordering of the blocks of $[\lambda]$ produces a homeomorphism between $\mathbf{X}^{[\lambda]} \subset \mathbf{X}^n$ and $\mathbf{X}^k$. Moreover, this becomes an isometry by rescaling the ith coordinate of $\mathbf{X}^k$ by $\sqrt{j}$, where j is the size of the corresponding block in $[\lambda]$.*

Proof. Pick a bijection $[k] \to [\lambda]$ ordering the blocks of $[\lambda]$ and define a bijection between $\mathbf{X}^k$ and $\mathbf{X}^{[\lambda]}$ as described in Remark 6.5. This function is continuous with a continuous inverse. Moreover, when restricted to a single coordinate of $\mathbf{X}^k$ and the corresponding block of coordinates in $\mathbf{X}^{[\lambda]}$, this is the long thin diagonal embedding of Definition 6.2, which accounts for the stretch factors. $\square$

Proposition 6.7 (Stratum metrics). *If $[\lambda] \vdash [n]$ is a set partition with k blocks, then the stratum $\mathbf{X}_{[\lambda]} \subset \mathbf{X}^n$ is homeomorphic to $\mathrm{CONF}_k(\mathbf{X})$. Moreover, this homeomorphism can be promoted to an isometry by rescaling the ith coordinate of $\mathrm{CONF}_k(\mathbf{X})$ by $\sqrt{j}$, where j is the size of the corresponding block in $[\lambda]$.*

Proof. The map in Proposition 6.6 sends $\mathrm{CONF}_k(\mathbf{X})$ to $\mathbf{X}_{[\lambda]}$. $\square$

Proposition 6.8 (Stratum closures). *The closure of $\mathrm{CONF}_n(\mathbf{X})$ is $\mathbf{X}^n$, and for each set partition $[\lambda]$, the closure of the stratum $\mathbf{X}_{[\lambda]}$ is the subspace $\mathbf{X}^{[\lambda]}$.*

Proof. For the types of spaces considered here (Remark 1.3), it is easy to see that every point in $\mathbf{X}^n$ is a limit of points where the coordinates are distinct. Thus the closure of $\mathrm{CONF}_n(\mathbf{X})$ is $\mathbf{X}^n$ and, by Proposition 6.6, the closure of $\mathbf{X}_{[\lambda]}$ contains all of $\mathbf{X}^{[\lambda]}$. Conversely, the closure of $\mathbf{X}_{[\lambda]}$ is contained in $\mathbf{X}^{[\lambda]}$ since any convergent sequence of points where specific coordinates are always equal has a limit where those coordinates remain equal. $\square$

6.2. **Multiset strata.** The horizontal map $\mathrm{SHAPE} \colon \mathrm{MULT}_n(\mathbf{X}) \to \mathrm{INTPART}_n$ in Figure 3 on page 11 subdivides $\mathrm{MULT}_n(\mathbf{X})$ into strata we call $\mathrm{MULT}_\lambda(\mathbf{X})$ and into subspaces we call $\mathrm{MULT}^\lambda(\mathbf{X})$. The special case where $\mathbf{X}$ is the interval $\mathbf{I} = [x_\ell, x_r]$ is important in Part 3.

Definition 6.9 (Orthoschemes). The cell structure on $\mathbf{I}^n$ of Example 6.1 has $n!$ top-dimensional simplices, it admits a cellular action by SYM_n via permuting

$$\begin{array}{ccc}
 & \text{distinct} & \text{arbitrary} \\
\text{labeled} & \text{CONF}_n(\mathbf{X}) \hookrightarrow & \mathbf{X}^n \\
 & \text{SET} \downarrow & \downarrow \text{MULT} \\
\text{unlabeled} & \text{SET}_n(\mathbf{X}) \hookrightarrow & \text{MULT}_n(\mathbf{X})
\end{array}$$

FIGURE 21. Configuration spaces with points that are distinct and/or labeled. The horizontal maps are inclusions and the vertical maps are quotients. The one on the left is a covering map.

coordinates, and the orbifold quotient $\text{MULT}_n(\mathbf{I}) = \mathbf{I}^n/\text{SYM}_n$ can be identified with a single closed n-dimensional simplex. Since this simplex is the convex hull of n pairwise-orthogonal line segments with equal length, it is called a *standard n-orthoscheme* of side length s. This path of pairwise-orthogonal line segments through the vertex set is its *spine*. The closed cells of a standard n-orthoscheme are *non-standard orthoschemes* with a *spine* of pairwise-orthogonal line segments of length $(\sqrt{a_1})s, \dots, (\sqrt{a_k})s$ and $a_1 + \cdots + a_k \leq n$. See Figure 20 for an example and see [BM10] and [DMW20] for more on orthoschemes.

Definition 6.10 (Multiset strata). For each $\lambda \vdash n$ in INTPART_n, let $\text{MULT}_\lambda(\mathbf{X}) = \{M \in \text{MULT}_n(\mathbf{X}) \mid \text{SHAPE}(M) = \lambda\}$. These are the *strata of* $\text{MULT}_n(\mathbf{X})$, and $\text{MULT}_n(\mathbf{X})$ is a disjoint union of these nonempty subspaces. The indiscrete stratum $\text{MULT}_{[1^n]}$ is the isometric image of the long thin diagonal in $\mathbf{X}^n$ sent to $\text{MULT}_n(\mathbf{X})$. The discrete stratum is $\text{MULT}_{1^n}(\mathbf{X})$ is $\text{SET}_n(X)$, the collection of n distinct unlabeled points in $\mathbf{X}$, also known as the *unlabeled configuration space* $\text{UCONF}_n(\mathbf{X})$). The symmetric group acts freely on $\text{CONF}_n(\mathbf{X})$, $\text{SET}_n(\mathbf{X})$ is the quotient space $\text{CONF}_n(\mathbf{X})/\text{SYM}_n$, and the map $\text{SET}: \text{CONF}_n(\mathbf{X}) \to \text{SET}_n(\mathbf{X})$ which sends the n-tuple $\mathbf{x} = (x_1, \dots, x_n)$ to the n-element set $\text{SET}(\mathbf{x}) = \{x_1, \dots, x_n\}$ is an $n!$-sheeted covering map. See Figure 21.

Definition 6.11 (Multiset subspaces). Next let $\text{MULT}^\lambda(\mathbf{X}) = \{M \in \text{MULT}_n(\mathbf{X}) \mid \text{SHAPE}(M) \geq \lambda\}$. We call these the *subspaces of* $\text{MULT}_n(\mathbf{X})$ even though their structure is much more complicated than it is in the product case. As before each subspace $\text{MULT}^\lambda(\mathbf{X})$ is a disjoint union of strata:

$$\text{MULT}^\lambda(\mathbf{X}) = \bigsqcup_{\mu \geq \lambda} \text{MULT}_\mu(\mathbf{X}).$$

It is not too hard to see that for any set partition $[\lambda]$ with shape $\lambda = \text{SHAPE}([\lambda])$, the restricted map $\text{MULT}: \mathbf{X}_{[\lambda]} \to \text{MULT}_\lambda(\mathbf{X})$ is a covering map. This is because small changes to the coordinates of an n-tuple in the domain, with equal coordinates staying equal, correspond to small changes to the elements of the underlying set $S = \text{SET}(M)$ without changing their multiplicities. Although identifying the degree of the cover is, strictly speaking, unnecessary, the answer is straightforward and we have not seen it in the literature, so we pause to review the relevant combinatorics. We begin with a concrete example.

Example 6.12 (Preimages and symmetries). Let a, b, c, d and e be distinct points in $\mathbf{X}$ and let $\mathbf{x} = (a, b, a, c, d, c, e)$ be a 7-tuple in $\mathbf{X}^7$ with multiset $M = a^2 b^1 c^2 d^1 e^1$,

set partition $[\lambda] = 13|2|46|5|7$ and shape $\lambda = 2^2 1^3$ as in Example 1.1. Note that the set partition $[\lambda]$ and the multiset M do not uniquely determine $\mathbf{x}$. The set partition determines the blocks of equal coordinates, the multiset determines the set of coordinates to be assigned, and coordinate multiplicities must match the block sizes, but any assignment sending a and c to blocks 13 and 46, and b, d and e to blocks 2, 5 and 7 will work. The possible choices arise from the $|\mathrm{SYM}_\lambda| = 2! \cdot 3! = 12$ symmetries of the shape λ. Next, the set $\mathrm{MULT}^{-1}(M) \subset \mathbf{X}^7$ contains $\binom{n}{\lambda} = \binom{7}{2,1,2,1,1} = 1260$ 7-tuples, since this multinomial coefficient counts the number of rearrangements of two a's, one b, two c's, one d and one e. Finally, since the map from $\mathrm{MULT}^{-1}(M)$ to set partitions of shape λ is uniformly a 12-to-1 map, there are $\frac{1}{|\mathrm{SYM}_\lambda|}\binom{n}{\lambda} = \frac{1260}{12} = 105$ distinct set partitions with shape $\lambda = 2^2 1^3$.

Definition 6.13 (Symmetries of a shape). Let $\lambda = \lambda_1^{a_1} \lambda_2^{a_2} \cdots \lambda_\ell^{a_\ell}$ be an integer partition of n of length k and let $\mathbf{a} = (a_1, \ldots, a_\ell)$ be the exponents of λ. The *symmetry group of* λ is a subgroup of SYM_k. When the parts of λ are viewed as distinguishable, the group SYM_λ is the group of rearrangements of its k distinguished parts that maintain their weakly decreasing order. Concretely, the group is $\mathrm{SYM}_\lambda = \mathrm{SYM}_\mathbf{a} = \prod_{i=1}^\ell \mathrm{SYM}_{a_i}$ and it has size $|\mathrm{SYM}_\lambda| = \mathbf{a}! = \prod_{i=1}^\ell a_i!$. We also write $\binom{n}{\lambda}$ to denote the multinomial coefficient $\binom{\lambda}{a_1, \ldots, a_l}$.

Arguing as in Example 6.12 establishes the following three results.

Proposition 6.14 (Tuples with fixed multiset). *For any $M \in \mathrm{MULT}_n(\mathbf{X})$ with* $\mathrm{SHAPE}(M) = \lambda$, *there are $\binom{n}{\lambda}$ n-tuples $\mathbf{x} \in \mathbf{X}^n$ with $\mathrm{MULT}(\mathbf{x}) = M$.*

Proposition 6.15 (Tuples with fixed multiset and set partition). *Given a multiset $M \in \mathrm{MULT}_n(\mathbf{X})$ and a set partition $[\lambda] \vdash [n]$ with a common shape $\lambda = \mathrm{SHAPE}(M) = \mathrm{SHAPE}([\lambda])$, there are $|\mathrm{SYM}_\lambda|$ n-tuples $\mathbf{x} \in \mathbf{X}^n$ with $\mathrm{MULT}(\mathbf{x}) = M$ and $\mathrm{SETPART}(\mathbf{x}) = [\lambda]$.*

Proposition 6.16 (Set partitions with fixed shape). *For any integer partition $\lambda \vdash n$, there are $\frac{1}{|\mathrm{SYM}_\lambda|}\binom{n}{\lambda}$ set partitions $[\lambda] \vdash [n]$ with $\mathrm{SHAPE}([\lambda]) = \lambda$.*

Proof. Since the horizontal maps of Figure 3 are onto for any $\mathbf{X}$ considered here, let $M \in \mathrm{MULT}_n(\mathbf{X})$ be a multiset of shape λ. By Proposition 6.14 there are $\binom{n}{\lambda}$ n-tuples in $\mathbf{X}^n$ with multiset M and by Proposition 6.15 each set partition of shape λ accounts for $|\mathrm{SYM}_\lambda|$ of these tuples. The quotient of these two values counts the number of set partitions of shape λ. $\qquad\square$

With these counts, we can clarify the structure of the stratum MULT_λ. We start with a concrete example stated in the language of intermediate covers.

Example 6.17 (Stratum covers). The stratum $\mathbf{X}_{13|2|46|5|7}$ in X^7 is homeomorphic to $\mathrm{CONF}_5(\mathbf{X})$, but the corresponding stratum $\mathrm{MULT}_{2^2 1^3}$ in $\mathrm{MULT}_7(\mathbf{X})$ is not homeomorphic to $\mathrm{SET}_7(\mathbf{X})$. To see this, note that each element of $\mathrm{SET}_7(\mathbf{X})$ has 7! preimages in $\mathrm{CONF}_7(\mathbf{X})$, while each element of $\mathrm{MULT}_{2^2 1^3}(\mathbf{X})$ has only $|\mathrm{SYM}_{2^2 1^3}| = 2!3! = 12$ preimages in $\mathbf{X}^7$ (Proposition 6.15). Instead, $\mathrm{MULT}_{2^2 1^3}(\mathbf{X})$ is homeomorphic to the intermediate cover $\mathrm{SET}_{2,3}(\mathbf{X})$, which is a $\binom{5}{2,3} = 10$ sheeted cover of $\mathrm{SET}_5(\mathbf{X})$. And $\mathrm{CONF}_5(\mathbf{X})$ is a $2!3! = 12$ sheeted cover of $\mathrm{SET}_{2,3}(\mathbf{X})$. See Figure 22.

As Example 6.17 shows, the multiset strata $\mathrm{MULT}_\lambda(\mathbf{X})$ are, in general, intermediate covers between $\mathrm{CONF}_k(\mathbf{X})$ and $\mathrm{SET}_k(\mathbf{X})$.

$$
\begin{array}{ccc}
\mathbf{X}_{13|2|46|5|7} \xlongequal{\ \sim\ } \mathrm{Conf}_5(\mathbf{X}) & \qquad & \mathbf{X}_{[\lambda]} \xlongequal{\ \sim\ } \mathrm{Conf}_k(\mathbf{X}) \\
{\scriptstyle 2!3!}\Big\downarrow \qquad\qquad \Big\downarrow{\scriptstyle 2!3!} & & {\scriptstyle \mathbf{a}!}\Big\downarrow \qquad\qquad \Big\downarrow{\scriptstyle \mathbf{a}!} \\
\mathrm{Mult}_{2^2 1^3}(\mathbf{X}) \xlongequal{\ \sim\ } \mathrm{Set}_{2,3}(\mathbf{X}) & & \mathrm{Mult}_\lambda(\mathbf{X}) \xlongequal{\ \sim\ } \mathrm{Set}_{\mathbf{a}}(\mathbf{X}) \\
\Big\downarrow{\scriptstyle \binom{5}{2,3}} & & \Big\downarrow{\scriptstyle \binom{k}{\mathbf{a}}} \\
\mathrm{Set}_5(\mathbf{X}) & & \mathrm{Set}_k(\mathbf{X})
\end{array}
$$

FIGURE 22. The stratum $\mathrm{Mult}_\lambda(\mathbf{X})$ in $\mathrm{Mult}_n(\mathbf{X})$ is homeomorphic to an intermediate cover of $\mathrm{Set}_k(\mathbf{X})$, where $k = \mathrm{len}(\lambda)$.

Definition 6.18 (Intermediate covers)**.** Let $\mathbf{a} = (a_1, \cdots, a_\ell)$ be a tuple of positive integers with sum k. The *intermediate cover* $\mathrm{Set}_{\mathbf{a}}(\mathbf{X})$ is the space of subsets of $\mathbf{X}$ of size k, with elements labeled so that there are exactly a_i points with label i for each $i \in [\ell]$. The map that forgets the label is a covering map $\mathrm{Set}_{\mathbf{a}}(\mathbf{X}) \to \mathrm{Set}_k(\mathbf{X})$ of degree $\binom{k}{\mathbf{a}} = \binom{k}{a_1 \ \cdots \ a_\ell}$. If $f \colon [k] \to [\ell]$ is a function with the property that $|f^{-1}(i)| = a_i$ for all $i \in [\ell]$, then f induces a map $\mathrm{Conf}_k(\mathbf{X}) \to \mathrm{Set}_{\mathbf{a}}(\mathbf{X})$ which labels coordinates by their image under f, and this is an $\mathbf{a}$!-sheeted covering since permutations within preimages do not change the result.

This gives us a fairly precise description of the Mult map as a stratified covering.

Theorem 6.19 (Stratified covering map)**.** *The* Mult *map is a stratified covering map. Concretely, if $[\lambda] \vdash [n]$ is a set partition of shape $\lambda = \lambda_1^{a_1} \cdots \lambda_\ell^{a_\ell}$ with $\mathrm{len}(\lambda) = k$ and $\mathbf{a} = (a_1, \ldots, a_\ell)$ are the exponents of λ, then the stratum $\mathbf{X}_{[\lambda]}$ is homeomorphic to $\mathrm{Conf}_k(\mathbf{X})$, the stratum $\mathrm{Mult}_\lambda(\mathbf{X})$ is homeomorphic to the intermediate cover $\mathrm{Set}_{\mathbf{a}}(\mathbf{X})$, and the map* Mult *restricts to a covering map $\mathbf{X}_{[\lambda]} \twoheadrightarrow \mathrm{Mult}_\lambda(\mathbf{X})$ of degree $|\mathrm{Sym}_\lambda| = \mathbf{a}!$.*

Proof. There is a natural homeomorphism from $\mathrm{Mult}_\lambda(\mathbf{X})$ to $\mathrm{Set}_{\mathbf{a}}(\mathbf{X})$ which sends a multiset of shape λ to its underlying set of size k, where each element of the set is labeled by its multiplicity in the multiset. Meanwhile, we know by Proposition 6.7 that $\mathbf{X}_{[\lambda]}$ is homeomorphic to $\mathrm{Conf}_k(\mathbf{X})$ once we fix a bijection $[k] \to [\lambda]$. Finally, if we use the same bijection and the map $[k] \to [\lambda] \to [\ell]$ to construct a covering map $\mathrm{Conf}_k(\mathbf{X}) \to \mathrm{Set}_{\mathbf{a}}(\mathbf{X})$ as in Example 6.17, then the homeomorphism and the covers form the commuting square in Figure 22. $\square$

Corollary 6.20. *The map* Mult$\colon \mathbf{X}^n \to \mathrm{Mult}_n(\mathbf{X})$ *is locally onto.*

Proof. Fix $\mathbf{x} \in \mathbf{X}^n$ with multiset $M = \mathrm{Mult}(\mathbf{x})$, set partition $[\lambda] = \mathrm{SetPart}(\mathbf{x})$, and shape $\lambda = \mathrm{Shape}(\mathbf{x})$. The fact that $\mathbf{X}_{[\lambda]} \to \mathrm{Mult}_\lambda(\mathbf{X})$ is a covering map (Theorem 6.19) is sufficient to show that the image of a neighborhood of $\mathbf{x} \in \mathbf{X}_{[\lambda]}$ contains a neighborhood of M in $\mathrm{Mult}_\lambda(\mathbf{X})$. For the other strata near $\mathbf{x}$ and M we note that a small neighborhood of $\mathbf{x} \in \mathbf{X}_{[\lambda]}$ contains points in $\mathbf{X}_{[\mu]}$ if and only if $[\mu] \leq [\lambda]$ in $\mathrm{SetPart}_n$ and a small neighborhood of $M \in \mathrm{Mult}_\lambda(\mathbf{X})$ contains points in $\mathrm{Mult}_\mu(\mathbf{X})$ if and only if $\mu \leq \lambda$ in $\mathrm{IntPart}_n$. Since the set partitions below $[\lambda]$ map onto the integer partitions below λ, the image of this neighborhood contains multisets in $\mathrm{Mult}_\mu(\mathbf{X})$ near M for every $\mu \leq \lambda$. In particular, the portions of every stratum of $\mathrm{Mult}_n(\mathbf{X})$ with M in the boundary are covered by a portion of a stratum in $\mathbf{X}^n$ with $\mathbf{x}$ in its boundary. $\square$
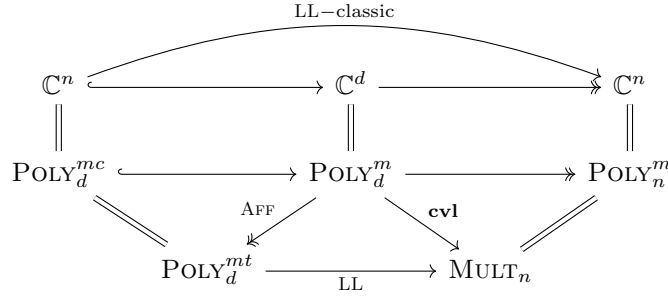
$$\text{LL-classic}$$

Figure 23. The classical Lyashko–Looijenga map is a map from $\mathbb{C}^n$ to $\mathbb{C}^n$ with $n = d - 1$. It can also be formulated as a map LL from Poly_d^{mt} to Mult_n.

7. Critical Values and Polynomials

This section describes a stratification of monic centered polynomials that turns the Lyashko–Looijenga map into a stratified covering map. After introducing our version of the LL map (7.1) we discuss polynomial strata (7.2).

7.1. **The LL map.** While the classical LL map is from $\mathbb{C}^n$ to $\mathbb{C}^n$, the version used here is a map from Poly_d^{mt}, the space of monic degree-d polynomials up to translation equivalence, to Mult_n, the space of multisets in $\mathbb{C}$ of size $n = d - 1$. The various spaces and maps discussed are shown in Figure 23.

Definition 7.1 (Critical value map). Let $\text{Mult}_n = \text{Mult}_n(\mathbb{C})$ be the space of n-element multisets in $\mathbb{C}$ (Definition 1.5). The *critical value map* $\mathbf{cvl} \colon \text{Poly}_d \to \text{Mult}_n$ sends a degree-d complex polynomial p to its n-element multiset $\mathbf{cvl}(p)$ of critical values in $\mathbb{C}$.

In Figure 23 the (diagonal) map $\mathbf{cvl}$ has been restricted to polynomials that are monic. Multisets in $\mathbb{C}$ are in natural bijection with monic polynomials.

Definition 7.2 (Multisets and monic polynomials). There is a natural bijection between Mult_n and Poly_n^m. The map $\text{Poly} \colon \text{Mult}_n \to \text{Poly}_n^m$ sends an n-element multiset $M \in \text{Mult}_n$ with $M = z_1^{m_1} z_2^{m_2} \cdots z_k^{m_k}$ and $\sum m_i = n$ to the polynomial $p = \text{Poly}(M)$ with $p(z) = (z - z_1)^{m_1}(z - z_2)^{m_2} \cdots (z - z_k)^{m_k}$. The inverse map $\mathbf{rts} \colon \text{Poly}_n^m \to \text{Mult}_n$ sends a polynomial to its multiset of roots.

Definition 7.2 is used in the lower righthand corner of Figure 23. Moreover, as discussed in Definition 2.1, $\text{Poly}_d^m = \mathbb{C}^d$ and $\text{Poly}_d^{mc} = \mathbb{C}^n$ using coefficients as coordinates, and these give the identifications in Figure 23 between the first and second rows. The classic version of the *Lyashko–Looijenga map* from $\mathbb{C}^n$ to $\mathbb{C}^n$ is shown in the top row. Theorem 5.1.1 of [LZ04] summarizes its key properties.

Theorem 7.3 (LL map). *The Lyashko–Looijenga map* $\text{LL} \colon \mathbb{C}^n \to \mathbb{C}^n$, *from the space of monic centered degree-d polynomials to the space of monic polynomials of degree $n = d - 1$, is a polynomial finite map of degree d^{d-2}.*

These properties make it well-suited for investigations by algebraic geometers. Here is a brief definition of the map and its key properties.

Definition 7.4 (LL map, classic version)**.** The classic version of the *Lyashko–Looijenga map* sends a monic centered polynomial p of degree d to the monic polynomial of degree $n = d - 1$ whose roots are the critical values of p. The coefficients of the polynomials in both the domain and range can be used as coordinates to give an induced map from $\mathbb{C}^n$ to $\mathbb{C}^n$. See Figure 23. It is a *polynomial* map because the coordinates in the range are defined by multivariable polynomial functions of the coordinates in the domain, and it is a *finite map of degree* d^{d-2} because a generic point in the range has exactly d^{d-2} preimages.

The bottom row of Figure 23 uses polynomials with an affine domain.

Definition 7.5 (Affine map)**.** We say that $p, q \colon \mathbb{C} \to \mathbb{C}$ are *equivalent up to translation* if there is a constant $b \in \mathbb{C}$ such that $q(z) = p(z + b)$. This is an equivalence relation; let $[p] = \{q \mid q(z) = p(z + b), b \in \mathbb{C}\}$ be the *translation equivalence class* of p. If POLY_d^{mt} denotes monic polynomials of degree d up to translation, then there is a quotient map $\mathrm{AFF} \colon \mathrm{POLY}_d^m \twoheadrightarrow \mathrm{POLY}_d^{mt}$ that sends p to $[p]$. We call this the *affine map* since the domain of each polynomial p becomes, in essence, an affine space with no fixed origin, instead of a 1-dimensional complex vector space.

Polynomials up to translation are equivalent to polynomials that are centered.

Remark 7.6 (Centering polynomials)**.** For monic polynomials, the coefficient of the term just below the leading term is the negative of the sum of its roots. In particular, $c_1 = 0$ and p is centered if and only if the average of the roots is at the origin. Under precomposition with a translation, the average of the roots is translated, and every equivalence class $[p]$ contains a unique representative that is centered. The map $\mathrm{POLY}_d^{mt} \to \mathrm{POLY}_d^{mc}$ sending $[p]$ to its centered representative is a section of the affine quotient map $\mathrm{AFF} \colon \mathrm{POLY}_d^m \twoheadrightarrow \mathrm{POLY}_d^{mt}$ and a homeomorphism.

Translation equivalence is a special case of a more general situation.

Remark 7.7 (Composing with linear functions)**.** Let $f(z) = az + b$ be an invertible linear transformation, let $g(z) = \frac{1}{a}(z - b)$ be its inverse, and recall that these maps are Euclidean similarities of the plane: translating, dilating, and rotating. Postcomposing $p \colon \mathbb{C} \to \mathbb{C}$ with f applies the similarity f to the coordinate system in the range. Concretely, if $q(z) = f(p(z)) = a \cdot p(z) + b$, then $\mathbf{cpt}(q) = \mathbf{cpt}(p)$ and $\mathbf{cvl}(q) = f(\mathbf{cvl}(p)) = a \cdot \mathbf{cvl}(p) + b$. Precomposing p with f applies the inverse similarity g to the coordinate system in the domain. If $q(z) = p(f(z)) = p(az + b)$, then $\mathbf{cpt}(q) = g(\mathbf{cpt}(p)) = \frac{1}{a}(\mathbf{cpt}(p) - b)$ and $\mathbf{cvl}(q) = \mathbf{cvl}(p)$.

This leads to the factorization of the critical value map shown in Figure 23.

Definition 7.8 (LL map)**.** By Remark 7.7, all of the polynomials in $[p]$ have the same multiset of critical values, so the critical value map $\mathbf{cvl} \colon \mathrm{POLY}_d^m \to \mathrm{MULT}_n$ factors through the affine map $\mathrm{AFF} \colon \mathrm{POLY}_d^m \twoheadrightarrow \mathrm{POLY}_d^{mt}$ sending $p \mapsto [p]$. Our version of the LL map is the induced map $\mathrm{LL} \colon \mathrm{POLY}_d^{mt} \to \mathrm{MULT}_n$. Because of the identifications on the left and right sides of Figure 23, this version of the LL map has many of the properties listed in Theorem 7.3, such as finitely many point preimages bounded above by d^{d-2}.

Of particular interest here are restrictions the LL map to polynomials with critical values is a specific portion of the range.

Definition 7.9 (Restricted maps). For any subspace $\mathbf{X} \subset \mathbb{C}$ (Remark 1.3), let $\text{POLY}_d(\mathbf{X})$ be the collection of polynomials whose critical values lie in $\mathbf{X}$, and we use superscripts to restrict attention to those that are monic (m), centered (c) or only considered up to translation (t). For any such $\mathbf{X}$, the lower portion of Figure 23 can be restricted in this subspace resulting in a *restricted* LL *map* $\text{LL} \colon \text{POLY}_d^{mt}(\mathbf{X}) \to \text{MULT}_n(\mathbf{X})$.

7.2. Polynomial strata. The stratification of multisets (Section 6) leads to a double stratification of polynomials based on critical point shape, critical value shape, and the arrow between them in the integer partition acyclic category.

Definition 7.10 (Polynomial strata). The space POLY_d has a double stratification by critical point shape and critical value shape. For any polynomial p of degree d, its *critical point shape* is $\lambda = \lambda(p) = \text{SHAPE}(\mathbf{cpt}(p))$, its *critical value shape* is $\mu = \mu(p) = \text{SHAPE}(\mathbf{cvl}(p))$, and the map from $\mathbf{cpt}(p)$ to $\mathbf{cvl}(p)$ determines an arrow $\lambda(p) \xrightarrow{p} \mu(p)$ in the acyclic category INTPART_n (Definition 1.10). Let $\text{POLY}_{\lambda \to \mu} = \{p \in \text{POLY}_d \mid \lambda(p) \xrightarrow{p} \mu(p) \text{ is } \lambda \to \mu\}$ be the "preimage" of an arrow in the acyclic category INTPART_n. The double stratification is

$$\text{POLY}_d = \bigsqcup_{\substack{\lambda, \mu \vdash n \\ \lambda \to \mu}} \text{POLY}_{\lambda \to \mu}.$$

Remark 7.11 (Extreme preimages). If p is a monic polynomial with an indiscrete critical value multiset, then it has an indiscrete critical point multiset (Lemma 2.14). In particular, the unique preimage of $\mathbf{cvl}(p) = \{c^n\}$ under the LL map is $[z^d + c] \in \text{POLY}_d^{mt}$. At the other extreme, a discrete multiset with n distinct critical values is a generic point with d^{d-2} preimages (Theorem 7.3).

The double stratification in Definition 7.10 factors through the affine map.

Definition 7.12 (Strata up to translation). For a fixed polynomial p, its critical values are invariant under translation (Remark 7.7), so the critical value shape $\mu(p)$ is a function of the translation equivalence class $[p]$. Its critical points are moved under translation, but this leaves their shape invariant, so the critical point shape $\lambda(p)$ is also a function of $[p]$. In particular, the double stratification of POLY_d^m factors through the affine map to give a double stratification of POLY_d^{mt} with $\text{POLY}_{\lambda \to \mu}^{mt} = \text{AFF}(\text{POLY}_{\lambda \to \mu}^m)$.

The double stratification is needed because of accidental equalities.

Definition 7.13 (Accidental equalities). When p is a polynomial with $\lambda(p) < \mu(p)$, there are distinct critical points $z_1 \neq z_2 \in \mathbf{cpt}(p)$ with equal critical values $p(z_1) = p(z_2) \in \mathbf{cvl}(p)$, and we say that p has *accidental equalities*.

The Chebyshev polynomial of the first kind, defined by the equation $T_d(\cos(\theta)) = \cos(d \cdot \theta)$, is an extreme example of this phenomenon. It has d distinct roots, all real, and $n = d - 1$ distinct real critical points. Every critical value, on the other hand, is either 1 or -1, so for d at least 4, $T_d(z)$ has accidental equalities. Such accidental equalities, however, have a limited impact on path lifting.

The LL map, like the MULT map, is a stratified covering map.

Theorem 7.14 (Stratified covering map). *For all integer partitions $\lambda, \mu \vdash n$ with $\lambda \to \mu$, the restricted map* $\text{LL} \colon \text{POLY}_{\lambda \to \mu}^{mt} \to \text{MULT}_\mu(\mathbb{C})$ *is a covering map.*

Theorem 7.14 is a consequence of [LZ04, Theorem 5.2.11] or [DM20, Theorem B], but in both cases a certain amount of interpretive work is necessary. A proof based on [DM20] is included in Appendix A.

Remark 7.15 (Constant finite point preimages)**.** Theorem 7.14 is the polynomial analogue of Theorem 6.19, but with less detail about the degrees of the covers. The degrees of the covers and a polynomial analogue of Proposition 6.16 has been established by Zvonkine [Zvo97]. In particular, the restricted map $\mathrm{LL}\colon \mathrm{POLY}^{mt}_{\lambda\to\mu}(\mathbb{C}) \to \mathrm{MULT}_\mu(\mathbb{C})$ has finite point preimages of constant size, and this constant can be derived from the combinatorics of $\lambda \to \mu$. See also [LZ04, Theorem 5.2.2].

Remark 7.16 (Empty strata)**.** For some arrows $\lambda \to \mu$ the subspace $\mathrm{POLY}^{mt}_{\lambda\to\mu}$ is empty. If p is a polynomial where $\mu(p)$ is the indiscrete partition, for example, then $\lambda(p)$ is also indiscrete (Remark 7.11). Thus $\mathrm{POLY}^{mt}_{\lambda\to\mu}$ is empty whenever μ is indiscrete and $\lambda \neq \mu$. Note that Theorem 7.14 remains vacuously true in this case since $\mathrm{POLY}^{mt}_{\lambda\to\mu}$ is a 0-sheeted cover of $\mathrm{MULT}_\mu(\mathbb{C})$.

The critical value map and the LL map are locally onto.

Lemma 7.17 (Locally onto)**.** *The map* $\mathbf{cvl}\colon \mathrm{POLY}^m_d \to \mathrm{MULT}_n(\mathbb{C})$ *is locally onto. As a consequence, the map* $\mathrm{LL}\colon \mathrm{POLY}^{mt}_d \to \mathrm{MULT}_n(\mathbb{C})$ *is also locally onto.*

Proof. The main result of [BCN02] is that the map from complex polynomials to critical values is onto. In fact, their proof easily extends to show that it is locally onto in the sense that for any polynomial p and for any neighborhood N of p in POLY^m_d the image $\mathbf{cvl}(N)$ contains a neighborhood of $\mathbf{cvl}(p)$. As a factor of the $\mathbf{cvl}$-map, the LL map inherits this property. $\qquad\square$

The stratified product, multiset and polynomial spaces $\mathbb{C}^n$, $\mathrm{MULT}_n(\mathbb{C})$, and $\mathrm{POLY}^{mt}_d(\mathbb{C})$, and the stratified maps MULT and LL connecting them, give all three spaces a stratified Euclidean metric.

Definition 7.18 (Stratified Euclidean metrics)**.** The natural Euclidean product metric on $\mathbb{C}^n$ has a Euclidean metric on each of its strata (Proposition 6.7), and since the MULT map is a stratified cover defined as the quotient by the isometric symmetric group action, there is a unique metric on $\mathrm{MULT}_n(\mathbb{C})$ that restricts to a local isometry for each covering map in the stratification. This is the *stratified Euclidean metric on* $\mathrm{MULT}_n(\mathbb{C})$. Simlilarly, the LL map is a stratified cover and there is a unique metric on $\mathrm{POLY}^{mt}_d(\mathbb{C})$ that restricts to a local isometry for each covering map in its stratification. This pulls the stratified Euclidean metric on $\mathrm{MULT}_n(\mathbb{C})$ back to $\mathrm{POLY}^{mt}_d(\mathbb{C})$, and is the *stratified Euclidean metric on* $\mathrm{POLY}^{mt}_d(\mathbb{C})$. Since the LL map and the MULT map use the same stratification in their common range, we have local isometries between strata neighborhoods of polynomials, multisets and n-tuples. Concretely, if p is a monic centered polynomial and $\mathbf{x}$ is an n-tuple with common multiset $M = \mathbf{cvl}(p) = \mathrm{MULT}(\mathbf{x})$, then there are small neighborhoods in the appropriate strata and local isometries so that $N_p \cong N_M \cong N_\mathbf{x}$.

Some cell structures on multiset spaces can also be lifted through the LL map.

Definition 7.19 (Stratified cell structures)**.** A cell structure on $\mathrm{MULT}_n(\mathbf{X})$ is a *stratified cell structure* if all points in the same open cell have the same shape. In other words, the stratification of $\mathrm{MULT}_n(\mathbf{X})$ into open cells is a refinement of the stratification $\mathrm{MULT}_n(\mathbf{X}) = \bigsqcup_{\lambda\vdash n} \mathrm{MULT}_\lambda(\mathbf{X})$ by the shape of these n-element

$$
\begin{array}{ccc}
\{0\} & \xrightarrow{\ \widetilde{\alpha}\ } & \mathbb{C}^n \\
\downarrow & {\scriptstyle \exists!\widetilde{\alpha}} & \downarrow {\scriptstyle \text{MULT}} \\
[0,1] & \xrightarrow{\ \alpha\ } & \text{MULT}_n(\mathbb{C}) \\
& {\scriptstyle \geq} & \downarrow {\scriptstyle \text{SHAPE}} \\
& & \text{INTPART}_n
\end{array}
\qquad
\begin{array}{ccc}
\{0\} & \xrightarrow{\ \widetilde{\alpha}\ } & \text{POLY}_d^{mt}(\mathbb{C}) \\
\downarrow & {\scriptstyle \exists!\widetilde{\alpha}} & \downarrow {\scriptstyle \text{LL}} \\
[0,1] & \xrightarrow{\ \alpha\ } & \text{MULT}_n(\mathbb{C}) \\
& {\scriptstyle \geq} & \downarrow {\scriptstyle \text{SHAPE}} \\
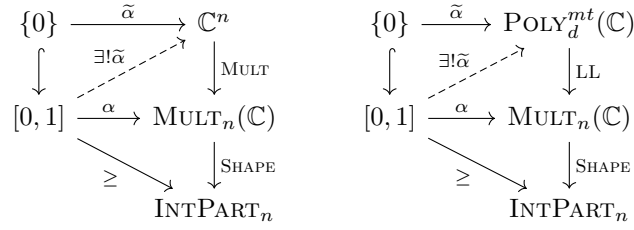& & \text{INTPART}_n
\end{array}
$$

FIGURE 24. Paths can be uniquely lifted through the MULT map (left) and the LL map (right) when the multiset path α has a weakly increasing shape.

multisets. The open cells in a stratified cell structure on $\text{MULT}_n(\mathbf{X})$ lift through the individual covering maps of the stratified LL map to provide the open cells of a cell structure on $\text{POLY}_d^{mt}(\mathbf{X})$. And with this lifted cell structure on the domain, the LL map becomes a cellular map.

8. UNIQUE PATH LIFTING

In this section we show that every path in $\text{MULT}_n(\mathbb{C})$ lifts through the MULT map and through the LL map, and this lift is unique when the shape of the path is weakly increasing. We focus first on the MULT map (8.1) and then the LL map (8.2).

8.1. **Path-lifting through the** MULT **map.** Lifting multiset paths to $\mathbb{C}^n$ is a simpler situation than lifting them through the LL map, which is why they are being considered first. The diagrams for the two situations are shown in Figure 24.

Definition 8.1 (Shapes and Multiset Paths). Let $\alpha\colon [0,1] \to \text{MULT}_n(\mathbb{C})$ be a path and note that since α is continuous, the points in the set underlying the multiset move around continuously in $\mathbb{C}$. For each $t \in [0,1]$, the multiset $\alpha(t)$ has a shape $\lambda(t) = \text{SHAPE}(\alpha(t))$ in INTPART_n that records its multiset of multiplicities. We say that α has a *weakly increasing shape* if for all $s \leq t$ in $[0,1]$, we have $\lambda(s) \leq \lambda(t)$ in INTPART_n. Equivalently, the points (with multiplicity) moving around in $\mathbb{C}$ are allowed to merge but not split, so that the size of the underlying set weakly decreases over time as the integer partition weakly increases. It has a *weakly decreasing shape* if $s \leq t$ in $[0,1]$ implies $\lambda(s) \geq \lambda(t)$ in INTPART_n, or equivalently, the underlying points are allowed to split but not merge. For any path $\alpha\colon [0,1] \to Y$, the *time reversal of* α is $\alpha^{\text{rev}}\colon [0,1] \to Y$ with $\alpha^{\text{rev}}(1-t) = \alpha(t)$. Note that α has a weakly increasing/decreasing shape if and only if α^{rev} has a weakly decreasing/increasing shape. Paths that remain in a single stratum $\text{MULT}_\lambda(\mathbb{C})$ have a *constant shape* $\lambda(t) = \lambda$ for all $t \in [0,1]$.

We begin with an easy observation.

Lemma 8.2 (Paths and Strata). *Let* $\alpha\colon [0,1] \to \text{MULT}_n(\mathbb{C})$ *be a multiset path and let* $\beta\colon [0,1] \to \mathbb{C}^n$ *be a path with* $\alpha = \text{MULT} \circ \beta$. *If* $\alpha(t)$ *has constant shape* μ *and* $\text{SETPART}(\beta(0)) = [\mu]$, *then* α *is a path in* $\text{MULT}_\mu(\mathbb{C})$ *and* β *is a path in* $\mathbb{C}_{[\mu]}$.

Proof. Since α has constant shape, it is a path in $\text{MULT}_\mu(\mathbb{C})$. View the path α as points with multiplicities moving around $\mathbb{C}$ without splitting or merging, and view $[\mu] = \text{SETPART}(\beta(0))$ as a way of replacing these multiplicities at the start point

with initial labels. The unique continuous way to lift α to a path β in $\mathbb{C}^n$ is to drag these initial labels along as the points move, and this unique lift stays in $\mathbb{C}_{[\mu]}$. $\quad\square$

The main result in this section is that path liftings always exist and the lifting is unique when the path to be lifted has a weakly increasing shape.

Theorem 8.3 (Lifting paths to $\mathbb{C}^n$)**.** *For any path $\alpha\colon [0,1] \to \text{Mult}_n(\mathbb{C})$ and for any lift of the start point $\alpha(0)$ to an n-tuple $\widetilde{\alpha}(0) \in \mathbb{C}^n$ with $\text{Mult}(\widetilde{\alpha}(0)) = \alpha(0)$, there always exists a lifted path $\widetilde{\alpha}\colon [0,1] \to \mathbb{C}^n$ with $\alpha = \widetilde{\alpha} \circ \text{Mult}$, and the lifted path $\widetilde{\alpha}$ is unique when α has weakly increasing shape.*

Proof. Since the map Mult is a locally onto (Corollary 6.20), every path in the range has at least one lift to the domain. Let β_1 and β_2 be two lifts of α and recall that the set $\{t \mid \beta_1(t) = \beta_2(t)\}$ where they agree is always a closed subset of $[0,1]$. If α has constant shape μ, then by Lemma 8.2, α is a path in $\text{Mult}_\mu(\mathbb{C})$ and both β_1 and β_2 are paths in $\mathbb{C}_{[\mu]}$. Since the restricted map $\text{Mult}\colon \mathbb{C}_{[\mu]} \to \text{Mult}_\mu(\mathbb{C})$ is a covering map (Theorem 6.19), unique path lifting for covers shows that β_1 and β_2 agree for all $t \in [0,1]$ and α has a unique lift in this case. To prove this when α has a weakly increasing but non-constant shape, it is sufficient to consider α where $\mu(t) = \mu(0)$ for all $0 \le t < 1$ and $\mu(0) < \mu(1)$. More complicated weakly increasing paths are concatenations of finitely many paths of this restricted type. Arguing as above for the subpaths restricted to $[0,t]$, we find that $\beta_1(t) = \beta_2(t)$ for all $t < 1$. But the portion on which they agree is closed so $\beta_1(1)$ and $\beta_2(1)$ are also equal. $\quad\square$

For the remainder of the section, we examine what can go wrong for paths that do not have weakly increasing shape. To start, paths with weakly decreasing shape can have multiple lifts, but only finitely many.

Corollary 8.4 (Finitely many lifts I)**.** *Let $\alpha\colon [0,1] \to \text{Mult}_n(\mathbb{C})$ be a path and let $\widetilde{\alpha}(0) \in \mathbb{C}^n$ be a lift of its start point $\alpha(0)$. If α has a weakly descreasing shape, then there exist at most $n!$ lifted paths $\widetilde{\alpha}\colon [0,1] \to \mathbb{C}^n$ with $\alpha = \text{Mult} \circ \widetilde{\alpha}$.*

Proof. Since α has a weakly decreasing shape, its time reversal α^{rev} has a weakly increasing shape. By Theorem 8.3, for every preimage of the endpoint $\alpha(1)$ in $\mathbb{C}^n$, there is a unique lifted path $\widetilde{\alpha}^{\text{rev}}$ that starts at this preimage. It must end at one of the preimages of $\alpha(0)$ and this defines a function from the preimages of $\alpha(1)$ to the preimages of $\alpha(0)$. The number of preimages of $\alpha(1)$ sent to a fixed preimage $\widetilde{\alpha}(0)$ of $\alpha(0)$ is equal to the number of lifts of α starting at $\widetilde{\alpha}(0)$. Since points in $\text{Mult}_n(\mathbb{C})$ have at most $n!$ preimages in $\mathbb{C}^n$, α has at most $n!$ lifts starting at $\widetilde{\alpha}(0)$. $\quad\square$

The upper bound of $n!$ occurs when the path goes from one extreme to the other.

Example 8.5 (Maximal number of lifts I)**.** Let $\alpha\colon [0,1] \to \text{Mult}_n(\mathbb{C})$ be any path that has a weakly decreasing shape which starts at an indiscrete multiset (with 1 point of multiplicity n) and ends at a discrete multiset (with n points of multiplicity 1). The start point $\alpha(0)$ has a unique preimage in $\mathbb{C}^n$ and the endpoint $\alpha(1)$ has $n!$ preimages in $\mathbb{C}^n$. The time-reversed path α^{rev} has a unique lift that starts at each of the preimages of $\alpha(1)$ and these lifts all end at the unique preimage of $\alpha(0)$. In particular, α has $n!$ distinct lifts that start at the unique preimage of $\alpha(0)$.

Finally, paths that are not weakly monotonic can have uncountably many lifts.

Example 8.6 (Uncountable lifts I)**.** For $n = 2$ and $\mathbb{R} \subset \mathbb{C}$, we give an explicit example of a path $\alpha\colon [0,1] \to \text{Mult}_2(\mathbb{R}) \subset \text{Mult}_2(\mathbb{C})$ that has uncountably many

lifts to $\mathbb{R}^2 \subset \mathbb{C}^2$. The space $\text{MULT}_2(\mathbb{R})$ is the closed half-plane obtained by folding the plane $\mathbb{R}^2$ across the line $y = x$, and we identify $\text{MULT}_2(\mathbb{R})$ with the lower half-plane $\{(x, y) \mid x \geq y\}$. Every path in the plane projects to a path in the half-plane by composing with the map MULT, and every path in the half-plane has at least one lift to the plane with a given lift of its starting point, but there is a choice of lift whenever the path in the half-plane leaves the diagonal boundary line. Let $s \colon [0, 1] \to \mathbb{R}$ be the continuous function

$$s(t) = \begin{cases} t \sin(\pi/t) & \text{if } t \neq 0 \\ 0 & \text{if } t = 0 \end{cases}$$

and let s_t be a shorthand for $s(t)$. Note that $s^{-1}(0) = \{t \in I \mid s_t = 0\}$ is the set $\{0\} \cup \{\frac{1}{k} \mid k \in \mathbb{N}\}$, and that the complement $I - s^{-1}(0)$ is a countable union of open intervals. Next, let $\beta \colon [0, 1] \to \mathbb{R}^2$ be the path where $\beta(t) = (s_t, -s_t)$ and let α be its projection: $\alpha = \text{MULT} \circ \beta$. The image of β is contained in the line $x + y = 0$ of slope -1, and it is on the diagonal $x = y$ exactly for $t \in s^{-1}(0)$. In the half-plane $\text{MULT}_2(\mathbb{R})$ we have $\alpha(t) = (|s_t|, -|s_t|)$. The path β is one lift of α that starts at the point $(0, 0)$ but there many others. For each open time interval between consecutive points where $\alpha(t)$ is in the boundary, there are two possible lifts, one above the diagonal line $y = x$ and one below. And since there are countably many such intervals, there are $2^{\aleph_0}$ possible lifts.

8.2. **Path-lifting through the LL map.** We now prove analogous results for path-lifting through the LL map. We start by establishing the analog of Lemma 8.2 using the metric complexes constructed in Part 1. Let $\square$ be a large rectangle in the range of p with $\mathbf{cvl}(p) \subset \text{int}(\square)$, and let $\mathbf{P}'_p$ be the corresponding metric rectangular critical point complex (Definition 3.22) with its CAT(0) metric (Remark 3.23).

Lemma 8.7 (Distances). *If z_1, z_2 are points in $\mathbf{P}'_p$ and the interior of the unique geodesic between them is disjoint from $\mathbf{cpt}(p)$, then the distance $d_{\mathbf{P}'_p}(z_1, z_2)$ between them in $\mathbf{P}'_p$ is equal to the distance $d_{\mathbf{Q}'_p}(p(z_1), p(z_2))$ between their images in $\mathbf{Q}'_p$.*

Proof. By Remark 3.23, p is a local isometry from the CAT(0) metric space $\mathbf{P}'_p$ to the CAT(0) metric space $\mathbf{Q}'_p$ except at the points in $\mathbf{cpt}(p)$. The unique geodesic from z_1 to z_2 is a local geodesic in $\mathbf{P}'_p$ and, because it has no critical points in its interior, it is sent to a local geodesic in the rectangular complex $\mathbf{Q}'_p$. A local geodesic in a Euclidean rectangle, however, is the unique geodesic between its endpoints. $\square$

Corollary 8.8 (Points and values). *If the minimum distance between distinct critical points in $\mathbf{P}'_p$ is ϵ, then the minimum distance between distinct critical values in $\mathbf{Q}'_p$ is at most ϵ. In particular, if the distinct critical values in $\mathbf{Q}'_p$ are at least ϵ-separated, the distinct critical points in $\mathbf{P}'_p$ are at least ϵ-separated.*

Proof. If $z_1, z_2 \in \mathbf{cpt}(p)$ are distinct critical points that realize the minimal distance ϵ, then there can be no critical point in the interior of the unique geodesic connecting them and, by Lemma 8.7, the distance between $p(z_1), p(z_2) \in \mathbf{cvl}(p)$ is exactly ϵ. $\square$

Note that the implications in Lemma 8.7 and Corollary 8.8 are not reversible. The Chebyshev polynomial T_d with $d \geq 4$ has distinct critical points with equal critical values. A small perturbation of T_d, breaking an accidental equality, has critical points that remain ϵ-separated, but critical values that are not. Corollary 8.8 can be reframed as an assertion about paths and strata.

Lemma 8.9 (Paths and strata). *Let $\alpha \colon [0,1] \to \mathrm{MULT}_n(\mathbb{C})$ be a multiset path and let $\beta \colon [0,1] \to \mathrm{POLY}_d^{mt}$ be a lift of α through the LL map, so that $\alpha = \mathrm{LL} \circ \beta$. If $\alpha(t)$ has a constant shape μ and $\beta(0)$ has shape $\lambda \to \mu$, then α is a path in the stratum $\mathrm{MULT}_\mu(\mathbb{C})$ and β is a path in the stratum $\mathrm{POLY}_{\lambda \to \mu}^{mt}$.*

Proof. That α is a path in $\mathrm{MULT}_\mu(\mathbb{C})$ is clear from its constant shape (Lemma 8.2). Moreover, since the interval $[0,1]$ is compact and the points with multiplicity in $\alpha(t)$ neither merge nor split, there exists an $\epsilon > 0$ such that the points with multiplicity in $\alpha(t)$ are ϵ-separated for every t. By Corollary 8.8, the distinct critical points of $\beta(t)$ are also ϵ-separated for every t. In particular, β must have constant critical point shape, and this shape must be $\mathrm{SHAPE}(\beta(0)) = \lambda$. $\square$

We now proceed as before. Any multiset path α with weakly increasing shape can be subdivided into finitely many subintervals where the shape is constant, and by Lemma 8.9, the only possible lifts of these subintervals through the LL map occur in specific polynomial strata. The main result in this section is a polynomial version of Theorem 8.3.

Theorem 8.10 (Lifting paths to $\mathrm{POLY}_d^{mt}(\mathbb{C})$). *For any path $\alpha \colon [0,1] \to \mathrm{MULT}_n(\mathbb{C})$ and for any lift of $\alpha(0)$ to $\widetilde{\alpha}(0) = [p] \in \mathrm{POLY}_d^{mt}(\mathbb{C})$ with $\mathrm{LL}(\widetilde{\alpha}(0)) = \mathbf{cvl}(p) = \alpha(0)$, there always exists a lifted path $\widetilde{\alpha} \colon [0,1] \to \mathrm{POLY}_d^{mt}(\mathbb{C})$ with $\alpha = \widetilde{\alpha} \circ \mathrm{LL}$, and the lifted path $\widetilde{\alpha}$ is unique when α has weakly increasing shape.*

Proof. Since the LL map is locally onto (Lemma 7.17), every path in the range has at least one lift to the domain. Let β_1 and β_2 be two lifts of α and recall that the set $\{t \mid \beta_1(t) = \beta_2(t)\}$ where they agree is always a closed subset of $[0,1]$. If α has constant shape μ, then by Lemma 8.9, α is a path in $\mathrm{MULT}_\mu(\mathbb{C})$ and both β_1 and β_2 are paths in $\mathrm{POLY}_{\lambda \to \mu}^{mt}$. Since the restricted map $\mathrm{LL} \colon \mathrm{POLY}_{\lambda \to \mu}^{mt} \to \mathrm{MULT}_\mu(\mathbb{C})$ is a covering map (Theorem 7.14), unique path lifting for covers shows that β_1 and β_2 agree for all $t \in [0,1]$ and α has a unique lift in this case. To prove this when α has a weakly increasing but non-constant shape, it is sufficient to consider α where $\mu(t) = \mu(0)$ for all $0 \le t < 1$ and $\mu(0) < \mu(1)$. More complicated weakly increasing paths are concatenations of finitely many paths of this restricted type. Arguing as above for the subpaths restricted to $[0,t]$, we find that $\beta_1(t) = \beta_2(t)$ for all $t < 1$. But the portion on which they agree is closed so $\beta_1(1)$ and $\beta_2(1)$ are also equal. $\square$

The consequences of Theorem 8.10 are similar to those of Theorem 8.3. Here are polynomial versions of Corollary 8.4, Example 8.5, and Example 8.6.

Corollary 8.11 (Finitely many lifts II). *Let $\alpha \colon [0,1] \to \mathrm{MULT}_n(\mathbb{C})$ be a path and let $\widetilde{\alpha}(0) \in \mathrm{POLY}_d^{mt}(\mathbb{C})$ be a lift of its start point. If α has a weakly decreasing shape, then there are at most d^{d-2} lifted paths $\widetilde{\alpha} \colon [0,1] \to \mathrm{POLY}_d^{mt}(\mathbb{C})$ with $\alpha = \mathrm{LL} \circ \widetilde{\alpha}$.*

The proof is similar to that of Corollary 8.4 and has been omitted.

Example 8.12 (Maximal number of lifts II). Let $\alpha \colon [0,1] \to \mathrm{MULT}_n(\mathbb{C})$ be a path with a weakly decreasing shape that starts at the indiscrete multiset and ends at a discrete multiset. By Remark 7.11, the start point has a unique preimage and the endpoint has d^{d-2} preimages in $\mathrm{POLY}_d^{mt}(\mathbb{C})$. Arguing as in Example 8.5 shows that α has exactly d^{d-2} lifts starting at the unique lift of the start point.

Example 8.13 (Uncountable lifts II). Let $\beta \colon [0,1] \to \mathrm{POLY}_3(\mathbb{C})$ be a continuous path in the space of monic cubic polynomials defined by setting $\beta(t) = p_t$ where

$p_t(z) = z^3 - \frac{3}{2}s_t z^2 + 1$ and s_t is as defined in Example 8.6. Let $\alpha\colon [0,1] \to \mathrm{Mult}_2(\mathbb{C})$ be defined by the composition $\alpha = \mathbf{cvl} \circ \beta$. Concretely, the derivative $p'_t(z)$ factors as $3z(z - s_t)$, $\mathbf{cpt}(p_t) = \{0, s_t\}$ and $\alpha(t) = \mathbf{cvl}(p_t) = \{1, 1 - \frac{1}{2}s_t^3\}$. By Remark 7.11, when $s_t = 0$ and $\alpha(t) = \{1^2\}$ is indiscrete, $[z^3 + 1]$ is its unique preimage under the LL map, and when $s_t \neq 0$ and $\alpha(t)$ is generic, there are $3^1 = 3$ preimages. As in Example 8.6, the set $s^{-1}(0) = \{0\} \cup \{\frac{1}{k} \mid k \in \mathbb{N}\}$ and its complement $I - s^{-1}(0)$ is a countable union of open intervals. For each open time interval between consecutive points where $\alpha(t)$ is indiscrete, there are three possible lifts. And since there are countably many such intervals, there are $3^{\aleph_0}$ possible lifts of α.

9. POLYNOMIAL HOMOTOPIES

Recall that $\mathrm{Poly}_d^{mt}(\mathbf{U})$ denotes the space of monic degree-d polynomials up to translation with critical values in the subspace $\mathbf{U} \subset \mathbb{C}$. For simplicity we call $\mathrm{Poly}_d^{mt}(\mathbf{U})$ the *polynomials over* $\mathbf{U}$. The goal of this section is to clarify how the polynomial space $\mathrm{Poly}_d^{mt}(\mathbf{U})$ changes as $\mathbf{U}$ changes. The first thing to point out is that there is something to prove. For example, if $f\colon \mathbb{C} \to \mathbb{C}$ is a homeomorphism with $f(\mathbf{U}) = \mathbf{V}$, is it true that the space $\mathrm{Poly}_d^{mt}(\mathbf{U})$ of polynomials over $\mathbf{U}$ and the space $\mathrm{Poly}_d^{mt}(\mathbf{V})$ of polynomials over $\mathbf{V}$ are homeomorphic? This is obvious for planar d-branched covers.

Example 9.1. Let $f\colon \mathbb{C} \to \mathbb{C}$ be a homeomorphism of $\mathbb{C}$ with $f(\bigcirc) = \square$, sending the closed unit disk $\bigcirc$ homeomorphically to a closed rectangle $\square$. If q is any planar d-branched cover with $\mathbf{cvl}(q) \subset \bigcirc$, then $f \circ q$ is a planar d-branched cover with $\mathbf{cvl}(f \circ q) \subset \square$, and composing in the other direction with f^{-1} shows that this establishes a bijection between the infinite-dimensional function space of planar d-branched covers with critical values in $\bigcirc$ and the infinite-dimensional function space of planar d-branched covers with critical values in $\square$. On the other hand, there is no homeomorphism $f\colon \mathbb{C} \to \mathbb{C}$ with $f(\bigcirc) = \square$ where $f \circ p$ is a *polynomial* for any polynomial p with $\mathbf{cvl}(p) \subset \bigcirc$.

One way to show that this is true for polynomials is to characterize monic centered polynomials by their multiset of critical values and the monodromy, and we use this perspective in Part 3. Here we take a more direct approach. For the subspaces of $\mathbb{C}$ under consideration (Remark 1.3), homeomorphic subspaces of $\mathbb{C}$ can slowly transition from one to the other via a homotopy of $\mathbb{C}$, which ends up inducing a homeomorphism of the polynomials over those subspaces.

Definition 9.2 (Homotopies). A *homotopy* is a continuous map $H\colon \mathbf{U} \times \mathbf{I} \to \mathbf{Y}$ with $\mathbf{I} = [0,1]$. We write $H(u,t) = h_t(u) = h^u(t)$ for each $u \in \mathbf{U}$ and $t \in \mathbf{I}$. These refer to the *time map* $h_t\colon \mathbf{U} \to \mathbf{Y}$, and the *path map* $h^u\colon \mathbf{I} \to \mathbf{Y}$. We also write u_t for $H(u,t) = h^u(t)$ and $\mathbf{U}_t$ for $H(\mathbf{U},t) = h_t(\mathbf{U})$, so that h^u is a path from u_0 to u_1 and H is a homotopy from $\mathbf{U}_0$ to $\mathbf{U}_1$.

A homotopy of the points in $\mathbb{C}$ induces, for each n, a homotopy of the tuples in $\mathbb{C}^n$ and a homotopy of multisets in $\mathrm{Mult}_n(\mathbb{C})$.

Definition 9.3 (Induced homotopies). Given a subset $\mathbf{U} \subseteq \mathbb{C}$, a *point homotopy* is a homotopy $H\colon \mathbf{U} \times \mathbf{I} \to \mathbb{C}$ from $\mathbf{U}_0$ to $\mathbf{U}_1$ inside $\mathbb{C}$. This induces a *tuple homotopy* $H^n\colon \mathbf{U}^n \times \mathbf{I} \to \mathbb{C}^n$ from $(\mathbf{U}_0)^n$ to $(\mathbf{U}_1)^n$ inside $\mathbb{C}^n$, obtained by applying the homotopy H to each factor of $\mathbf{U}^n$ simultaneously. Taking the quotient by the coordinate-permuting Sym_n action on $\mathbf{U}^n$ yields the *multiset homotopy* $H_n\colon \mathrm{Mult}_n(\mathbf{U}) \times \mathbf{I} \to \mathrm{Mult}_n(\mathbb{C})$ from $\mathrm{Mult}_n(\mathbf{U}_0)$ to $\mathrm{Mult}_n(\mathbf{U}_1)$ inside

$$
\begin{array}{ccc}
(z,t) \longmapsto H(z,t) & \mathbf{U} \times \mathbf{I} \xrightarrow{\ \ H\ \ } \mathbb{C} \\[2ex]
(\mathbf{z},t) \longmapsto H^n(\mathbf{z},t) & \mathbf{U}^n \times \mathbf{I} \xrightarrow{\ \ H^n\ \ } \mathbb{C}^n \\[1ex]
\Big\downarrow \qquad\qquad \Big\downarrow & \Big\downarrow{\scriptstyle \text{MULT}\times \mathbf{1}} \qquad\qquad \Big\downarrow{\scriptstyle \text{MULT}} \\[1ex]
(M,t) \longmapsto H_n(M,t) & \text{MULT}_n(\mathbf{U}) \times \mathbf{I} \xrightarrow{\ \ H_n\ \ } \text{MULT}_n(\mathbb{C})
\end{array}
$$

FIGURE 25. A point homotopy H, tuple homotopy H^n, and multiset homotopy H_n, with $z \in \mathbf{U}$, $\mathbf{z} \in \mathbf{U}^n$ and $M \in \text{MULT}_n(\mathbf{U})$.

$\text{MULT}_n(\mathbb{C})$; see Figure 25. Concretely, if $M \in \text{MULT}_n(\mathbf{U})$ and $\mathbf{z} \in \mathbf{U}^n$ is any n-tuple with $M = \text{MULT}(\mathbf{z})$, then $H_n(M,t) = \text{MULT}(H^n(\mathbf{z},t))$.

Definition 9.4 (Induced time maps and path maps). Let H be a point homotopy with induced tuple homotopy H^n and multiset homotopy H_n. The time maps are denoted $h_t \colon \mathbf{U} \to \mathbb{C}$ for H, $(h^n)_t \colon \mathbf{U}^n \to \mathbb{C}^n$ for H^n, and $(h_n)_t \colon \text{MULT}_n(\mathbf{U}) \to \text{MULT}_n(\mathbb{C})$ for H_n. Using the notation $\mathbf{U}_t = h_t(\mathbf{U})$, we have the following path maps: a *point path* $h^z \colon \mathbf{I} \to \mathbf{U}_t$ for H, a *tuple path* $(h^n)^{\mathbf{z}} \colon \mathbf{I} \to (\mathbf{U}_t)^n$ for H^n, and a *multiset path* $(h_n)^M \colon \mathbf{I} \to \text{MULT}_n(\mathbf{U}_t)$ for H_n.

The point paths in point homotopies may merge or split over time.

Definition 9.5 (Splitting and merging). Let $H \colon \mathbf{U} \times \mathbf{I} \to \mathbb{C}$ be a point homotopy. We say that H *splits points* if there are distinct points $u,v \in \mathbf{U}$ and distinct times $s < t \in \mathbf{I}$ such that $u_s = v_s$ and $u_t \neq v_t$. Similarly, we say that H *merges points* if there are distinct points $u,v \in \mathbf{U}$ and distinct times $s < t \in \mathbf{I}$ such that $u_s \neq v_s$ and $u_t = v_t$. When H does not split points it is *nonsplitting* and when it does not merge points it is *nonmerging*. A point homotopy *preserves points* if it is both nonsplitting and nonmerging. In particular, for a point-preserving homotopy, $u_t = v_t$ at some time $s \in \mathbf{I}$ if and only if $u_t = v_t$ for all $t \in \mathbf{I}$.

Nonsplitting homotopies can be initially simplified.

Remark 9.6 (Initial inclusions). When H is a nonsplitting point homotopy, points with $u_0 = v_0$ stay together throughout, so the entire homotopy H factors through the quotient map $h_0 \times \mathbf{1} \colon \mathbf{U} \times \mathbf{I} \twoheadrightarrow \mathbf{U}_0 \times \mathbf{I}$ to produce a simpler point homotopy $H' \colon \mathbf{U}_0 \times \mathbf{I} \to \mathbb{C}$. This allows us to assume without loss of generality that all nonsplitting homotopies are injective at time $t = 0$ with $\mathbf{U} = \mathbf{U}_0$.

A nonsplitting point homotopy leads to multiset paths that are uniquely liftable.

Remark 9.7 (Nonsplitting). Let $H \colon \mathbf{U} \times \mathbf{I} \to \mathbb{C}$ be a point homotopy and let H_n be the corresponding multiset homotopy. When H is nonsplitting, the points in a multiset path can merge but not split, which means that they have a weakly increasing shape. In particular, multiset paths in H_n satisfy the necessary conditions to be uniquely liftable through the LL map (Theorem 8.10).

One consequence of Remark 9.7 is homotopy at the level of polynomial spaces.

Definition 9.8 (Polynomial homotopies). Let $H \colon \mathbf{U} \times \mathbf{I} \to \mathbb{C}$ be a nonsplitting point homotopy with $\mathbf{U} = \mathbf{U}_0 \subset \mathbb{C}$. We can use Theorem 8.10 to define a function $\widetilde{H}_n \colon \text{POLY}_d^{mt}(\mathbf{U}) \times \mathbf{I} \to \text{POLY}_d^{mt}(\mathbb{C})$ as follows. Let p be a monic degree-d polynomial with $[p] \in \text{POLY}_d^{mt}(\mathbf{U})$ and let $M = \text{LL}([p]) = \mathbf{cvl}(p) \in \text{MULT}_n(\mathbf{U})$. By

$$\begin{array}{ccc}
\text{POLY}_d^{mt}(\mathbf{U}) \times \mathbf{I} & \xrightarrow{\widetilde{H}_n} & \text{POLY}_d^{mt}(\mathbb{C}) \\
\downarrow{\scriptstyle \text{LL} \times 1} & & \downarrow{\scriptstyle \text{LL}} \\
\text{MULT}_n(\mathbf{U}) \times \mathbf{I} & \xrightarrow{H_n} & \text{MULT}_n(\mathbb{C})
\end{array}$$

FIGURE 26. The polynomial homotopy $\widetilde{H}_n$ can be viewed as a lift of the multiset homotopy H_n through the LL map, i.e. this diagram commutes.

$$\begin{array}{ccc}
\text{POLY}_{\lambda\to\mu}^{mt}(\mathbf{U}) & \xrightarrow{(\widetilde{h}_n)_t} & \text{POLY}_{\lambda\to\mu}^{mt}(\mathbf{U}_t) \\
\downarrow{\scriptstyle \text{LL}} & & \downarrow{\scriptstyle \text{LL}} \\
\text{MULT}_\mu(\mathbf{U}) & \xrightarrow{(h_n)_t} & \text{MULT}_\mu(\mathbf{U}_t)
\end{array}$$

FIGURE 27. The time map $(\widetilde{h}_n)_t$ is a lift of the time map $(h_n)_t$ through the LL map when restricted to a stratum in the double stratification of $\text{POLY}_d^{mt}(\mathbb{C})$.

Remark 9.7, the multiset path $\alpha = (h_n)^M \colon \mathbf{I} \to \text{MULT}_n(\mathbb{C})$ starting at M has a weakly increasing shape and $[p]$ is a lift of its starting point $\alpha(0)$ through the LL map. Next, by Theorem 8.10 there is a unique lift of α to a path $\beta \colon \mathbf{I} \to \text{POLY}_d^{mt}(\mathbf{U})$ that starts at $[p]$. Finally, we define $\widetilde{H}_n$ at the point $([p], t) \in \text{POLY}_d^{mt}(\mathbf{U}) \times \mathbf{I}$ to be $\beta(t)$. By construction, $\text{LL} \circ \widetilde{H}_n = H_n \circ (\text{LL} \times 1)$ (see Figure 26), so $\widetilde{H}_n$ is a continuous map which we refer to as a *polynomial homotopy*.

10. POLYNOMIAL SPACES

In this section we establish the homeomorphisms and compactifications shown in Figure 28 and the quotients and deformation retractions shown in Figure 29. The relationships between these polynomial spaces mirror the relationships between subspaces of $\mathbb{C}$ used to define them, and this is what prompted our introduction of a visual shorthand (Definition 1.2). We begin by establishing continuous maps between polynomial spaces.

Remark 10.1 (Time maps). Let $H \colon \mathbf{U} \times \mathbf{I} \to \mathbb{C}$ be a nonsplitting point homotopy and let $\widetilde{H}_n$ be the corresponding polynomial homotopy. For any $s < t$ in $\mathbf{I}$, we can restrict $\mathbf{I}$ to the interval $[s, t]$ and apply Remark 9.6 to obtain the point and multiset time maps $h_t \colon \mathbf{U}_s \to \mathbf{U}_t$ and $(h_n)_t \colon \text{MULT}_n(\mathbf{U}_s) \to \text{MULT}_n(\mathbf{U}_t)$ respectively. The polynomial homotopy $\widetilde{H}_n$ is then defined by lifting the multiset paths in H_n, which gives us the polynomial time map $(\widetilde{h}_n)_t \colon \text{POLY}_d^{mt}(\mathbf{U}_s) \to \text{POLY}_d^{mt}(\mathbf{U}_t)$. In particular, this is a continuous map from one polynomial space to another.

Proposition 10.2 (Homeomorphisms). *Let $\mathbf{U}$ be a compact subset of $\mathbb{C}$ and let $H \colon \mathbf{U} \times \mathbf{I} \to \mathbb{C}$ be a point-preserving homotopy. Then for all $s < t$ in $\mathbf{I}$, the spaces $\text{POLY}_d^{mt}(\mathbf{U}_s)$ and $\text{POLY}_d^{mt}(\mathbf{U}_t)$ are homeomorphic.*

Proof. First, consider the restricted map $H \colon \mathbf{U} \times [s, t] \to \mathbb{C}$ and its time reversal $H^{\text{rev}} \colon \mathbf{U} \times [s, t] \to \mathbb{C}$ defined by $H^{\text{rev}}(u, x) = H(u, s + t - x)$. Since $h_t \colon \mathbf{U}_s \to \mathbf{U}_t$

and the time reversal $h_s^{\text{rev}} \colon \mathbf{U}_t \to \mathbf{U}_s$ are inverses of one another, each time map is a bijection, and since $\mathbf{U}$ is compact, it is also a homeomorphism. Since H is nonsplitting, we can apply Remark 10.1 to see that the polynomial time map is a continuous function $(\widetilde{h}_n)_t \colon \text{POLY}_d^{mt}(\mathbf{U}_s) \to \text{POLY}_d^{mt}(\mathbf{U}_t)$. Since H is nonmerging, the time reversal H^{rev} is a nonsplitting point homotopy which yields the continuous time map $(\widetilde{h}_n)_s^{\text{rev}} \colon \text{POLY}_d^{mt}(\mathbf{U}_t) \to \text{POLY}_d^{mt}(\mathbf{U}_s)$. Finally, the fact that h_t and h_s^{rev} are inverses tells us that $(\widetilde{h}_n)_t$ and $(\widetilde{h}_n)_s^{\text{rev}}$ are inverses of one another, so the proof is complete. $\qquad\square$

The following corollary is an immediate application of Proposition 10.2.

Corollary 10.3 (Topological variations). *If $\mathbf{U}$ and $\mathbf{V}$ are two closed intervals, two closed topological disks, two closed annuli, or two closed circles embedded in $\mathbb{C}$ (so that there is a point-preserving homotopy $\mathbf{U}$ to $\mathbf{V}$ inside $\mathbb{C}$), then $\text{POLY}_d^{mt}(\mathbf{U})$ and $\text{POLY}_d^{mt}(\mathbf{V})$ are homeomorphic.*

The homeomorphisms produced by Proposition 10.2 and Corollary 10.3 are not canonically defined, but there are sufficiently many to justify de-emphasizing the fine details of the shapes listed in Definition 1.2.

Remark 10.4 (Shapes). The parenthetical point-preserving homotopy condition in the statement of Corollary 10.3 is, strictly speaking, unnecessary since all embeddings of these simple spaces into $\mathbb{C}$ are connected by point-preserving homotopies, and more exotic possibilities would detract from our main point. For any reasonably nice class of embeddings (such as all closed Euclidean rectangles in $\mathbb{C}$) there are more or less obvious point-preserving homotopies between them. And by Proposition 10.2 there are homeomorphisms between the corresponding polynomial spaces. In particular, $\text{POLY}_d^{mt}(\blacksquare)$ can be discussed without specifying the precise closed rectangle, since there is only one such space up to a choice of homeomorphism.

Lemma 10.5 (Closed and bounded). *If $\mathbf{U} \subset \mathbb{C}$ is closed/bounded/compact, then $\mathbf{U}^n$, $\text{MULT}_n(\mathbf{U})$ and $\text{POLY}_d^{mt}(\mathbf{U})$ are closed/bounded/compact.*

Proof. The properties of being closed, bounded and/or compact pass through finite direct products and these properties also project and lift through surjections where there is a finite upper bound on the size of a point preimage. $\qquad\square$

Lemma 10.6 (Nested compact sets). *Let U and V be open subsets of $\mathbb{C}$, and suppose they can be expressed as the unions of nested compact sets $\mathbf{U}_1 \subset \mathbf{U}_2 \subset \cdots$ and $\mathbf{V}_1 \subset \mathbf{V}_2 \subset \cdots$ respectively. If there is a homotopy from U to V such that the restriction to each $\mathbf{U}_i$ is point-preserving, then $\text{POLY}_d^{mt}(U) \cong \text{POLY}_d^{mt}(V)$.*

Proof. By Proposition 10.2 and Lemma 10.5, $\text{POLY}_d^{mt}(\mathbf{U}_i)$ and $\text{POLY}_d^{mt}(\mathbf{V}_i)$ are compact and homeomorphic. Since $\text{POLY}_d^{mt}(U)$ and $\text{POLY}_d^{mt}(V)$ are each the nested union of these homeomorphic compact sets, it follows that the two polynomial spaces are homeomorphic as well. $\qquad\square$

We are now ready to prove Theorem E.

Theorem 10.7 (Theorem E). *The complex plane $\mathbb{C}$, the punctured plane $\mathbb{C}_\mathbf{0}$ and the real line $\mathbb{R}$ are homeomorphic to the open rectangle $\square$, the open annulus $\odot$ and the open interval $\multimap$ respectively, and these induce homeomorphisms of polynomial spaces $\text{POLY}_d^{mt}(\mathbb{C}) \cong \text{POLY}_d^{mt}(\square)$, $\text{POLY}_d^{mt}(\mathbb{C}_\mathbf{0}) \cong \text{POLY}_d^{mt}(\odot)$ and $\text{POLY}_d^{mt}(\mathbb{R}) \cong \text{POLY}_d^{mt}(\multimap)$.*

Proof. Let $\square \subset \mathbb{C}$ be an open rectangle and let $H \colon \mathbb{C} \times \mathbf{I} \to \mathbb{C}$ be the standard point-preserving homotopy from $\mathbb{C}$ (viewed simply as the plane) to $\square$ obtained by rescaling the real and imaginary coordinates separately. For each positive integer k, let $\mathbf{U}_k \subset \mathbb{C}$ be the closed square of side length k centered at the origin. Then $\mathbb{C}$ is the union of the compact sets $\mathbf{U}_1 \subset \mathbf{U}_2 \subset \cdots$, and H transforms these to a sequence of homeomorphic nested compact sets $\mathbf{V}_1 \subset \mathbf{V}_2 \subset \cdots$ with $\square$ as their union. By Lemma 10.6, $\mathrm{POLY}_d^{mt}(\mathbb{C}) \cong \mathrm{POLY}_d^{mt}(\square)$. The other two homeomorphisms follow from similar arguments. $\qquad \square$

Next, we consider the compatibility of the homeomorphisms above with natural compactifications.

Proposition 10.8 (Special compactifications)**.** *Let $\mathbf{U} \subset \mathbb{C}$ be a closed interval $\rightarrowtail$ / closed square $\blacksquare$ / closed disk $\bigcirc$ / closed annulus $\circledcirc$ and let U be the corresponding open interval $\multimap$ / open square $\blacksquare$ / open disk $\bullet$ / open annulus $\odot$, so that $\mathbf{U}$ is the compact closure of U. Then the compact closure of U^n in $\mathbb{C}^n$ is $\mathbf{U}^n$, the compact closure of $\mathrm{MULT}_n(U)$ in $\mathrm{MULT}_n(\mathbb{C})$ is $\mathrm{MULT}_n(\mathbf{U})$, and the compact closure of $\mathrm{POLY}_d^{mt}(U)$ in $\mathrm{POLY}_d^{mt}(\mathbb{C})$ is $\mathrm{POLY}_d^{mt}(\mathbf{U})$.*

Proof. By Lemma 10.5, $\mathbf{U}^n$, $\mathrm{MULT}_n(\mathbf{U})$ and $\mathrm{POLY}_d^{mt}(\mathbf{U})$ are compact and closed, so it is clear that the closure of the U-version is contained in the $\mathbf{U}$-version in each case. In the other direction, there exist point-preserving homotopies H that shrink $\mathbf{U}$ into the interior of U in each case, and the time-reversed version H' expands a closed subspace of U, homeomorphic to $\mathbf{U}$, to all of $\mathbf{U}$. Once we lift H' to a tuple, multiset and polynomial homotopy, it becomes clear that every tuple / multiset / polynomial in $\mathbf{U}^n$ / $\mathrm{MULT}_n(\mathbf{U})$ / $\mathrm{POLY}_d^{mt}(\mathbf{U})$ is the endpoint of a path that otherwise remains in U^n / $\mathrm{MULT}_n(U)$ / $\mathrm{POLY}_d^{mt}(U)$. In particular, the version with $\mathbf{U}$ is contained in the closure of the version with U. $\qquad \square$

As an immediate consequence, we obtain a proof of Theorem F.

Theorem 10.9 (Theorem F)**.** *The polynomial spaces $\mathrm{POLY}_d^{mt}(\blacksquare)$, $\mathrm{POLY}_d^{mt}(\circledcirc)$ and $\mathrm{POLY}_d^{mt}(\rightarrowtail)$ are compactifications of $\mathrm{POLY}_d^{mt}(\blacksquare)$, $\mathrm{POLY}_d^{mt}(\odot)$ and $\mathrm{POLY}_d^{mt}(\multimap)$.*

Proof. This follows from Proposition 10.8 and Theorem E. $\qquad \square$

A simple argument shows that some polynomial spaces are dense in others.

Remark 10.10 (Dense)**.** Let $H \colon \mathbb{T} \times \mathbf{I} \to \mathbb{C}$ be a point-preserving homotopy that rigidly rotates the unit circle and let p be any polynomial where -1 is a critical value. By choosing an appropriate portion of circle rotation over time and lifting this to a path of polynomials in $\mathrm{POLY}_d^{mt}(\bigcirc)$, we can see $[p] \in \mathrm{POLY}_d^{mt}(\bigcirc)$ is a limit of polynomials in $\mathrm{POLY}_d^{mt}(\bigcirc)$. In particular, $\mathrm{POLY}_d^{mt}(\bigcirc)$ is dense in $\mathrm{POLY}_d^{mt}(\bigcirc)$.

Example 10.11 (Homeomorphisms and compactifications)**.** Figure 28 shows a variety of inclusions, homeomorphisms and compactifications of polynomial spaces over $\mathbb{R}$, $\mathbb{C}$, $\mathbb{C}_{\mathbf{0}}$, $\mathbb{T}$, an open interval $\multimap$, an open rectangle $\blacksquare$, an open disk $\bullet$, an open annulus $\odot$, a closed interval $\rightarrowtail$, a closed rectangle $\blacksquare$, a closed disk $\bigcirc$, a closed annulus $\circledcirc$ and a circle $\bigcirc$. The inclusions are immediate: if $V \subset U$, then $\mathrm{POLY}_d^{mt}(V) \subset \mathrm{POLY}_d^{mt}(U)$ by definition. The homeomorphisms follow from Proposition 10.2 and the obvious point-preserving homotopies. And the compactifications follow from Proposition 10.8.

$$\mathrm{POLY}_d^{mt}(\mathbb{R}) \hookrightarrow \mathrm{POLY}_d^{mt}(\mathbb{C}) = \mathrm{POLY}_d^{mt}(\mathbb{C}) \leftarrow \mathrm{POLY}_d^{mt}(\mathbb{C_0}) \leftarrow \mathrm{POLY}_d^{mt}(\mathbb{T})$$

$$\big\updownarrow\cong \qquad \big\updownarrow\cong \qquad \big\updownarrow\cong \qquad \big\updownarrow\cong \qquad \big\|$$

$$\mathrm{POLY}_d^{mt}(\multimap) \hookrightarrow \mathrm{POLY}_d^{mt}(\blacksquare) \overset{\cong}{\leftrightarrow} \mathrm{POLY}_d^{mt}(\bullet) \leftarrow \mathrm{POLY}_d^{mt}(\odot) \leftarrow \mathrm{POLY}_d^{mt}(\bigcirc)$$

$$\big\downarrow{\scriptstyle\mathrm{CMPT}} \qquad \big\uparrow{\scriptstyle\mathrm{CMPT}} \qquad \big\uparrow{\scriptstyle\mathrm{CMPT}} \qquad \big\uparrow{\scriptstyle\mathrm{CMPT}} \qquad \big\|$$

$$\mathrm{POLY}_d^{mt}(\multimap) \hookrightarrow \mathrm{POLY}_d^{mt}(\square) \overset{\cong}{\leftrightarrow} \mathrm{POLY}_d^{mt}(\bigcirc) \leftarrow \mathrm{POLY}_d^{mt}(\circledcirc) \leftarrow \mathrm{POLY}_d^{mt}(\bigcirc)$$

FIGURE 28. Homeomorphisms and compactifications of spaces of polynomial over $\mathbb{R}$, $\mathbb{C}$, $\mathbb{C_0}$, $\mathbb{T}$, an interval, a rectangle, a disk, an annulus, a circle and their interiors.

Proposition 10.12 (Special quotients)**.** *There is a surjective quotient map from* $\mathrm{POLY}_d^{mt}(\multimap)$ *to* $\mathrm{POLY}_d^{mt}(\bigcirc)$ *where the only identifications are among the polynomials with a critical value at an endpoint of the interval. Similarly, there is a surjective quotient map from* $\mathrm{POLY}_d^{mt}(\square)$ *to* $\mathrm{POLY}_d^{mt}(\circledcirc)$ *where the only identifications are among the polynomials with a critical value in the left or right side of the rectangle.*

Proof. A closed interval in $\mathbb{C}$ can be stretched around and moved in a point-preserving way until identifying its endpoints at time $t = 1$ to form an embedded circle. For example, if $U = \multimap$ is embedded in $\mathbb{C}$ as the left half of the unit circle $\mathbb{T}$ and parameterized as $U = \{e(s) \mid s \in [-\frac{1}{4}, \frac{1}{4}]\}$ using Definition 4.1, then the map $H \colon U \times \mathbf{I} \to \mathbb{T}$ that sends $(e(s), t)$ to $e((1 + t) \cdot s)$ is a nonsplitting point homotopy with these properties. This map is point-preserving except that at time $t = 1$, its length has doubled, covering all of $\mathbb{T}$ with the endpoints overlapping at $e(\frac{1}{2}) = e(-\frac{1}{2}) = -1$. In particular, if H' is H restricted to $V \times \mathbf{I}$ where V is U with both endpoints removed, then H' is point-preserving. The time $t = 1$ map of the polynomial homotopy $\widetilde{H}_n$ is a map q that sends $\mathrm{POLY}_d^{mt}(\multimap)$ to $\mathrm{POLY}_d^{mt}(\bigcirc)$ (Lemma 10.1), and the restricted version $\widetilde{H'_n}$ is a homeomorphism between $\mathrm{POLY}_d^{mt}(\multimap)$ and $\mathrm{POLY}_d^{mt}(\bigcirc)$ (Lemma 10.6). Since $\mathrm{POLY}_d^{mt}(\multimap)$ is the closure of $\mathrm{POLY}_d^{mt}(\multimap)$ (Lemma 10.5) and $\mathrm{POLY}_d^{mt}(\bigcirc)$ is dense in $\mathrm{POLY}_d^{mt}(\bigcirc)$ (Remark 10.10), the map q is surjective. And the homeomorphic embedding of the polynomials with all critical values in the interior of the interval means that the only identifications are among those polynomials with critical values at the endpoints. The argument in the second case is nearly identical except that the unit circle is expanded to include a closed interval of possible positive magnitudes. $\qquad\square$

The special quotient from $\mathrm{POLY}_d^{mt}(\square)$ to $\mathrm{POLY}_d^{mt}(\circledcirc)$ is best understood through an example. See Example 15.2.

Definition 10.13 (Deformation retracting homotopies)**.** Recall that a *deformation retraction* from a topological space $\mathbf{U}$ to a subspace $\mathbf{V}$ is a map $H \colon \mathbf{U} \times \mathbf{I} \to \mathbf{U}$ such that $h_0(u) = u$, $h_t(v) = v$ and $h_1(u) \in \mathbf{V}$ for all $u \in \mathbf{U}$, $v \in \mathbf{V}$ and $t \in \mathbf{I}$. Let $\mathbf{V} \subset \mathbf{U}$ be subspaces of $\mathbb{C}$ and let $H \colon \mathbf{U} \times \mathbf{I} \to \mathbb{C}$ be a nonsplitting point homotopy. We say that H is a *nonsplitting deformation retracting point homotopy from* $\mathbf{U}$ *to* $\mathbf{V}$ if the image of H lies in $\mathbf{U}$ and H, with the range restricted to $\mathbf{U}$, is a deformation retraction from $\mathbf{U}$ to $\mathbf{V}$.

$$\begin{array}{ccc}
\mathrm{POLY}_d^{mt}(\blacksquare) & \xrightarrow{\quad LL \quad} & \mathrm{MULT}_n(\blacksquare) \\
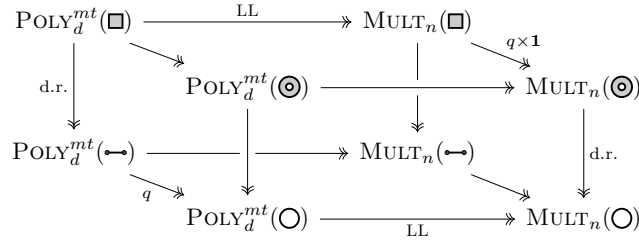\end{array}$$

FIGURE 29. The left-to-right LL maps, back-to-front quotient maps, and the top-to-bottom deformation retractions for the $2n$-dimensional cell complexes associated with the four key shapes.

Proposition 10.14 (Deformation retractions). *If H is a nonsplitting deformation retracting point homotopy from $\mathbf{U}$ to $\mathbf{V}$ inside $\mathbb{C}$, then there is a $\widetilde{H}_n$-induced deformation retraction from $\mathrm{POLY}_d^{mt}(\mathbf{U})$ to $\mathrm{POLY}_d^{mt}(\mathbf{V})$ inside $\mathrm{POLY}_d^{mt}(\mathbb{C})$.*

Proof. At time $t = 0$, H is the identity map on $\mathbf{U}$ and $\widetilde{H}_n$ is the identity map on $\mathrm{POLY}_d^{mt}(\mathbf{U})$, and since the range of H remains in $\mathbf{U}$, the range of $\widetilde{H}_n$ remains in $\mathrm{POLY}_d^{mt}(\mathbf{U})$. Next, a multiset in $\mathbf{V}$ remains fixed under H_n and the unique lift of this constant multiset path is a constant polynomial path. Thus, $\widetilde{H}_n$ restricts the identity map on $\mathrm{POLY}_d^{mt}(V)$ at each time t. Finally, at time $t = 1$ the range of H is in $\mathbf{V}$, so at time $t = 1$ the range of $\widetilde{H}_n$ is in $\mathrm{POLY}_d^{mt}(\mathbf{V})$. $\qquad\square$

We now establish the last of our main tools.

Theorem 10.15 (Theorem G). *A deformation retraction of $\square$ onto any embedded arc $\rightarrowtail$ induces a deformation retraction from $\mathrm{POLY}_d^{mt}(\blacksquare)$ to $\mathrm{POLY}_d^{mt}(\rightarrowtail)$. Similarly, the deformation retraction of $\circledcirc$ onto any core curve $\bigcirc$ induces a deformation retraction from $\mathrm{POLY}_d^{mt}(\circledcirc)$ to $\mathrm{POLY}_d^{mt}(\bigcirc)$.*

Proof. This follows immediately from Proposition 10.14. $\qquad\square$

The results from this section establish the maps between the polynomial space on the lefthand side of Figure 29. The two back-to-front quotient maps are the special quotients of Proposition 10.12. The two top-to-bottom deformation retractions follow from the obvious nonsplitting deformation retracting point homotopies from a closed rectangle to a horizontal line segment and from a closed annulus to a circle. Finally, if we choose quotients and deformation retractions that commute at the level of subspaces of $\mathbb{C}$, the corresponding polynomial versions also commute. The maps between the multiset spaces on the right are induced by the same set of point homotopies, and the LL map sends the four polynomial spaces on left to the four multiset spaces on the right.

Part 3. Geometric Combinatorics

The goal of Part 3 is to prove Theorems A, B, C, and D, which are assertions about metric cell structures for the polynomial spaces $\text{POLY}_d^{mt}(\mathbf{X})$ when $\mathbf{X}$ is ↬, ◯, □, or ◉, respectively. Part 3 is structured as follows. In Section 11, we recall the monodromy action of a planar branched cover and discuss its relationship with the side permutations defined in Section 5. In Section 12 we prove Theorem A, in Section 13 we proof Theorem B, in Section 14 we prove Theorem C, and in Section 15 we prove Theorem D.

11. Monodromy and Side Permutations

There is a direct connection between the monodromy action of a branched cover and the side permutations defined in Section 5. We begin with the general results (11.1) and then connect them to the combinatorics of our complexes (11.2).

11.1. **Monodromy.** The monodromy action of a branched cover is a classical notion. Here we recall the basic definitions and record a useful characterization of polynomials (Proposition 11.6). For a different perspective on some of the monodromy, see [DM22, §9].

Definition 11.1 (Monodromy). Let $p \colon \mathbb{C} \to \mathbb{C}$ be a planar d-branched cover and let z be a regular point in the range. Regular paths based at z in the range lift to d paths that permute the d preimages of z in the domain. This *monodromy action* can be encoded in a group homomorphism $\pi_1(\mathbb{C} \setminus \mathbf{cvl}(p), z) \to \text{SYM}_d$. Both the topology of the connected d-sheeted cover and the monodromy action can be reconstructed from this group homomorphism. See [Hat02] for details.

Definition 11.2 (Constellations). When p has ℓ distinct critical values, the fundamental group $\pi_1(\mathbb{C} \setminus \mathbf{cvl}(p), z)$ is a free group $\mathbb{F}_\ell$ of rank ℓ, and the map $\mathbb{F}_\ell \to \text{SYM}_d$ can be described by the image of an ordered basis, i.e. by an ordered ℓ-tuple of permutations $\mathbf{g} = [g_1 \; g_2 \; \cdots \; g_\ell] \in (\text{SYM}_d)^\ell$. One way of producing ℓ loops that represent an ordered basis of $\mathbb{F}_\ell$ comes from drawing a star graph with ℓ arcs from z to the ℓ critical values with disjoint interiors. The ℓ loops are those that travel along one of these arcs, stopping just short of a critical value, going clockwise around the critical value, and returning along the same arc to z. These loops define a basis for the free group $\mathbb{F}_\ell$. When the basis elements and the corresponding permutations are linearly ordered according to the clockwise order that the arcs leave z, the product of these ℓ permutations in this order is a d-cycle. In [LZ04] these are called *constellations*. In the generic case where there are n critical values of multiplicity 1, the g_i are transpositions and the n-tuple $\mathbf{g}$ is a minimum length factorization of a fixed d-cycle into $n = d - 1$ transpositions.

A continuous motion of the critical values that keeps them distinct but returns them setwise to their original positions alters the monodromy action in predictable ways. In the generic polynomial case, there is a BRAID_n action on n-tuples of transpositions.

Definition 11.3 (Hurwitz action). Let G be a group and denote each n-tuple $\mathbf{g}$ in G^n by a row vector of the form $\mathbf{g} = [g_1 \; g_2 \; \cdots \; g_n]$, and let $\{\beta_1, \ldots, \beta_{n-1}\}$ be the standard generating set for the n-strand braid group BRAID_n. The *Hurwitz action*

of $\textsc{Braid}_n$ on G^n is defined by setting $\beta_i \cdot \mathbf{g}$ equal to

$$\beta_i \cdot [g_1 \ \cdots \ g_{i-1} \ \underline{g_i \ g_{i+1}} \ g_{i+2} \ \cdots \ g_n] = [g_1 \ \cdots \ g_{i-1} \ \underline{g_{i+1} \ g_i^{g_{i+1}}} \ g_{i+2} \ \cdots \ g_n]$$

where the altered portion has been underlined and x^y denotes the conjugate $y^{-1}xy$. This is called an *elementary Hurwitz move*. One easily verifies that this action satisfies the relations in the standard presentation of $\textsc{Braid}_n$. Under the Hurwitz action, the product of the entries in this order remains constant.

Hurwitz defined this action in his 1891 paper [Hur91] well before Artin's formal introduction of braid groups as an object of study [Art25, Art47]. In the generic case, the action is transitive.

Remark 11.4 (Hurwitz transitivity). It is well-known that there are exactly d^{d-2} ways to factor the d-cycle $\delta = (1 \ 2 \ \cdots d)$ into $n = d - 1$ transpositions, which correspond to the d^{d-2} maximal chains in $\textsc{NCPerm}_d = \textsc{NCPart}_d$, and to the d^{d-2} n-dimensional simplices in $|\textsc{NCPerm}_d|_\Delta = |\textsc{NCPart}_d|_\Delta$. And the Hurwitz action is transitive on these sets [BDSW14]. In fact, for any permutation $\pi \in \textsc{Sym}_d$ of absolute length k (Definition 4.18), the $\textsc{Braid}_k$ action on factorizations of π into a product of k transpositions is also transitive. This is clear since the factorizations and the transitivity take place cycle by disjoint cycle. This more general property is known as *local Hurwitz transitivity*.

This action can be used to distinguish the d^{d-2} generic monic centered polynomials with the same set of n distinct critical values.[3] More generally, monic centered polynomials are distinguished by their critical values and their monodromy actions (Proposition 11.6). This elementary result is not usually stated in these terms, so we include a proof. We begin with a special case.

Lemma 11.5 (Monodromy and critical values). *Monic centered polynomials with the same generic set of critical values and the same monodromy action are equal.*

Proof. Let p and q be generic monic centered polynomials of degree d with $\mathbf{cvl}(p) = \mathbf{cvl}(q) = M$ with $\textsc{Shape}(M) = 1^n$ as their common (multi)set of critical values. We know that there are exactly d^{d-2} polynomials in $\textsc{Poly}_d^{mc}(\mathbb{C})$ with $\mathbf{cvl}(p) = M$ (Theorem 7.3). Next, any braided motion of the n critical points extends to a point-preserving homotopy of $\mathbb{C}$, which induces an automorphism of $\textsc{Poly}_d^{mc}(\mathbb{C})$ (Lemma 10.6). As a consequence there exists a polynomial in $\textsc{Poly}_d^{mc}(\mathbb{C})$ with $\mathbf{cvl} = M$ for each of the d^{d-2} possible monodromy actions in the orbit of the Hurwitz action (Remark 11.4). In other words, the map from the d^{d-2} polynomials in $\textsc{Poly}_d^{mc}(\mathbb{C})$ with $\mathbf{cvl} = M$ to the d^{d-2} possible monodromies is onto, and therefore also injective. $\square$

Proposition 11.6 (Monodromy and critical values). *Monic centered polynomials with the same multiset of critical values and the same monodromy action are equal.*

Proof. Let p and q be monic centered polynomials of degree d with $\mathbf{cvl}(p) = \mathbf{cvl}(q) = M$, $S = \textsc{Set}(M)$ and $\ell = |S| = |M|_{\textsc{Set}}$. Let $\mathbf{U} \subset \mathbb{C}$ be a small closed neighborhood of S and note that $\textsc{Mult}_n(U)$ is a small open neighborhood of M in $\textsc{Mult}_n(\mathbb{C})$. Let p_1 and q_1 be generic polynomials in $\textsc{Mult}_n(U)$ near p and q (Lemma 7.17). By dragging their critical values around inside $\mathbf{U}$ we may assume

---

[3]Recall that monic centered polynomials are the distinguished representatives of equivalence classes of monic polynomials up to precomposition with a translation (Remark 7.6).

that $\mathbf{cvl}(p_1) = \mathbf{cvl}(q_1) = M_1$ of shape 1^n. By Remark 11.4 and Lemma 11.5 we know that there is a braided motion of M_1 which transforms p_1 into q_1, but more is true. Let π^i be the monodromy permutation corresponding to the unique critical value of M in the component $\mathbf{U}_i$, (coming from an arc from z to $\partial\mathbf{U}_i$, clockwise around the boundary of $\mathbf{U}_i$ and then back to z) and note that π^i is the same permutation for both p and q since their monodromy actions agree, and for their perturbations p_1 and q_1 since the loop remains regular and the permutation unchanged as p and q are perturbed. For an appropriate choice of little loops, π^i can be factored into transpositions coming from the elements of M_1 in $\mathbf{U}_i$. In particular, both p_1 and q_1 produce local transposition factorizations of π^i. Local Hurwitz transitivity means that the transposition factorization of π^i coming from p_1 can be transformed into the transposition factorization of π^i coming from q_1 by only moving the critical values of M_1 inside $\mathbf{U}_i$. Once all of these local modifications are made in each component of $\mathbf{U}_i$, the transformed p_1 has the same monodromy as q_1 and they are equal by Lemma 11.5. By picking $\mathbf{U}$ to be an arbitrarily small neighborhood of S, one can show that the distance from p to p_1 to q_1 to q in POLY_d^{mt} is also arbitrarily small. Thus $p = q$. $\qquad\square$

11.2. **Side permutations.** We now connect the monodromy action to the side permutations defined in Section 5. Let $p \in \mathrm{POLY}_d^{mt}(\square)$ be a polynomial with $\mathbf{cvl}(p) \subset \square$ and let $\mathbf{Q}_p$ be its regular value complex. The basepoint $z = (x_\ell, y_b) \in \mathbf{Q}_p$ is regular by construction and its d indexed preimages $\{z_1, \ldots, z_d\}$ are arranged in counterclockwise order in the boundary of $\mathbf{P}_p$ (Definition 5.2). The connection between the *monodromy action* of $\pi_1(\mathbf{Q}_p - \mathbf{cvl}(p), z)$ on the preimages of z and NCPERM_d is straightforward up to a choice of conventions.

Definition 11.7 (Monodromy and $\mathbf{Q}_p$). Permutations typically compose as functions from right-to-left, while paths are often concatenated from left-to-right. To reconcile this difference, the monodromy permutation is defined with a change of direction. If γ is an oriented path based at z that represents an element of $\pi_1(\mathbf{Q}_p - \mathbf{cvl}(p), z)$, the *monodromy permutation* of γ is the permutation whose disjoint cycles list the indices of the preimages of z as they occur when the lifted paths are traced in the *opposite* direction. This converts the right monodromy action defined by oriented paths to a left action by monodromy permutations. The change of direction ensures that left-to-right path concatenation matches right-to-left permutation composition. For example, if $\mathbf{V}$ is a closed disk in $\mathbf{Q}_p$ with $z \in \partial\mathbf{V}$ and $\mathbf{U} = p^{-1}(\mathbf{V})$ as its preimage in $\mathbf{P}_p$, the *clockwise* loop around $\partial\mathbf{V}$ lifts to clockwise arcs in $\partial\mathbf{U}$, but the monodromy permutation is the *counterclockwise* order in which the indexed preimages of z occur in boundary cycles of the components of $\mathbf{U}$. Compare this with Example 4.21.

As an illustration, consider side surfaces and the associated side permutations.

Lemma 11.8. *For each polynomial $p \in \mathrm{POLY}_d^{mt}(\square)$ the d-cycle $\delta = (1\ 2\ \cdots\ d)$ can be factored as $\delta = \pi_i^L \cdot \pi_i^R$ for each $i \in [k]$, and as $\delta = \pi_j^T \cdot \pi_j^B$ for each $j \in [l]$.*

Proof. Let $\mathbf{V}_i^L$ and $\mathbf{V}_i^R$ the be left and right side surfaces of $\mathbf{Q}$ determined by the arc α_i. Let γ be the clockwise path around $\mathbf{Q}_p$ based at z, let γ^L be the clockwise path around $\partial\mathbf{V}_i$ based at z, and let γ^R be the path from z to b_i in $\mathbf{B}$, clockwise around $\partial\mathbf{V}_i^R$, and from b_i back to z in $\mathbf{B}$. The concatenation $\gamma^L.\gamma^R$ is homotopic to γ inside $\mathbb{C} \setminus \mathbf{cvl}(p)$. The monodromy permutations of γ^L and γ^R are the side

permutations π_i^L and π_i^R, and the monodromy permutation of γ is $\delta = (12 \cdots d)$. Finally the composition $(\pi_i^L)(\pi_i^R)$ is δ, by the argument in Example 4.21. The top-bottom case is nearly identical. $\qquad \square$

The fact that permutation composition comes from concatenating clockwise boundary cycles based at z explains the need to multiply top then bottom and left then right. Lemma 11.8 extends to more general subsurfaces.

Definition 11.9 (Interval permutations). For each subinterval $[x_{i_1}, x_{i_2}] \subset \mathbf{I}_p$, the *interval subsurface* $\mathbf{V}_{i_1,i_2}^I = \mathbf{V}_{i_1}^R \cap \mathbf{V}_{i_2}^L$ is the subrectangle $[x_{i_1}, x_{i_2}] \times \mathbf{J}_p \subset \mathbf{Q}_p$. For each subinterval $[y_{j_1}, y_{j_2}] \subset \mathbf{J}_p$, the *interval subsurface* $\mathbf{V}_{j_2,j_1}^J = \mathbf{V}_j^T \cap \mathbf{V}_{j'}^B$ is the rectangle $\mathbf{I}_p \times [y_{j_1}, y_{j_2}] \subset \mathbf{Q}_p$. Note that the order of the subscripts $j_1 < j_2$ have been switched in the notation $\mathbf{V}_{j_2,j_1}^J$ to reflect the counterclockwise order that ℓ_{j_2} and ℓ_{j_1} occur in the boundary cycle $\partial \mathbf{Q}_p$. This swap simplifies the statement of Lemma 11.11 below. The preimage subsurfaces are denoted $\mathbf{U}_{i_1,i_2}^I = p^{-1}(\mathbf{V}_{i_1,i_2}^I)$ and $\mathbf{U}_{j_2,j_1}^J = p^{-1}(\mathbf{V}_{j_2,j_1}^J)$. Since many of these subsurfaces do not contain the basepoint z, we connect $\mathbf{V}_{i_1,i_2}^I$ to z with the portion of $\mathbf{B}$ from z to b_{i_1}, and we connect $\mathbf{V}_{j_2,j_1}^J$ to z with the portion of $\mathbf{L}$ from z to ℓ_{j_1}. In particular, the clockwise loop around $\partial \mathbf{V}_{i_1,i_2}^I$ *based at z via* $\mathbf{B}$ is the concatenation of the path from z to b_{i_1} in $\mathbf{B}$, the clockwise loop around $\partial \mathbf{V}_{i_1,i_2}^I$, and the return path from b_{i_1} to z in $\mathbf{B}$. The monodromy permutation for this path is the *interval permutation* $\pi_{i_1,i_2}^I = \mathrm{PERM}([\lambda_{i_1,i_2}^I])$ of the *interval partition* $[\lambda_{i_1,i_2}]^I = \mathrm{NCPART}^B(\mathbf{U}_{i_1,i_2}^I)$. Similarly, the clockwise loop around $\mathbf{V}_{j_2,j_1}^J$ *based at z via* $\mathbf{L}$ is the concatenation of the path from z to ℓ_{j_1} in $\mathbf{L}$, the clockwise loop around $\partial \mathbf{V}_{j_2,j_1}^J$, and the return path from ℓ_{j_1} to z in $\mathbf{L}$. And the monodromy permutation for this path is the *interval permutation* $\pi_{j_2,j_1}^J = \mathrm{PERM}([\lambda_{j_2,j_1}^J])$ of the *interval partition* $[\lambda_{j_2,j_1}]^J = \mathrm{NCPART}^L(\mathbf{U}_{j_2,j_1}^J)$.

Remark 11.10 (Sides and intervals). Side surfaces are examples of subinterval surfaces, meaning side partitions are examples of subinterval partitions and side permutations are examples of subinterval permutations. For example, $\mathbf{Q}_p = \mathbf{V}_{\ell,r}^I = \mathbf{V}_{t,b}^J$, so $\delta = \pi_{\ell,r}^I = \pi_{b,t}^J$. Similarly, $\mathbf{V}_i^L = \mathbf{V}_{\ell,i}^I$, $\mathbf{V}_i^R = \mathbf{V}_{i,r}^I$, $\mathbf{V}_j^T = \mathbf{V}_{t,j}^J$ and $\mathbf{V}_j^B = \mathbf{V}_{j,b}^J$, so $\pi_i^L = \pi_{\ell,i}^I$, $\pi_i^R = \pi_{i,r}^I$, $\pi_j^T = \pi_{t,j}^T$ and $\pi_j^B = \pi_{j,b}^J$.

We have the following generalization of Lemma 11.8.

Lemma 11.11 (Factoring side permutations). *For each triple $i_1 < i_2 < i_3$ in $[k]$, there is a horizontal factorization $\pi_{i_1,i_3}^I = (\pi_{i_1,i_2}^I)(\pi_{i_2,i_3}^I)$, and for each triple $j_1 < j_2 < j_3$ in $[l]$, there is a vertical factorization $\pi_{j_3,j_1}^J = (\pi_{j_3,j_2}^J)(\pi_{j_2,j_1}^J)$.*

Proof. The rectangles $\mathbf{V}_{i_1,i_2}^I$ and $\mathbf{V}_{i_2,i_3}^I$ overlap on the vertical arc α_{i_2}, so a clockwise loop around $\mathbf{V}_{i_1,i_2}^I$ based at z via $\mathbf{B}$, followed by a clockwise loop around $\mathbf{V}_{i_2,i_3}^I$ based at z via $\mathbf{B}$, is homotopy equivalent in $\mathbb{C} \setminus \mathbf{cvl}(p)$ to a clockwise loop around $\mathbf{V}_{i_1,i_3}$ based at z via $\mathbf{B}$. The corresponding permutation factorization follows by Definition 11.1. Similarly the rectangles $\mathbf{V}_{j_3,j_2}^J$ and $\mathbf{V}_{j_2,j_1}^J$ overlap on the horizontal arc β_{j_2}, and a clockwise loop around $\mathbf{V}_{j_3,j_2}^J$ based at z via $\mathbf{L}$, followed by a clockwise loop around $\mathbf{V}_{j_2,j_1}^J$ based at z via $\mathbf{L}$, is homotopy equivalent in $\mathbb{C} \setminus \mathbf{cvl}(p)$ to a clockwise loop around $\mathbf{V}_{j_3,j_1}^J$ based at z via $\mathbf{L}$. $\qquad \square$

Let $\sigma_i = \pi_{i,i+1}^I$ be the permutation from a single edge subinterval of $\mathbf{I}$, and let $\tau_j = \pi_{j+1,j}^J$ be the permutation from a single edge subinterval of $\mathbf{J}$. We call these

basic horizontal side permutations and *basic vertical side permutations* respectively. In this language we have the following corollary where we have factored horizontally and vertically as much as possible.

Corollary 11.12 (Side constellations). *For each polynomial $p \in \text{POLY}_d^{mt}(\square)$ the d-cycle δ can be factored into basic horizontal side permutations $\delta = \pi_1^L \cdot \sigma_1 \cdot \sigma_2 \cdots \sigma_{k-1} \cdot \pi_k^R$ with corresponding horizontal side constellation $[\pi_1^L \ \sigma_1 \ \sigma_2 \ \cdots \ \sigma_{k-1} \ \pi_k^R]$, and into basic vertical side permutations $\delta = \pi_l^T \cdot \tau_{l-1} \cdots \tau_2 \cdot \tau_1 \cdot \pi_1^B$ with corresponding vertical side constellation $[\pi_l^T \ \tau_{l-1} \ \cdots \ \tau_2 \ \tau_1 \ \pi_1^B]$.*

Proof. By Lemma 11.11 we have $\delta = \pi_{\ell,r}^I = (\pi_{\ell,1}^I)(\pi_{1,2}^I)(\pi_{2,3}^I)\cdots(\pi_{k-1,k}^I)(\pi_{k,r}^I)$ from the edges of $\mathbf{I}_p$, and $\delta = \pi_{t,b}^J = (\pi_{l,1}^J)(\pi_{l,l-1}^J)\cdots(\pi_{3,2}^J)(\pi_{2,1}^J)(\pi_{1,b}^J)$ from the edges of $\mathbf{J}_p$. The statement simply uses simpler names for the factors (Remark 11.10). $\square$

When the critical values of a permutation have distinct real or distinct imaginary parts, one side chain determines the monodromy.

Remark 11.13 (Side constellations and monodromy). Let $p \in \text{POLY}_d^{mt}(\square)$ be a polynomial. If the critical values in $\mathbf{cvl}(p)$ have distinct real parts, then the left side chain determines the monodromy of p. In fact, the loops based at z around the single edge subsurfaces $\mathbf{V}_{i,i+1}^I$ which contain a (necessarily unique) critical value are a basis for the free group $\pi_1(\mathbf{Q}_p \setminus \mathbf{cvl}(p), z)$. In particular, the $(k+2)$-tuple $[\pi_1^L \ \sigma_1 \ \sigma_2 \ \cdots \ \sigma_k \ \pi_k^R]$ is almost a constellation of permutations encoding the monodromy map (Definition 11.2). When the left side of $\square$ is regular, the first column of $\mathbf{Q}_p$ is regular, the first entry π_1^L is the identity permutation and it is not needed. When the right side of $\square$ is regular, the last column of $\mathbf{Q}_p$ is regular, the last entry π_1^R is the identity permutation and it is not needed. Once any initial and/or final identity permutations are removed, what remains is the tuple of permutations that encode the monodromy action. Similarly, if the critical values in $\mathbf{cvl}(p)$ have distinct imaginary parts, then the bottom side chain determines the monodromy of p. The argument is analogous.

12. INTERVALS AND THEOREM A

This section introduces and analyzes a metric cell structure on $\text{POLY}_d^{mt}(\rightarrowtail)$, thereby proving Theorem A. Let $\rightarrowtail = \mathbf{I} = [x_\ell, x_r]$ be a closed interval in $\mathbb{R}$, so that $(\rightarrowtail)^n = \mathbf{I}^n$ is an n-cube. Recall that the space $\text{MULT}_n(\rightarrowtail) = \text{MULT}_n(\mathbf{I})$ is a standard n-orthoscheme (Definition 6.9). We begin with an example illustrating how to go from a multiset in $\rightarrowtail$ to a point in a face of this simplex.

Example 12.1. Let $\mathbf{I} = [x_\ell, x_r]$ be an interval, and let $M = x_\ell^3 x_1^4 x_2^1 x_3^2 x_r^1$ be an 11-element multiset in $\mathbf{I}$. The multiset M labels a point in the 11-dimensional orthoscheme $\text{MULT}_{11}(\mathbf{I})$, and we can separate out the metric and combinatorial information that M contains. There are 3 points $C = \{x_1, x_2, x_3\}$ in the interior of $\mathbf{I}$, and a 5-tuple $\mathbf{m} = [3\ 4\ 1\ 2\ 1]$ that records the multiplicities of the 5 vertices of the 3-subdivided interval $\mathbf{I}_C$. The open 3-simplex containing the point labeled by M is determined by the 5-tuple $\mathbf{m}$ and the exact point in this open 3-simplex is determined by location of the 3-element set C in the interior of $\mathbf{I}$. See Figure 30.

Definition 12.2 (Multisets in an interval). An arbitrary element $M \in \text{MULT}_n(\rightarrowtail)$ with $\rightarrowtail = \mathbf{I} = [x_\ell, x_r]$ can be written in the form $M = x_\ell^{m_\ell} x_1^{m_1} \cdots x_k^{m_k} x_r^{m_r}$. It can also be split into two pieces of information. Adding the elements of M as vertices of
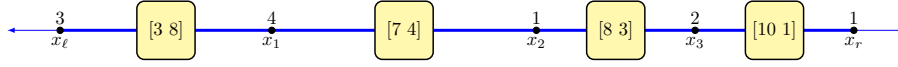
FIGURE 30. The multiset $M = x_\ell^3 x_1^4 x_2^1 x_3^2 x_r^1 \in \text{MULT}_{11}(\mathbf{I})$ labels a point in a 3-dimensional face of the 11-dimensional simplex $\text{MULT}_{11}(\mathbf{I})$. The 3-dimensional face is determined by the linear composition $\mathbf{m} = \text{COMP}(M) = [3\ 4\ 1\ 2\ 1]$ and the four vertex labels $[3\ 8]$, $[7\ 4]$, $[8\ 3]$ and $[10\ 1]$ below $\mathbf{m}$ in the linear composition order. The exact point in this open 3-simplex is determined by location of the 3-element set $C = \{x_1, x_2, x_3\}$ in I. The vertices below the linear composition are shown superimposed on the 4 edges of the 3-subdivided interval $\mathbf{I}_C$.

$\mathbf{I}$ creates a subdivided interval $\mathbf{I}_C$, where $C = \{x_1, \ldots, x_k\} = \text{SET}(M) \cap I$ records the elements of M in the interior of $\mathbf{I}$ indexed in the left-to-right order they occur (Definition 3.2). There is also a $(k+2)$-tuple $\mathbf{m} = [m_\ell\ m_1\ \cdots\ m_k\ m_r]$ that records the multiplicities of the vertices of $\mathbf{I}_C$ in the multiset M, listed in the same left-to-right order. We say $\mathbf{m} = \text{COMP}(M)$ is the *linear composition* of M. Since there need not be elements of M at either end of $\mathbf{I} = \bullet\!\!-\!\!\bullet$, we have $m_\ell, m_r \geq 0$, but $m_i > 0$ for $i \in [k]$. The linear composition $\mathbf{m}$ of length $k+2$ determines the open k-simplex of the n-orthoscheme $\text{MULT}_n(\bullet\!\!-\!\!\bullet)$ and the choice of a k-element subset $C \subset I$ specifies a point in that open k-simplex. Note that M can be reconstructed from C and $\mathbf{m}$.

Figure 31 shows a standard 3-dimensional orthoscheme $\text{MULT}_3(\mathbf{I})$ with the linear compositions that label its faces. The face poset of simplex $\text{MULT}_n(\bullet\!\!-\!\!\bullet)$ is the finite poset of linear compositions of n.

Definition 12.3 (Linear compositions). A *linear composition of n with length $k+2$* is a row vector $\mathbf{m} = [m_\ell\ m_1\ \cdots\ m_k\ m_r]$ of sum n with integers $m_\ell, m_r \geq 0$ and $m_i > 0$ for $i \in [k]$. For $k > 0$, an *elementary merge* of $\mathbf{m}$ replaces two adjacent entries with their sum. This produces a new linear composition of n of length $(k-1) + 2 = k + 1$. Let $\text{COMP}_n(\bullet\!\!-\!\!\bullet)$ denote the set of all linear compositions of n together with the partial order $\mathbf{m} \geq \mathbf{m}'$ if there is a sequence of elementary merges that starts at $\mathbf{m}$ and ends at $\mathbf{m}'$. The graded poset $\text{COMP}_n(\bullet\!\!-\!\!\bullet)$ has a unique maximal element $[0\ 1\ 1\ \cdots\ 1\ 0]$ and $n + 1$ minimal elements $[m_\ell\ m_r]$ with $m_\ell, m_r \geq 0$ and $m_\ell + m_r = n$.

Multisets in an interval and the corresponding linear compositions are explored with more detail in [DM24].

Remark 12.4 (Stratified cell structure). Let $\text{COMP}: \text{MULT}_n(\bullet\!\!-\!\!\bullet) \to \text{COMP}_n(\bullet\!\!-\!\!\bullet)$ be the map that sends $M \mapsto \text{COMP}(M)$ (Definition 12.2). The COMP map determines the simplicial cell structure on $\text{MULT}_n(\bullet\!\!-\!\!\bullet)$ in the sense that M_1 and M_2 belong to the same open simplicial face if and only if $\text{COMP}(M_1) = \text{COMP}(M_2)$. Moreover, since $\text{SHAPE}(M)$ is the multiset of positive entries in $\text{COMP}(M)$, the simplicial cell structure is a stratified cell structure in the sense of Definition 7.19. As a consequence there is an induced cell structure on $\text{POLY}_d^{mt}(\bullet\!\!-\!\!\bullet)$ and the LL map becomes a cellular map $\text{LL}: \text{POLY}_d^{mt}(\bullet\!\!-\!\!\bullet) \to \text{MULT}_n(\bullet\!\!-\!\!\bullet)$. Since the generic degree is d^{d-2} (Theorem 7.3), the cell structure on $\text{POLY}_d^{mt}(\bullet\!\!-\!\!\bullet)$ is built out of d^{d-2} standard n-orthoschemes. There is also an induced simplicial cell structure on the n-cube
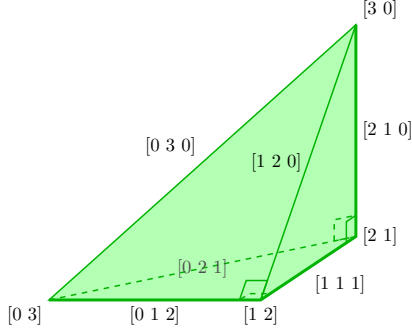
FIGURE 31. The faces of the 3-orthoscheme $\mathrm{MULT}_3(\rightarrowtail)$ have linear composition labels. The linear composition labels of its 0-cells and 1-cells are shown. The open 3-cell has label $[0\ 1\ 1\ 1\ 0]$ and the four 2-cells have labels $[0\ 1\ 1\ 1]$ (bottom), $[0\ 1\ 2\ 0]$ (front), $[0\ 2\ 1\ 0]$ (back), and $[1\ 1\ 1\ 0]$ (right). Its spine is the thick path from $[0\ 3]$ to $[1\ 2]$ to $[2\ 1]$ to $[3\ 0]$.

$$\mathrm{POLY}_d^{mt}(\rightarrowtail) \xrightarrow{\ d^{d-2}\ } \mathrm{MULT}_n(\rightarrowtail) \xleftarrow{\ n!\ } (\rightarrowtail)^n$$

FIGURE 32. Three cell complexes related to a closed interval $\rightarrowtail$, all with simplicial orthoscheme metrics. The LL map on the left and the MULT map on the right are cellular maps with respect to these cell structures.

$(\rightarrowtail)^n$ that turns the MULT map into a cellular map. This is the typical subdivision of the n-cube into $n!$ standard n-orthoschemes that are permuted by the symmetric group action. See Figure 32.

We are now ready to prove Theorem A.

Theorem 12.5 (Theorem A). *The space $\mathrm{POLY}_d^{mt}(\rightarrowtail)$ of polynomials with critical values in a closed interval (with the stratified Euclidean metric) is isometric to the order complex $|\mathrm{NCPART}_d|_\Delta$ (with the orthoscheme metric).*

Proof. Let $\square$ be a closed rectangle $\mathbf{Q}' = \mathbf{I}' \times \mathbf{J}' = \square$, let $\rightarrowtail$ be $\mathbf{I}' \times \{y_1\}$ for some $y_1 \in \mathbf{J}'$, and let $\mathrm{GEOCOM}\colon \mathrm{POLY}_d^{mt}(\rightarrowtail) \to |\mathrm{NCPERM}_d^L|_\Delta$ be the GEOCOM map of Definition 5.12 with the domain restricted to the subspace $\mathrm{POLY}_d^{mt}(\rightarrowtail)$ and the range projected onto the first factor. We show that this version of the GEOCOM map is a bijective cellular homeomorphism. The cellular nature of the map is immediate from the way the cell structures were defined on the domain and range. In particular, different polynomials in the same cell differ only in their barycentric coordinates and these coordinates are used in all three spaces $\mathrm{MULT}_n(\rightarrowtail)$, $\mathrm{POLY}_d^{mt}(\rightarrowtail)$ and $|\mathrm{NCPERM}_d^L|_\Delta$. This also shows that the local metrics are preserved.

To see that GEOCOM is surjective, note that the image contains at least one point in each of the d^{d-2} open top-dimensional cells of $|\mathrm{NCPERM}_d|_\Delta$ by Remark 11.4, it contains all of these points because the map is cellular, and it contains the union of the closed top-dimensional cells because the image is compact and thus closed (Proposition 10.8). Finally, every point in $|\mathrm{NCPERM}_d|_\Delta$ is in the image,

because every point is in the boundary of a top-dimensional cell. This is the order complex version of the fact that every chain of noncrossing permutations extends to a maximal chain.

To see that GEOCOM is also injective, suppose $p, q \in \text{POLY}_d^{mt}(\leftrightarrow)$ have the same image $\text{GEOCOM}(p) = \text{GEOCOM}(q)$. This means that p and q lie in the same simplex of $\text{POLY}_d^{mt}(\leftrightarrow)$ and have the same left side chains, which means that p and q have the same monodromy (Remark 11.13). Moreover, the multiplicity of the unique critical value in an edge of $\mathbf{I}'_p$ is determined by the absolute length of the basic horizontal side permutations σ_i (Corollary 11.12), so $\mathbf{cvl}(p)$ and $\mathbf{cvl}(q)$ have the same linear composition $\mathbf{m}$. Next, the fact that p and q are sent to the same point in this simplex means that they have the same barycentric coordinates. The barycentric coordinates encode relative widths (Definition 3.2) and we can use these to reconstruct the locations of the critical values in $\mathbf{I}'$. Since p and q have the same set of critical values with the same multiplicities, we have $\mathbf{cvl}(p) = \mathbf{cvl}(q)$ as multisets. By Proposition 11.6, $p = q$ and GEOCOM is injective. Finally, as a bijective map from a compact space to a Hausdorff space, it is a homeomorphism. $\square$

The metric simplicial complex $\text{POLY}_d^{mt}(\leftrightarrow) = |\text{NCPART}_d|_\Delta$ is also the branched line complex $\text{BR}_d^m(\leftrightarrow)$ whose points are labeled by marked d-branched lines.

Definition 12.6 (Branched lines). Let $\mathbf{I}' = [x'_\ell, x'_r]$ be an interval in $\mathbb{R}$ and let $\mathbf{I} = [x_\ell, x_r]$ be an interval that contains $\mathbf{I}'$ in its interior. For each polynomial $p \in \text{POLY}_d^{mt}(\mathbf{I}')$, there is a preimage branched line $p^{-1}(\mathbf{I})$ which is a metric banyan (Example 3.19). It is a single banyan rather than a banyan grove because the interval $\mathbf{I}$ contains all of the critical values of p. The endpoints of $\mathbf{I}$, being regular, have d preimages each that can be marked / labeled as through they were representative points on the left and right sides of a d-branched rectangle $\mathbf{P}_p$. Let $\text{BR}_d^m(\mathbf{I}')$ be the space of all such marked metric banyans / marked branched lines. The procedure just described gives a map $\text{POLY}_d^{mt}(\mathbf{I}')$ to $\text{BR}_d^m(\mathbf{I}')$. Next, from a marked metric banyan, it is possible to read off the left side partitions and the relative widths of the intervals between the critical values. In other words, the marked metric banyan contains the same information as the corresponding point in $|\text{NCPART}_d|_\Delta$, and we have a map $\text{BR}_d^m(\mathbf{I}') \to |\text{NCPART}_d|_\Delta$. Finally, Theorem A provides a map back from $|\text{NCPART}_d|_\Delta \to \text{POLY}_d^{mt}(\mathbf{I}')$. One can trace through the definitions of these maps to see that they are consistent and thus all three are bijections. It is in this sense that the space of monic centered degree-d polynomials with critical values in a fixed interval is the same as the space of marked d-branched lines.

13. CIRCLES AND THEOREM B

We now derive Theorem B from Theorem A. First, recall the definition of the dual braid complex.

Definition 13.1 (Dual braid complex). The *dual braid complex* K_d is a quotient space of the order complex $|\text{NCPERM}_d|_\Delta$. Recall that there is an ordered k-simplex in $|\text{NCPERM}_d|_\Delta$ for each chain $\pi_0 < \pi_1 < \cdots < \pi_k$ of noncrossing permutations. The *edge labels* of this k-simplex are $\sigma_i = \pi_{i-1}^{-1}\pi_i$ and the corresponding *factorization* of $\delta = (1\ 2\ \cdots\ d)$ has constellation $[\pi^L\ \sigma_1\ \sigma_2\ \cdots\ \sigma_k\ \pi^R]$ where $\pi^L = \pi_0$ and $\pi^R = (\pi_k)^{-1}\delta$. The possibly trivial permutation π^L determines the vertex where the ordered k-simplex starts in $|\text{NCPERM}_d|_\Delta$, and the possibly trivial permutation

π^R determines the vertex where it ends. The edge labels are nontrivial. In the dual braid complex K_d, two simplices are identified if and only if they have the same sequence of edge labels. The result is a Δ-complex with one vertex and d^{d-2} top-dimensional cells that are standard n-orthoschemes.

Definition 13.2 (Standard representatives)**.** For every equivalence class of simplices in $|\mathrm{NCPERM}_d|_\Delta$ that are identified to form one simplex in the dual braid complex K_d, there is a standard representative where π^R is the identity. Concretely, if $[\pi^L \ \sigma_1 \ \sigma_2 \ \cdots \ \sigma_k \ \pi^R]$ is a constellation where π^R is nontrivial, then its standard representative is $[\pi^L_{\mathrm{new}} \ \sigma_1 \ \sigma_2 \ \cdots \ \sigma_k \ \pi^R_{\mathrm{new}}]$ where π^R_{new} is the identity and π^L_{new} is $\delta \cdot \pi^R \cdot \delta^{-1} \cdot \pi^L$.

Theorem 13.3 (Theorem B)**.** *The space* $\mathrm{POLY}^{mt}_d(\bigcirc)$ *of polynomials with critical values in a circle is homeomorphic to a quotient of the complex* $\mathrm{POLY}^{mt}_d(\rightarrowtail)$ *by face identifications. As a metric Δ-complex,* $\mathrm{POLY}^{mt}_d(\bigcirc)$ *is the dual braid complex K_d with the orthoscheme metric.*

Proof. Let $\rightarrowtail$ be a closed horizontal interval in $\mathbb{R}$. As $\rightarrowtail$ is dragged around to form a circle $\bigcirc$ at time $t = 1$, the polynomials in $\mathrm{POLY}^{mt}_d(\rightarrowtail)$, with their monodromy and critical value characterization, are dragged around to the polynomials in $\mathrm{POLY}^{mt}_d(\bigcirc)$. This process is completely reversible except for polynomials with critical values at both endpoints of $\rightarrowtail = [x_\ell, x_r]$. When p is a polynomial of this type, its endpoint critical values are merged at time $t = 1$ and the corresponding monodromy permutations around these critical values, defined by appropriate paths based at z, are multiplied. In particular, if p has horizontal side constellation $[\pi^L_1 \ \sigma_1 \ \sigma_2 \ \cdots \ \sigma_k \ \pi^R_1]$ (Corollary 11.12) then the final polynomial with one fewer critical value has a monodromy constellation of the form $[\pi^L_{\mathrm{new}} \ \sigma_1 \ \sigma_2 \ \cdots \ \sigma_k \ \pi^R_{\mathrm{new}}]$ where π^R_{new} is the identity and π^L_{new} is $\delta \cdot \pi^R_1 \cdot \delta^{-1} \cdot \pi^L_1$. The conjugation of π^R_1 by δ represents a change of path surrounding the critical value at x_r so that the clockwise loop around x_r concatenated with the standard clockwise loop around x_ℓ is homotopic to a loop surrounding both which is dragged to a clockwise loop around their merged critical value. Finally, the constellations label the faces of $\mathrm{POLY}^{mt}_d(\rightarrowtail)$ and each particular point is encoded in the metric information of the relative widths of the edges in $\mathbf{I}'_p$. Since the endpoint identification only changes the monodromy and leaves the metric information unchanged, the induced identification on $\mathrm{POLY}^{mt}_d(\rightarrowtail)$ is an isometric face identification. It is also clear from the labels that this is the same identification as that used to create the dual braid complex (Definition 13.2). $\qquad\square$

Definition 13.4 (Branched circles)**.** Let $\mathbf{U}$ be a closed disk that contains $\bigcirc$ in its interior. We give $\mathbf{U}$ a minimal cell structure so that $\bigcirc$ is a subcomplex. It has two vertices, three edges and two 2-cells. There is one vertex v in $\bigcirc$ and another vertex u in $\partial\mathbf{U}$. The rest of $\bigcirc$ is an open edge as is the rest of $\partial\mathbf{U}$. The third edge e connects u and v. For any particular polynomial $p \in \mathrm{POLY}^{mt}_d(\bigcirc)$, the preimage of $\mathbf{U}$ is a nonsingular disk diagram and the preimages of u can be marked and cyclically labeled by the set $[d]$. The preimage of $\bigcirc$ is a metric cactus (Example 3.20). We use the regular point $u \in \partial\mathbf{U}$ as the basepoint for the monodromy action on the preimages of u and we call cyclically marked preimages of u a *marking*. Let $\mathrm{BR}^m_d(\bigcirc)$ be the space of all such marked metric cacti / marked branched circles. The procedure just described gives a map $\mathrm{POLY}^{mt}_d(\bigcirc)$ to $\mathrm{BR}^m_d(\bigcirc)$, and from each marked metric cactus it is possible to read off the monodromy and to recover the

$$\begin{array}{ccccc}
\text{POLY}_d^{mt}(\mathbf{Q}) & \xrightarrow{\ \ d^{d-2}\ \ } & \text{MULT}_n(\mathbf{Q}) & \xleftarrow{\ \ n!\ \ } & \mathbf{Q}^n \\
\downarrow{\scriptstyle 1} & & \downarrow{\scriptstyle n!} & & \parallel{\scriptstyle 1} \\
\text{POLY}_d^{mt}(\mathbf{I}) \times \text{POLY}_d^{mt}(\mathbf{J}) & \xrightarrow{(d^{d-2})^2} & \text{MULT}_n(\mathbf{I}) \times \text{MULT}_n(\mathbf{J}) & \xleftarrow{(n!)^2} & \mathbf{I}^n \times \mathbf{J}^n
\end{array}$$

FIGURE 33. Six complexes related to a rectangle $\square = \mathbf{Q} = \mathbf{I} \times \mathbf{J}$, all with bisimplicial orthoscheme metrics. The horizontal maps are LL maps and MULT maps and the vertical maps come from deformation retracting onto the sides of $\square$. The numbers on the arrows indicate the generic degree of these cellular maps.

map from the metric branched circle to $\bigcirc$, including the location and multiplicity of the critical values. In particular, it is possible to recover the multiset $\mathbf{cvl}(p)$. With the monodromy and the critical value multiset we recover the polynomial p. Thus the map from polynomials to marked branched circles is injective and it is not too hard to show that it is also onto. It is in this sense that the space of monic centered degree-d polynomials with critical values in a fixed circle is the same as the space of marked d-branched circles.

14. RECTANGLES AND THEOREM C

This section introduces and analyzes a metric cell structure on $\text{POLY}_d^{mt}(\square)$, thereby proving Theorem C. The cell structure and the method of proof are patterned after the linear case.

Definition 14.1 (Bisimplicial cells). Let $\square$ be a closed rectangle $\mathbf{Q} = \mathbf{I} \times \mathbf{J}$ as in Definition 3.6 where $\mathbf{I}$ and $\mathbf{J}$ are intervals of length s and t respectively. By focusing on the real and imaginary coordinates separately, the product space $(\square)^n = \mathbf{Q}^n$ can be viewed as $\mathbf{I}^n \times \mathbf{J}^n$, an n-cube of side length s times an n-cube of side length t. If we quotient by the full action of $\text{SYM}_n \times \text{SYM}_n$ with the first symmetric group acting on the real coordinates and second acting on the imaginary coordinates, the quotient space is $\text{MULT}_n(\mathbf{I}) \times \text{MULT}_n(\mathbf{J})$, a direct product of a standard n-orthoscheme of side length s with a standard n-orthoscheme of side length t. We call this an oriented *bisimplex* or an *biorthoscheme* when we are viewing it as a metric object. The space $\text{MULT}_n(\mathbf{Q})$ is an intermediate space where we only quotient by the diagonal action of SYM_n on the two factor n-cubes. The cells of $\text{MULT}_n(\mathbf{Q})$ are orbits of cells in $\mathbf{Q}^n$. In particular, in these $2n$-dimensional spaces, $\mathbf{Q}^n$ with its $(n!)^2$ top-dimensional cells which are the product of two n-orthoschemes. and $\text{MULT}_n(\mathbf{Q})$ has $n!$ top-dimensional biorthoschemes. This complete our description of the righthand square of Figure 33.

To clarify the cell structure we focus on the projections onto $\mathbf{I}$ and $\mathbf{J}$.

Definition 14.2 (Multisets in a rectangle). For each n-element multiset $M \in \text{MULT}_n(\mathbf{Q})$, let $C = \Re(M) \cap I$ with $k = |C|$, let $D = \Im(M) \cap J$ with $l = |D|$, and let $\mathbf{I}_C$, $\mathbf{J}_D$ and $\mathbf{Q}_{C,D}$ be the corresponding subdivisions of $\mathbf{I}$, $\mathbf{J}$ and $\mathbf{Q}$. All of the elements of M are at the vertices of $\mathbf{Q}_{C,D}$ and as in the linear case, we can split M into a combinatorial part and a metric part. The combinatorial aspect is a $(k+2) \times (l+2)$ grid is nonnegative integers that record the multiplicities of the vertices of $\mathbf{Q}_{C,D}$. The metric part are the numbers $\text{BARY}(\mathbf{I}_C)$ and $\text{BARY}(\mathbf{J}_D)$ which

record the relative widths of the columns and rows of cells in $\mathbf{Q}_{C,D}$ respectively. The combinatorics determine the open bisimplicial cell and the barycentric coordinates determine the point in the cell. The numbers $\mathrm{BARY}(\mathbf{I}_C)$ determine the point in the first simplex and the numbers $\mathrm{BARY}(\mathbf{J}_D)$ determine the point in the second simplex.

Remark 14.3 (Cellular maps). Since varying the widths and heights of the rectangles does not change the shape of the multiset, the cell structure described in Definition 14.2 is a stratified cell structure on $\mathrm{MULT}_n(\mathbf{Q})$, and so by Definition 7.19 it induces a stratified cell structure on $\mathrm{POLY}_d^{mt}(\mathbf{Q})$ built out of biorthoschemes, turning the horizontal LL map in the upper left part of Figure 33 into a cellular map. The induced map from $\mathrm{POLY}_d^{mt}(\mathbf{Q})$ in the upper left to biorthoscheme $\mathrm{MULT}_n(\mathbf{I}) \times \mathrm{MULT}_n(\mathbf{J})$ is completely determined by the horizontal and vertical barycentric coordinates. Next consider the LL $\times$ LL map from $\mathrm{POLY}_d^{mt}(\mathbf{I}) \times \mathrm{POLY}_d^{mt}(\mathbf{J})$ to $\mathrm{MULT}_n(\mathbf{I}) \times \mathrm{MULT}_n(\mathbf{J})$. This is already known to be cellular by the results in Section 12. Finally, the vertical map on the left is the GEOCOM map of Section 5 with the range relabeled using Theorem A. The definitions are consistent, this map is also cellular and the lefthand square commutes.

To complete the proof of Theorem C we only need to show that the vertical GEOCOM map on the left-hand side is injective.

Theorem 14.4 (Theorem C). *The space* $\mathrm{POLY}_d^{mt}(\square)$ *of polynomials with critical values in a closed rectangle (with the stratified Euclidean metric) is isometric to a subcomplex of* $|\mathrm{NCPERM}_d|_\Delta \times |\mathrm{NCPERM}_d|_\Delta$ *(with the orthoscheme metric).*

Proof. Let $\square$ be a closed rectangle $\mathbf{Q}' = \mathbf{I}' \times \mathbf{J}' = \square$ and note that the GEOCOM map is cellular and metric-preserving on each open cell by Remark 14.3. Once we show it is injective, its image is a subcomplex and the proof is complete. To see injectivity, suppose we are given a point $\mathrm{GEOCOM}(p)$ in the interior of a product of two orthoschemes in $|\mathrm{NCPERM}_d^L|_\Delta \times |\mathrm{NCPERM}_d^B|_\Delta$ that came from a polynomial $p \in \mathrm{POLY}_d^{mt}(\square)$. This point can be expressed as a pair of side chains $\pi_1^L < \pi_2^L < \cdots < \pi_k^L$ and $\pi_1^B < \pi_2^B < \cdots < \pi_l^B$ and the (ordered) barycentric coordinates in each (ordered) factor simplex. The left noncrossing permutations π_i^L can be converted first to left noncrossing partitions $[\lambda_i]^L$ (Definition 4.17) and then to top-bottom matchings $[\mu_i]^{TB}$ (Proposition 4.15), which we can draw as noncrossing multiarcs in a standard d-branched rectangle $\mathbf{P}$, with the arcs of $[\mu_i]^{TB}$ connecting the d points $t_{m,i}$ in the top sides $\{T_m\}$ to the d points $b_{m,i}$ in the bottom sides $\{B_m\}$. This is the multiarc $\widetilde{\alpha}_i$. Similarly, the chain of noncrossing bottom permutations π_j^B allow us to draw the multiarc $\widetilde{\beta}_j$. Together this reconstructs the full 1-skeleton of the regular point complex $\mathbf{P}_p$. By adding in the bounded regions as 2-cells we recover all of the regular point complex $\mathbf{P}_p$. Next, we reconstruct the critical point complex $\mathbf{P}_p'$ as the cellular dual of $\mathbf{P}_p$, then the critical value complex $\mathbf{Q}_p'$ and the critical complex map $\mathbf{P}_p' \to \mathbf{Q}_p'$ from $\mathbf{P}_p'$ (Definition 3.22). From the critical complex map we also know the multiplicity of each vertex in $\mathbf{Q}_p'$. This is the combinatorial information contained in the multiset $\mathbf{cvl}(p)$. Together with the barycentric coordinates, we can reconstruct the critical value multiset $M = \mathbf{cvl}(p)$. Finally, the cellular critical complex map $\mathbf{P}_p' \to \mathbf{Q}_p'$ determines the branched cellular regular complex map $\mathbf{P}_p \to \mathbf{Q}_p$. From the d-sheeted cover between their 1-skeletons one can read off the monodromy action. By Proposition 11.6 this means that we
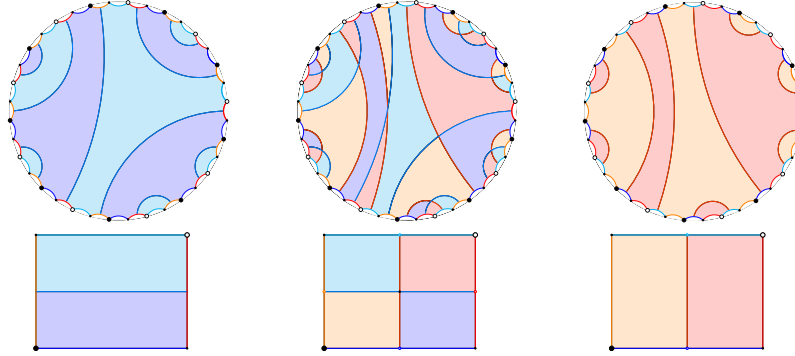
FIGURE 34. The left-right matching shown in the upper left and the bottom-top matching shown on the upper right combine to form the basketball in the middle.

can reconstruct p from its image under the GEOCOM map, and the GEOCOM map is injective. □

From the generic degrees of the maps, it is clear that the subcomplex in the image of the GEOCOM map only contains $d^{d-2} \cdot n!$ of the $(d^{d-2})^2$ top-dimensional bisimplices. Here is one natural way to characterize which vertices, and more generally which simplices are in this subcomplex.

Definition 14.5 (Basketballs). The vertices of $\text{POLY}_d^{mt}(\square)$ correspond to polynomials where the multiset $\mathbf{cvl}(p)$ is contained in the four corners of $\square$. The left and bottom chains become single noncrossing permutations π_1^L and π_1^B, which encode a top-bottom matching $[\mu_1]^{TB}$ and a left-right matching $[\mu_1]^{LR}$, or more topologically the multiarc $\widetilde{\alpha}_1$ and the multiarc $\widetilde{\beta}_1$, which are the preimage under p of a regular vertical arc α_1 and a regular horizontal arc β_1. The lift of this regular "plus sign" in $\square$ must be d "plus signs" in the d-branched $4d$-gon. This is illustrated in Figure 34. The resulting combinatorial structure is what Martin, Savitt and Singer call a *basketball* [MSS07]. See [GS88, Sjo15] for more background and [Sav09] for more on basketballs. As described in [MSS07, Theorem 2.8], basketballs are in one-to-one correspondence with the noncrossing partitions of $[4d]$ in which each block has size 4. They also show that the number of basketballs is the Fuss–Catalan number $C_d^{(4)} = \frac{1}{3d+1}\binom{4d}{d}$, and each is obtained from a polynomial in the manner described here. Thus, the image of GEOCOM is a subcomplex of $|\text{NCPERM}_d^L|_\Delta \times |\text{NCPERM}_d^B|_\Delta$ with $C_d^{(4)}$ vertices. More generally, a chain of left side permutations and a chain of bottom side permutations describe a bisimplex in the image of the GEOCOM map if and only if for every choice of left permutation π_i^L and choice of bottom permutation π_j^R, the combination encodes a pair of multiarcs that form a basketball.

Definition 14.6 (Branched rectangles). Let $\square = \mathbf{Q}' = \mathbf{I}' \times \mathbf{J}'$ be a closed rectangle contained in the interior of a larger closed rectangle $\mathbf{Q} = \mathbf{I} \times \mathbf{J}$ based at its bottom left corner z and add an edge from z to the bottom left corner of $\mathbf{Q}'$. This gives $\mathbf{Q}$ a cell structure. For each polynomial $p \in \text{POLY}_d^{mt}$, the preimage disk $\mathbf{P} = p^{-1}(\mathbf{Q})$ receives a cell structure and it contains the metric critical value complex $\mathbf{P}'_p$ as a subcomplex built out of Euclidean rectangles. There is also the natural labeling of
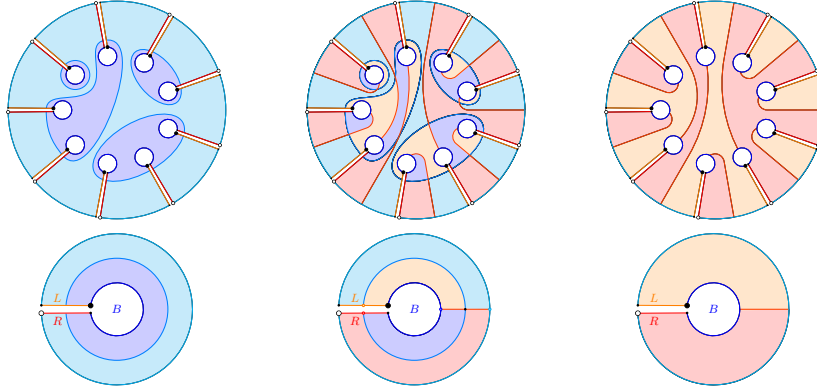
FIGURE 35. A standard version of a left-right matching and a
compatible bottom-top matching, when the rectangle in $\mathbb{C}$ has been
moved by a point-preserving homotopy so that the left and right
sides nearly touch and the bottom side nearly encloses a disk in
the interior of the closed annulus about to be formed.

the preimages of z (Definition 5.2). We call this a *marked d-branched rectangle*. Let
$\mathrm{BR}_d^m(\blacksquare)$ be the collection of all marked d-branched rectangles. As described in the
proof of Theorem C, the marked d-branched rectangle is sufficient information to
reconstruct p, and it is also not too hard to prove that every possible such marked
d-branched rectangle arises from some polynomial. It is in this sense that the space
of monic centered degree-d polynomials with critical values in a fixed rectangle is
the same as the space of marked d-branched rectangles.

15. ANNULI AND THEOREM D

In this section we prove Theorem D by performing a gluing of $\square$ into $\circledcirc$ similar
to gluing of $\multimap$ into $\bigcirc$ in the proof of Theorem B in Section 13.

Theorem 15.1 (Theorem D). *The space $\mathrm{POLY}_d^{mt}(\circledcirc)$ of polynomials with critical
values in a closed annulus is homeomorphic to a quotient of $\mathrm{POLY}_d^{mt}(\square)$ by face
identifications.*

Proof. Let $H: \square \times [0,1] \to \mathbb{C}$ be a nonsplitting homotopy that is point preserving
except at time $t = 1$ when it identifies the left and right sides to create a closed an-
nulus $\circledcirc$ with the top side becoming the outer circle and the bottom side becoming
the inner circle. As described in Definition 9.8 this induces to a polynomial homo-
topy $\widetilde{H}_n: \mathrm{POLY}_d^{mt}(\square) \times [0,1] \to \mathrm{POLY}_d^{mt}(\mathbb{C})$. For each polynomial $p \in \mathrm{POLY}_d^{mt}(\square)$,
we have continuously deforming polynomials $p_t = (\widetilde{h}_n)_t(p) \in \mathrm{POLY}_d^{mt}(h_t(\square))$. By
Proposition 10.2, this in turn induces a quotient of the space $\mathrm{POLY}_d^{mt}(\square)$ that be-
comes $\mathrm{POLY}_d^{mt}(\circledcirc)$. We can say something a bit more precise. The shape of the
multiset $\mathbf{cvl}(p_t)$ changes at time $t = 1$ if and only if there are critical values at a
point in the left and right sides of $\square$ at the same height—so they become one point at
time $t = 1$. When this happens, the corresponding monodromy permutations, from
appropriate loops based at a regular basepoint, are multiplied. Distinct points in
the same open bisimplex of $\mathrm{POLY}_d^{mt}(\square)$ only differ in the relative metrics assigned to

the horizontal and vertical subdivisions. The identification process is independent of these metrics which means that the quotient is by face identifications. $\square$

Example 15.2. As described in the proof of Theorem D, there is a continuous deformation from $\square$ at time $t = 0$ to $\odot$ at time $t = 1$. This determines a continuous deformation from a branched rectangle to a branched annulus. We illustrate the process for a vertex of $\text{POLY}_d^{mt}(\square)$. The left-right and bottom-top matchings obtained by pulling back a "plus sign" in $\square$ to a d-branched $4d$-gon are shown in Figure 34, along with the basketball formed by the union of both matchings. The effect of the continuous deformation of $\square$ into $\odot$ on this basketball is illustrated in Figure 35, and this represents a vertex of $\text{POLY}_d(\odot)$. This is a "standardized" version of what is happening topologically. For the actual continuously deforming polynomial p_t under the corresponding polynomial homotopy (Definition 9.8), there is a more concrete version which has this cell structure. It starts with a standard form like Figure 34, and ends near time $t = 1$ as an embedded complex in $\mathbb{C}$ in which the left and right sides with matching subscripts are about to meet, as in Figure 35.

Remark 15.3 (From rectangular to polar)**.** The transition from focusing on the rectangular coordinates of the critical values to focusing on their polar coordinates involves continuously varying the collection of polynomials under consideration using a polynomial homotopy. In particular, maintaining the same geometric and combinatorial data means changing the polynomial under consideration. Conversely, keeping the polynomial constant means drastically changing the geometric combinatorics. For example, polynomials might be in a lower dimensional cell if there are coincidences in the coordinates of its critical values, but one can have coincidences in one coordinate system without having them in the other.

Just as we can view $\text{POLY}_d^{mt}(\square)$ as a subcomplex of $|\text{NCPART}_d^L| \times |\text{NCPART}_d^B|$, the proof above shows that $\text{POLY}_d^{mt}(\odot)$ is isomorphic to a subcomplex of the direct product $K_d \times |\text{NCPART}_d^B|$, where K_d is the dual braid complex (Definition 13.1). We call this subcomplex the (marked) branched annulus complex $\text{BR}_d^m(\odot)$. Rather than define it explicitly, we comment on standard names for its bisimplices and refer the reader to the first article in this series [DM22].

Definition 15.4 (Standard representatives)**.** For every equivalence class of bisimplices in the branched rectangle complex $\text{BR}_d^m(\square)$ that are identified to form one bisimplex in the branched annulus complex $\text{BR}_d^m(\odot)$, there is a standard representative where the right side of $\square$ is regular. In particular, the vertices of the branched annulus complex are labeled by polynomials p where the multiset $\mathbf{cvl}(p)$ lives in the endpoints of the left side $\mathbf{L}$ of $\square$. By Theorem A applied to $\text{BR}_d^m(\mathbf{L})$, these are indexed by noncrossing partitions and $\text{BR}_d^m(\odot)$ has exactly C_d vertices, where C_d is a Catalan number. The process of standardizing the pair of side chain labels of a bisimplex is straightforward on the left side permutation chain. It is exactly as described in Definition 13.2. The impact on the bottom side permutation chain, however, is more difficult to characterize cleanly. See the discussion in [DM22].

Appendix A. A Proof of Theorem 7.14

This appendix derives Theorem 7.14 from Theorem B in [DM20]. In that article all of the polynomials satisfy $p(0) = 0$, but here we use a slight generalization.

Definition A.1 (Base Pair). Let $\text{POLY}_d^{m,b\to c} = \{p \in \text{POLY}_d^m \mid p(b) = c\}$ be the subset of POLY_d^m sending b to c. We call $b \to c$ the point/value *base pair* for this subspace. The polynomials in $\text{POLY}_d^{m,b\to c}$ are indexed by their critical points. For example, if $\mathbf{cpt}(p) = z_1^{m_1} \cdots z_k^{m_k}$, then $p'(z) = d \cdot (z - z_1)^{m_1} \cdots (z - z_k)^{m_k}$ and

$$p(z) = d \cdot \left(\int_b^z (w - z_1)^{m_1} \cdots (w - z_k)^{m_k} \, dw \right) + c.$$

The space of monic centered polynomials is homemorphic to the space of monic polynomials up to translation (Remark 7.6), and the space of monic polynomials with a fixed base pair $b \mapsto c$ is a d-sheeted cover of these spaces, so long as we restrict our attention to polynomials with critical values that avoid c.

Remark A.2 (Base Pairs and Covers). If $\mathbf{c} = \{c\}$, then the restricted affine map $\text{AFF} \colon \text{POLY}_d^{m,b\to c}(\mathbb{C}_\mathbf{c}) \to \text{POLY}_d^{mt}(\mathbb{C}_\mathbf{c})$ is a d-sheeted covering map. The restriction to polynomials with critical values in $\mathbb{C}_\mathbf{c}$ means that for these polynomials, c has d distinct preimages. For each preimage there is a unique representative of the translation equivalence class where this preimage is labeled b. Also note that since the cover map preserves the shapes of the critical points and critical values, it restricts to d-sheeted covering maps $\text{AFF} \colon \text{POLY}_{\lambda\to\mu}^{m,b\to c}(\mathbb{C}_\mathbf{c}) \to \text{POLY}_{\lambda\to\mu}^{mt}(\mathbb{C}_\mathbf{c})$.

The following definitions are slight variations of those in [DM20] and [BCN02].

Definition A.3 (**cpt** to **cvl**). Let $b \to c$ be a base pair, let $\mathbf{m} = (m_1, \ldots, m_k)$ be a k-tuple of positive integers with $n = m_1 + \cdots + m_k$, and let $\mathbf{z_m} = (z_1, \ldots, z_k)$ be a point in $\mathbb{C}^k$ where the subscript $\mathbf{m}$ reminds us that coordinates in $\mathbf{z_m}$ come with assigned multiplicities. Let

$$p_\mathbf{m}^{b\to c}(z) = p_{\mathbf{m},\mathbf{z_m}}^{b\to c}(z) = d \cdot \left(\int_b^z (w - z_1)^{m_1} \cdots (w - z_k)^{m_k} \, dw \right) + c$$

be the unique monic polynomial with $\mathbf{cpt}(p) = z_1^{m_1} \cdots z_k^{m_k}$ that sends b to c. The map $\theta_\mathbf{m}^{b\to c} \colon \mathbb{C}^k \to \mathbb{C}^k$, defined by sending each $\mathbf{z_m}$ to

$$\theta_\mathbf{m}^{b\to c}(\mathbf{z_m}) = (\theta_{\mathbf{m},1}^{b\to c}(\mathbf{z_m}), \ldots, \theta_{\mathbf{m},k}^{b\to c}(\mathbf{z_m})) = (p_\mathbf{m}^{b\to c}(z_1), \ldots, p_\mathbf{m}^{b\to c}(z_k))$$

takes the critical points of $p_\mathbf{m}^{b\to c}$ to the critical values of $p_\mathbf{m}^{b\to c}$.

Theorem B of [DM20] describes a factorization of the determinant of the $k \times k$ Jacobian matrix $\mathbf{J}_\mathbf{m}^{b\to c}$, defined by $(\mathbf{J}_\mathbf{m}^{b\to c})_{ij} = \frac{\partial}{\partial z_i} \theta_{\mathbf{m},j}^{b\to c}(\mathbf{z_m}) = \frac{\partial}{\partial z_i} p_\mathbf{m}^{b\to c}(z_j)$.

Lemma A.4 (Invertibility). *Let $b \to c$ be a base pair, let $\mathbf{m} = (m_1, \ldots, m_k)$ be a k-tuple of positive integers with $m_1 + \cdots + m_k = n$, and let $\mathbf{z_m} = (z_1, \ldots, z_k) \in \mathbb{C}^k$. The determinant of the Jacobian $\mathbf{J}_\mathbf{m}^{b\to c}$ of the map $\theta_\mathbf{m}^{b\to c} \colon \mathbb{C}^k \to \mathbb{C}^k$ factors as follows:*

$$\det \mathbf{J}_\mathbf{m}^{b\to c} = \frac{d^k}{\binom{n}{m_1,\ldots,m_k}} \left(\prod_{j\in[k]} (b - z_j)^{m_j} \right) \left(\prod_{\substack{i,j\in[k]\\i\neq j}} (z_i - z_j)^{m_j} \right).$$

Thus $\mathbf{J}_\mathbf{m}^{b\to c}$ is invertible if and only if $z_1, \ldots, z_k$ are distinct and not equal to b. In particular, $\theta_\mathbf{m}^{b\to c} \colon \text{CONF}_k(\mathbb{C}_\mathbf{b}) \to \mathbb{C}^k$ is a local homeomorphism.

Proof. There have been two modifications compared to Theorem B in [DM20]. First, the polynomial $p_\mathbf{m}^{b\to c}$ has been multiplied by d so that $p_\mathbf{m}^{b\to c}$ is monic. This adds a factor of d to every entry of the k-by-k matrix $\mathbf{J}_\mathbf{m}^{b\to c}$ and a factor of d^k to the

$$
\begin{array}{ccc}
\mathbf{z_m} & \overset{\theta^{b\to c}_{\mathbf{m}}}{\longmapsto} & \mathbf{w_m} \\
\Vert\cong & & \Vert\cong \\
\mathbf{z} & \overset{\theta^{b\to c}_{[\lambda]}}{\longmapsto} & \mathbf{w} \\
\Vert & & \Vert \\
\mathbf{z} & \overset{\theta^{b\to c}_{[\lambda]}}{\longmapsto} & \mathbf{w} \\
\downarrow & & \downarrow \\
p & & \\
\downarrow & & \downarrow \\
[p] & \overset{\mathrm{LL}}{\longmapsto} & \mathbf{cvl}(p) \\
\Vert & & \Vert \\
[p] & \overset{\mathrm{LL}}{\longmapsto} & \mathbf{cvl}(p)
\end{array}
\qquad
\begin{array}{ccc}
\mathrm{CONF}_k(\mathbb{C_b}) & \overset{\theta^{b\to c}_{\mathbf{m}}}{\longrightarrow} & \mathbb{C}^k \\
\Vert\cong & & \Vert\cong \\
(\mathbb{C_b})_{[\lambda]} & \overset{\theta^{b\to c}_{[\lambda]}}{\longrightarrow} & \mathbb{C}^{[\lambda]} \\
\uparrow & & \uparrow \\
Z & \overset{\theta^{b\to c}_{[\lambda]}}{\longrightarrow} & W \\
\downarrow & & \downarrow \\
\mathrm{POLY}^{m,b\to c}_{\lambda\to\mu}(\mathbb{C_c}) & & {\scriptstyle\mathrm{MULT}} \\
\downarrow & & \downarrow \\
\mathrm{POLY}^{mt}_{\lambda\to\mu}(\mathbb{C_c}) & \overset{\mathrm{LL}}{\longrightarrow} & \mathrm{MULT}_\mu(\mathbb{C_c}) \\
\downarrow & & \downarrow \\
\mathrm{POLY}^{mt}_{\lambda\to\mu} & \overset{\mathrm{LL}}{\longrightarrow} & \mathrm{MULT}_\mu(\mathbb{C})
\end{array}
$$

FIGURE 36. The local behavior of the stratified LL map is related to the local behavior of the stratified **cpt**-to-**cvl**-map $\theta^{b\to c}_{\mathbf{m}}$. In the square between the second and third rows Z is the restriction of $(\mathbb{C_b})_{[\lambda]}$ to the preimage of $W = (\mathbb{C_c})_{[\mu]}$ under $\theta^{b\to c}_{[\lambda]}$. The spaces $\mathrm{CONF}_k(\mathbb{C_b}) \cong (\mathbb{C_b})_{[\lambda]}$ and $\mathbb{C}^k \cong \mathbb{C}^{[\lambda]}$ in the top two rows are $2k$-dimensional manifolds and the other 7 spaces are 2ℓ-dimensional manifolds, where k and ℓ are the number of distinct critical points and critical values, respectively. Every arrow is an inclusion or a local homeomorphism.

factored determinant. Next, the shift from base pair $p(0) = 0$ to base pair $p(b) = c$ introduces the constant b into the factorization. The constant c plays no role. $\square$

The map $\theta^{b\to c}_{\mathbf{m}}$ can also be reformulated as a map between subspaces of $\mathbb{C}^n$.

Remark A.5 (Subspaces of $\mathbb{C}^n$). Let $[\lambda] \vdash [n]$ be a set partition with k blocks indexed by the order they occur in the standard shorthand (Definition 1.4). For $\mathbf{z} \in \mathbb{C}^{[\lambda]} \subset \mathbb{C}^n$, let z_i be the common value of the coordinates indexed by the ith block, let $\mathbf{z_m} = (z_1, \ldots, z_k)$, and let $\mathbf{m} = (m_1, \ldots, m_k)$ where m_i is the size of the ith block. For $\mathbf{z} \in \mathbb{C}^{[\lambda]}$ with $[\lambda] = 124|3|57|6$, we have $\mathbf{z} = (z_1, z_1, z_2, z_1, z_3, z_4, z_3)$, $\mathbf{z_m} = (z_1, z_2, z_3, z_4)$ and $\mathbf{m} = (m_1, m_2, m_3, m_4) = (3, 1, 2, 1)$. The map from $\mathbf{z} \mapsto \mathbf{z_m}$ is an isomorphism $\mathbb{C}^{[\lambda]} \cong \mathbb{C}^k$ (Proposition 6.6). To indicate that the domain and range are replaced with the subspace $\mathbb{C}^{[\lambda]} \subset \mathbb{C}^n$ where $[\lambda]$ is any set partition whose i^{th} block has size m_i, we replace the subscript $\mathbf{m}$ on $\theta^{b\to c}_{\mathbf{m}}$ with $[\lambda]$. Under this homeomorphism, the subspace $\mathrm{CONF}_k(\mathbb{C_b}) \subset \mathbb{C}^k$, where $\theta^{b\to c}_{\mathbf{m}}$ is a local homeomorphism, becomes $(\mathbb{C_b})_{[\lambda]} \subset \mathbb{C}^{[\lambda]}$, where $\theta^{b\to c}_{[\lambda]}$ is a local homeomorphism. See the top two rows of Figure 36.

Every polynomial p is part of a commuting diagram as in Figure 36.

Remark A.6 (Commuting Maps). Let p be a monic degree-d polynomial with critrical point shape $\lambda = \lambda(p) \vdash n$ and critical value shape $\mu = \mu(p) \geq \lambda$. The

equivalence class $[p]$ lies in $\mathrm{POLY}^{mt}_{\lambda \to \mu}$ and the LL map send $[p]$ to the mulitset $M = \mathbf{cvl}(p) \in \mathrm{MULT}_\mu(\mathbb{C})$. For any $c \notin \mathbf{cvl}(p)$ and any $b \in p^{-1}(c)$, $[p]$ is in $\mathrm{POLY}^{mt}_{\lambda \to \mu}(\mathbb{C}_\mathbf{c})$ and p is in $\mathrm{POLY}^{m,b\to c}_{\lambda \to \mu}(\mathbb{C}_\mathbf{c})$. Next, let $\mathbf{z}$ be an n-tuple listing the n critical points of p with the appropriate multiplicities and let $[\lambda] = \mathrm{SETPART}(\mathbf{z}) \vdash [n]$ be its set partition. Note that $\mathbf{z} \in (\mathbb{C}_\mathbf{b})_{[\lambda]}$ by construction and its image, $\mathbf{w} = \theta^{b\mapsto c}_{[\lambda]}(\mathbf{z})$ is in $W = (\mathbb{C}_\mathbf{c})_{[\mu]}$ for some set partition $[\mu] \geq [\lambda]$ whose shape is $\mu = \mu(p)$ and $\mathrm{MULT}(\mathbf{w}) = \mathbf{cvl}(p)$. We define Z as the restriction of $(\mathbb{C}_\mathbf{b})_{[\lambda]}$ to the preimage of $W = (\mathbb{C}_\mathbf{c})_{[\mu]}$ under $\theta^{b\to c}_{[\lambda]}$, and note that p can be reconstruction as $p = p^{b\to c}_\mathbf{m}$. Writing $\mathbf{z}_\mathbf{m}$ and $\mathbf{w}_\mathbf{m}$ for the images of $\mathbf{z}$ and $\mathbf{w}$ under the isomorphism from $\mathbb{C}^{[\lambda]}$ to $\mathbb{C}^k$ completes the construction of the commuting diagram containing the polynomial p as shown in Figure 36.

Theorem A.7 (Stratified covering map)**.** *For all integer partitions $\lambda, \mu \vdash n$ with $\lambda \to \mu$, the restricted map* LL$\colon \mathrm{POLY}^{mt}_{\lambda \to \mu} \to \mathrm{MULT}_\mu(\mathbb{C})$ *is a covering map.*

Proof. We first show that the restricted map LL$\colon \mathrm{POLY}^{mt}_{\lambda \to \mu} \to \mathrm{MULT}_\mu(\mathbb{C})$ is a local homeomorphism. Let p be a representative of $[p] \in \mathrm{POLY}^{mt}_{\lambda \to \mu}$ and pick a base pair $b \to c$ and an ordering of the n critical points of p to construct the maps in Figure 36 as described in Remark A.6. Since $b \notin \mathbf{cpt}(p)$ and $c \notin \mathbf{cvl}(p)$, the restriction to LL$\colon \mathrm{POLY}^{mt}_{\lambda \to \mu}(\mathbb{C}_\mathbf{c}) \to \mathrm{MULT}_\mu(\mathbb{C}_\mathbf{c})$ in the penultimate row does not change the local neighborhood of $[p]$ in the domain or $\mathbf{cvl}(p)$ in the range. Next note that the map $\mathrm{MULT}\colon W = (\mathbb{C}_\mathbf{c})_{[\mu]} \to \mathrm{MULT}_\mu(\mathbb{C}_\mathbf{c})$ is a covering map (Theorem 6.19), and so is the map $\mathrm{POLY}^{b\to c}_{\lambda \to \mu}(\mathbb{C}_\mathbf{c}) \to \mathrm{POLY}^{mt}_{\lambda \to \mu}$ (Remark A.2). Thus, if the two maps emerging from Z are local homeomorphisms, so is the LL map in a neighborhood of $[p]$. The space $W = (\mathbb{C}_\mathbf{c})_{[\mu]}$ is a 2ℓ-dimensional manifold inside the $2k$-dimensional manifold $\mathbb{C}^{[\lambda]}$, where k and ℓ are the number of blocks in $[\lambda]$ and $[\mu]$, or the number of distinct critical points and distinct critical values, respectively. The space Z is the preimage of the 2ℓ-dimensional manifold W under the local homeomorphism $\theta^{b\to c}_{[\lambda]}$ (Remark A.5), restricted to the open $2k$-dimensional submanifold $(\mathbb{C}_\mathbf{c})_{[\lambda]}$, which makes it a 2ℓ-dimensional manifold mapped to W by a local homeomorphism. Finally, the map from Z to $\mathrm{POLY}^{b\to c}_{\lambda \to \mu}(\mathbb{C}_\mathbf{c})$ merely erases the indexing from the critical points of p, so it is also a covering map. This shows that the LL map in the bottom row is locally a homeomorphism. To show that it is, in fact, a covering map, it suffices to note that it is a surjective local homeomorphism between Hausdorff spaces with constant finite size point preimages (Remark 7.15). $\square$

References

[A'C20]   Norbert A'Campo, *Signatures of monic polynomials*, In the tradition of Thurston—geometry and topology, Springer, Cham, [2020] ©2020, pp. 527–543. MR 4264587

[A'C22]   _____, *Flow box decomposition for gradients of univariate polynomials, billiards on the Riemann sphere, tree-like configurations of vanishing cycles for A_n curve singularities and geometric cluster monodromy*, EMS Surv. Math. Sci. **9** (2022), no. 2, 389–414. MR 4659688

[AP24]   Norbert A'Campo and Athanase Papadopoulos, *Geometry on surfaces, a source for mathematical developments*, Surveys in Geometry II, Springer, Cham, 2024, pp. 7–70. MR 4769423

[Art25]   Emil Artin, *Theorie der Zöpfe*, Abh. Math. Sem. Univ. Hamburg **4** (1925), no. 1, 47–72. MR 3069440

[Art47]   E. Artin, *Theory of braids*, Ann. of Math. (2) **48** (1947), 101–126. MR 19087

[BBG⁺19] B. Baumeister, K.-U. Bux, F. Götze, D. Kielak, and H. Krause, *Non-crossing partitions*, Spectral structures and topological methods in mathematics, EMS Ser. Congr. Rep., EMS Publ. House, Zürich, [2019] ©2019, pp. 235–274. MR 4248147

[BCN02] A. F. Beardon, T. K. Carne, and T. W. Ng, *The critical values of a polynomial*, Constr. Approx. **18** (2002), no. 3, 343–354.

[BDSW14] Barbara Baumeister, Matthew Dyer, Christian Stump, and Patrick Wegener, *A note on the transitive Hurwitz action on decompositions of parabolic Coxeter elements*, Proc. Amer. Math. Soc. Ser. B **1** (2014), 149–154. MR 3294251

[Bes03] David Bessis, *The dual braid monoid*, Ann. Sci. École Norm. Sup. (4) **36** (2003), no. 5, 647–683. MR 2032983

[BH99] Martin R. Bridson and André Haefliger, *Metric spaces of non-positive curvature*, Grundlehren der Mathematischen Wissenschaften [Fundamental Principles of Mathematical Sciences], vol. 319, Springer-Verlag, Berlin, 1999. MR 1744486

[Bia97] Philippe Biane, *Some properties of crossings and partitions*, Discrete Math. **175** (1997), no. 1-3, 41–53. MR 1475837

[Bia22] Andrea Bianchi, *Partially multiplicative quandles and simplicial Hurwitz spaces*, Preprint, 2022.

[Bia23] Andrea Bianchi, *Moduli spaces of Riemann surfaces as Hurwitz spaces*, Adv. Math. **430** (2023), Paper No. 109217, 62. MR 4621956

[BKL98] Joan Birman, Ki Hyoung Ko, and Sang Jin Lee, *A new approach to the word and conjugacy problems in the braid groups*, Adv. Math. **139** (1998), no. 2, 322–353. MR 1654165

[BM10] Tom Brady and Jon McCammond, *Braids, posets and orthoschemes*, Algebr. Geom. Topol. **10** (2010), no. 4, 2277–2314.

[Bra01] Thomas Brady, *A partial order on the symmetric group and new $K(\pi,1)$'s for the braid groups*, Adv. Math. **161** (2001), no. 1, 20–40.

[Cal22] Danny Calegari, *Sausages and butcher paper*, Recent progress in mathematics, KIAS Springer Ser. Math., vol. 1, Springer, Singapore, [2022] ©2022, pp. 155–200. MR 4510957

[CD95] Ruth Charney and Michael W. Davis, *The $K(\pi,1)$-problem for hyperplane complements associated to infinite reflection groups*, J. Amer. Math. Soc. **8** (1995), no. 3, 597–627. MR 1303028

[Com] N. Combe, *Geometric invariants of the configuration space of d marked points on the complex plane*, (2019).

[CP91] Fabrizio Catanese and Marco Paluszny, *Polynomial-lemniscates, trees and braids*, Topology **30** (1991), no. 4, 623–640.

[CW91] Fabrizio Catanese and Bronislaw Wajnryb, *The fundamental group of generic polynomials*, Topology **30** (1991), no. 4, 641–651.

[DM20] Michael Dougherty and Jon McCammond, *Critical points, critical values, and a determinant identity for complex polynomials*, Proc. Amer. Math. Soc. **148** (2020), no. 12, 5277–5289. MR 4163840

[DM22] _____, *Geometric combinatorics of polynomials I: The case of a single polynomial*, J. Algebra **607** (2022), 106–138.

[DM24] _____, *Continuous noncrossing partitions and the dual braid complex*, Preprint, 2024.

[DMW20] Michael Dougherty, Jon McCammond, and Stefan Witzel, *Boundary braids*, Algebr. Geom. Topol. **20** (2020), no. 7, 3505–3560.

[DPS22] Emanuele Delucchi, Giovanni Paolini, and Mario Salvetti, *Dual structures on Coxeter and Artin groups of rank three*, June 2022, arXiv:2206.14518 [math].

[EMHZZ96] Mohamed El Marraki, Nicolas Hanusse, Jörg Zipperer, and Alexander Zvonkin, *Cacti, braids and complex polynomials*, Sém. Lothar. Combin. **37** (1996), Art. B37b, 36. MR 1462334

[FM94] William Fulton and Robert MacPherson, *A compactification of configuration spaces*, Ann. of Math. (2) **139** (1994), no. 1, 183–225. MR 1259368

[Gau99] Carl Friedrich Gauss, *Demonstratio nova theorematis omnem functionem algebraicam rationalem integram unius variabilis in factores reales primi vel secundi gradus resolvi posse*, Ph.D. thesis, Universität Helmstedt, 1799.

[GS88] S. M. Gersten and John R. Stallings, *On Gauss's first proof of the fundamental theorem of algebra*, Proc. Amer. Math. Soc. **103** (1988), no. 1, 331–332. MR 938691

[Hae91] André Haefliger, *Complexes of groups and orbihedra*, Group theory from a geometrical viewpoint (Trieste, 1990), World Sci. Publ., River Edge, NJ, 1991, pp. 504–540. MR 1170375

[Hat02] Allen Hatcher, *Algebraic topology*, Cambridge University Press, Cambridge, 2002. MR 1867354

[HKS16] Thomas Haettel, Dawid Kielak, and Petra Schwer, *The 6-strand braid group is* CAT(0), Geom. Dedicata **182** (2016), 263–286. MR 3500387

[Hua24] Jingyin Huang, *Cycles in spherical deligne complexes and application to $k(\pi,1)$-conjecture for Artin groups*, Preprint, 2024.

[Hur91] A. Hurwitz, *Ueber Riemann'sche Flächen mit gegebenen Verzweigungspunkten*, Math. Ann. **39** (1891), no. 1, 1–60. MR 1510692

[Jeo23] Seong Gu Jeong, *The seven-strand braid group is* CAT(0), Manuscripta Math. **171** (2023), no. 3-4, 563–581. MR 4597707

[Koz08] Dmitry Kozlov, *Combinatorial algebraic topology*, Algorithms and Computation in Mathematics, vol. 21, Springer, Berlin, 2008. MR 2361455

[Kre72] G. Kreweras, *Sur les partitions non croisées d'un cycle*, Discrete Math. **1** (1972), no. 4, 333–350. MR 309747

[LZ04] Sergei K. Lando and Alexander K. Zvonkin, *Graphs on surfaces and their applications*, Encyclopaedia of Mathematical Sciences, vol. 141, Springer-Verlag, Berlin, 2004, With an appendix by Don B. Zagier, Low-Dimensional Topology, II. MR 2036721

[McC] Jon McCammond, *Noncrossing hypertrees*, Preprint 2017. `arXiv:1707.06634`.

[McC06] ———, *Noncrossing partitions in surprising locations*, Amer. Math. Monthly **113** (2006), no. 7, 598–610. MR 2252931

[McC24] ———, *Polynomials and the dual braid complex*, Oberwolfach Mini-Workshop: Artin Groups meet Triangulated Categories, 2024.

[MS17] Jon McCammond and Robert Sulway, *Artin groups of Euclidean type*, Inventiones mathematicae **210** (2017), no. 1, 231–282 (en).

[MSS07] Jeremy L. Martin, David Savitt, and Ted Singer, *Harmonic algebraic curves and noncrossing partitions*, Discrete Comput. Geom. **37** (2007), no. 2, 267–286. MR 2295058

[Nek14] Volodymyr Nekrashevych, *Combinatorial models of expanding dynamical systems*, Ergodic Theory Dynam. Systems **34** (2014), no. 3, 938–985.

[Pao21] Giovanni Paolini, *The dual approach to the $k(\pi,1)$ conjecture*, Preprint, 2021.

[PS21] Giovanni Paolini and Mario Salvetti, *Proof of the $K(\pi,1)$ conjecture for affine Artin groups*, Inventiones mathematicae **224** (2021), no. 2, 487–572 (en).

[Sal22] Paolo Salvatore, *A cell decomposition of the Fulton MacPherson operad*, J. Topol. **15** (2022), no. 2, 443–504. MR 4441597

[Sal23] Nick Salter, *Stratified braid groups: monodromy*, Preprint, 2023.

[Sal24] ———, *Monodromy of stratified braid groups, II*, Preprint, 2024.

[Sav09] David Savitt, *Polynomials, meanders, and paths in the lattice of noncrossing partitions*, Trans. Amer. Math. Soc. **361** (2009), no. 6, 3083–3107. MR 2485419

[Sjo15] Jon A. Sjogren, *Polynomial roots and open mappings*, 2015.

[Sta15] Richard P. Stanley, *Catalan numbers*, Cambridge University Press, New York, 2015. MR 3467982

[TBY+22] William P. Thurston, Hyungryul Baik, Gao Yan, John H. Hubbard, Kathryn A. Lindsey, Tan Lei, and Dylan P. Thurston, *Degree-d-invariant laminations*, Collected works of William P. Thurston with commentary. Vol. III. Dynamics, computer science and general interest, Amer. Math. Soc., Providence, RI, [2022] ©2022, Reprint of [4205644], pp. 223–289. MR 4556605

[Weg20] Elias Wegert, *Seeing the monodromy group of a Blaschke product*, Notices Amer. Math. Soc. **67** (2020), no. 7, 965–975.

[Zvo97] Dimitri Zvonkine, *Multiplicities of the Lyashko-Looijenga map on its strata*, C. R. Acad. Sci. Paris Sér. I Math. **324** (1997), no. 12, 1349–1353. MR 1457085

Email address: `doughemj@lafayette.edu`

Department of Mathematics, Lafayette College, Easton, PA 18042

Email address: jon.mccammond@math.ucsb.edu

Department of Mathematics, UC Santa Barbara, Santa Barbara, CA 93106